Modifications to the Spectrum of Radiation from Black Holes

George Johnson

New College

University of Oxford

A thesis submitted for the degree of

Doctor of Philosophy

Hilary 2020

Acknowledgements

First and foremost I wish to thank my parents and my sister for their unwavering love and support throughout the last four years. They have been the foundation beneath this entire project, and a constant source of joy and comfort. I would like to thank my supervisor John March-Russell for his guidance throughout my degree, and for enabling me to pursue my interests within theoretical physics directly, even as they evolved. I would like also to thank those teachers at school and at university who encouraged me to aim continually high, and whose knowledge and wisdom have informed the way I think today. For their kindness and patience, I would like to thank the friends I met in Oxford — in particular Alex, Callum, and Will — with whom I have made a great many wonderful memories. For providing within Oxford a beautiful corner which I quickly came to call home, and for facilitating much of the life I led outside of my studies, I would like to thank New College and the staff who work there. Finally, none of this would have been possible without the financial support of a studentship from STFC.

Statement of Originality

This thesis is wholly the work of the author. No part of this thesis has been submitted for any other qualification.

Chapters 3, 4, and 5 are based respectively on the work in:

- G. Johnson and J. March-Russell, *Hawking Radiation of Extended Objects*, JHEP **04** (2020) 205, [hep-th/1812.10500].
- G. Johnson, *Tunnelling of Charged Particles from Black Holes*, JHEP **03** (2020) 038, [hep-th/1911.12379].
- G. Johnson, *Primordial Black Hole Constraints with Large Extra Dimensions*, JCAP **09** (2020) 046, [astro-ph/2005.07467].

Abstract

Despite their name, there is clear theoretical evidence that black holes emit radiation. The nature and spectrum of this radiation depends on many features of the black hole and the emitted particles. With the profound implications that black hole evaporation has on our understanding of the marriage of quantum mechanics and general relativity, it is essential to study the details of this radiation in new contexts.

In this thesis we examine certain important modifications to the spectrum of radiation from black holes that can occur. Firstly, we study the case that the particles emitted by the black hole are spatially extended, rather than pointlike, and find that the rate of emission is suppressed by a factor which depends sensitively on the size of the particle. We then study the emission of electrically charged particles from black holes from a perspective that elucidates the physical picture of emission; namely, in terms of tunnelling of particles both through the horizon and the external electric field. We finally consider the cosmological consequences of modifying the mass-temperature relation of black holes by supposing that they can radiate into higher dimensions. In particular, we argue that current constraints on the density of black holes in the universe are evaded in certain extra-dimensional theories, in which black holes are substantially colder than their four-dimensional counterparts.

Contents

1 Introduction

It has been over 100 years since the birth of the general theory of relativity. In this time, the principles of quantum mechanics and the principle of relativity have been synthesised into the modern quantum theory of fields, an effort culminating in the Standard Model of particle physics, thought to describe all known microscopic phenomena. By contrast, comparatively little has been learned about the quantum theory of gravitation in this time. Attempts to apply standard quantum field theoretic methods to the gravitational field lead to paradox and contradiction. In the study of black holes these theoretical conflicts are often thrown into sharp relief; yet by the same token, the physics of black holes often provides the greatest clues as to the ultimate ultraviolet nature of gravity.

The most immediate obstacle to quantizing general relativity is that the Einstein-Hilbert action is not renormalisable. When expanded in perturbations to the metric, the action contains terms suppressed by powers of the Planck mass M_P. For energies much less than M_P, the quantum theory of general relativity will give reliable answers for scattering amplitudes and decay rates, but once energies reach M_P, the theory is not to be trusted. For any other non-renormalisable theory, this would be the end of the story. However, for gravity there is a straightforward classical expectation for high-energy scattering: if we try to compress a large enough energy into a small enough space, we should produce a black hole. The horizon thus appears to hide information about the high-energy behaviour of gravity, and the theory is non-predictive only within a window of the Planck scale.

The horizon of a black hole is a subtle object. The classical behaviour of black holes is governed by a series of laws remarkably analogous to the laws of thermodynamics. They suggest that we should associate an entropy to a black hole proportional to the area of its horizon. But the entropy of an object should be a measure of the number of internal microstates consistent with the coarse-grained state of the object. We thus expect a quantum description of black holes to involve degrees of freedom that scale in number not with the volume of the black hole, but with the area. This simple idea is at the heart of holography and the AdS/CFT correspondence — the proposal that a quantum theory of gravity is equivalent to an ordinary quantum field theory defined in one fewer spacetime dimensions, with the dynamics of the gravitational theory determined by degrees of freedom living on the spacetime's boundary [1–3].

If black holes are to be considered thermodynamic objects, they must radiate. It was the discovery of Hawking in 1974 [4, 5] that such radiation is a necessary consequence of the quantum mechanical behaviour of matter in a black hole background, and that the temperature of this radiation is precisely as expected from the laws of black hole mechanics. In turn this discovery led to the famous information problem — that the process of formation and evaporation of a black hole seems to violate quantum mechanical unitarity. Rescuing this seems to require a radical shift in our understanding of physics: it appears we are forced either to abandon locality, to accept that quantum field theory breaks down not just at the Planck mass but on macroscopic distance scales, or something more extreme.

Attempts to construct a consistent theory of radiation from black holes hence provides profound insights into which principles of physics we should expect to be present, and which we may have to forgo, in the correct quantum theory of gravity.

1.1 A brief history

The first black hole solution to Einstein's field equations was discovered by Schwarzschild in 1916, though it was not until Finkelstein in 1958 [6] that the causal structure of the solution was understood. The singularity theorems of Hawking and Penrose

in the late 1960s [7] cemented the idea that these solutions were not mathematical curiosities, and that generically such singularities would form in our universe.

Since this time there has been a variety of observational evidence for the existence of black holes. The motion of the stars in the centre of our galaxy indicates that they are orbiting an object of mass approximately four million times that of the Sun [8]. The object itself is not visible, and the size of the object as constrained by the closest orbit is consistent with no conventional astrophysical object besides a black hole. More direct evidence came in 2015, with the discovery of gravitational waves by LIGO [9]. From numerical studies of general relativity it was inferred from the waveform that the gravitational waves were produced by the inward spiral and merger of two black holes, each several times the mass of the Sun. Most recently, in 2019 the Event Horizon Telescope announced that it had captured an image of the accretion disc around a supermassive black hole, in the centre of the galaxy Messier 87 [10]. With both electromagnetic and gravitational probes of the near-horizon geometry an experimental reality, rigorous testing of the classical theory of black holes is now possible.

The first prediction of emission by black holes was due to Zeldovich in 1970 [11]. He discovered that rotating black holes amplify any incident particle flux (at sufficiently low energies), and that this should lead to the quantum mechanical phenomenon of spontaneous particle emission. This process is analogous to the spontaneous production of charged particles that occurs in a strong electric field. Since the process occurs outside the black hole horizon, within the so-called ergosphere, there is no conflict with the defining feature of a classical black hole — that nothing can escape from its interior. The emission of particles is always such as to reduce the angular momentum of the black hole, and ceases once the black hole stops rotating.

Understanding of emission from black holes underwent a radical shift with the work of Hawking in 1974 [4, 5]. Hawking discovered that even a non-rotating black hole emits radiation, despite the absence of any classical amplification process, and that this evaporation could in principle continue until the black hole disappeared entirely. Though this radiation is weak, and would be undetectable for black holes

formed by stellar collapse, its deep theoretical implications have placed the precise nature of the radiation as a central question in the field of black hole physics.

Since this time, the existence of thermal radiation from a black hole has been re-established from several different perspectives. We discuss some of these in Chapter 2. The calculation of Hawking has been extended to a large class of black hole solutions [12–14], with more precise quantitative formulae for the emission rate derived [15,16]. With Hawking's result lending strong support to the existence of black hole entropy, it is natural to ask whether it can be given a statistical mechanical interpretation. The first progress in this direction was due to Strominger and Vafa [17], who demonstrated that the Bekenstein-Hawking expression for the entropy could be reproduced in the context of certain string theories by counting black hole microstates. Since then, a great deal of work has been done in understanding the relevant quantum corrections to the entropy [18,19] and further elucidating its microscopic origin [20–23].

The existence of Hawking radiation also has important implications for cosmology. Though large black holes are astronomically faint, primordial black holes that are hypothesised to have been produced in the early universe [24] are small enough to be radiating at an appreciable rate. The effects of this radiation on the evolution of the universe has also been the subject of much research [25].

1.2 Open problems

Here we outline two open problems in physics which are of particular relevance to this thesis, as well as the directions in which we expect to find a solution.

Firstly, as already alluded to, the precise nature of Hawking radiation is not fully understood. The calculation of Hawking is certainly approximate, and the spectrum of radiation will be modified, at the very least, by the following effects [26]. Firstly, Hawking's original derivation assumes a black hole background which is unchanged throughout the emission process. It is hence valid only in the adiabatic approximation in which the surface gravity κ is slowly varying. For wavepackets that cannot be localised on timescales smaller than that associated with the change in surface gravity,

Hawking's analysis does not apply. There is hence an infrared cut-off to Hawking radiation, given by $\omega \gtrsim \sqrt{\dot{\kappa}}$ [27]. Secondly, there is a natural ultraviolet cut-off to Hawking radiation. Purely energetic considerations forbid photons with energy greater than the black hole mass from being emitted. A marginally more detailed kinematic argument implies the photon energy is bounded by $\omega \leq M/2$. Thirdly, the interaction of the radiation with the gravitational field *outside* the horizon, after it has been produced, can lead to quantitatively and qualitatively large effects on the nature of the spectrum. These effects are captured by so-called greybody factors, which will form the subject of much of this thesis.

Among the most important unsolved problems in theoretical physics is the nature of the dark matter in the universe. There is now widespread astrophysical evidence that the visible matter in the universe constitutes only about one fifth of all matter. Among other sources, this evidence comes from the velocity profiles of galaxies, from gravitational lensing around galaxy clusters, from the anisotropies in the cosmic microwave background, and from galactic collisions [28–31].

It is usually assumed that dark matter is some as-yet undiscovered elementary particle, that interacts only very weakly with the particles of the Standard Model. However, there is one natural solution to the dark matter problem which does not require any extension to known physics — namely that the dark matter consists of black holes which formed very early in the universe's history [24]. Understanding precisely how these primordial black holes formed is an important open question, as is computing the observational consequences of a cosmic black hole background. Indeed, there is now a large variety of constraints on the density of primordial black holes in the universe, across a wide range of possible masses. Some of these constraints arise from the effects of the Hawking radiation these black holes are expected to emit; it is thus interesting to consider how they might differ if the nature of the radiation were modified. We defer a detailed discussion of these constraints to Chapter 5.

1.3 This thesis

Motivated by the questions of the previous section, in this thesis we consider how the spectrum of radiation from black holes depends on the nature of the black hole and of the emitted particles, and examine the phenomenological implications of a modified emission spectrum. In particular, in Chapter 3 we study the properties of emission from black holes of objects which are spatially extended, as opposed to pointlike. In Chapter 4 we consider radiation of charged particles by charged black holes. In this context there are two possible emission mechanisms; we consider the interplay of these two processes, and provide an interpretation of their combined effect in terms of quantum mechanical tunnelling. In Chapter 5 we examine how the fraction of dark matter that black holes could constitute is sensitive to the properties of their evaporation. In particular, we study the modifications to the density constraints that occur when primordial black holes are taken to radiate into higher dimensions.

We will adopt throughout the convention $c = \hbar = \epsilon_0 = k_B = 1$. We will retain the Planck mass $M_P = \sqrt{1/G}$ explicitly in Chapter 5, and elsewhere set it to unity. We will use T to denote the temperature of a black hole, except in Chapter 4 where T will denote a transmission probability and $T_{\rm BH}$ the black hole temperature. We use the mostly plus metric convention $- + + +$.

2

Background Theory

In this chapter we review some of the general theory of black holes and of the theory of quantum fields in black hole backgrounds.

2.1 Black hole solutions in general relativity

A black hole spacetime is one in which there is some region — termed the interior of the black hole — from which no signal can reach future null infinity. Under suitable regularity conditions (excluding, for instance, trivial black hole spacetimes such as Minkowski spacetime with points removed), time-independent black holes in four dimensions are completely characterised by three parameters: their mass M, their angular momentum J, and their charges Q_i under any $U(1)$ gauge symmetries that may be present [32–36].

The metric that describes such a black hole is the Kerr-Newman metric, a solution of the Einstein-Maxwell equations. Defining $a = J/M$, the metric is given by

$$\begin{aligned} \mathrm{d}s^2 = -\frac{\Delta - a^2 \sin^2\theta}{\Sigma}\mathrm{d}t^2 - 2a\sin^2\theta\,\frac{r^2+a^2-\Delta}{\Sigma}\mathrm{d}t\,\mathrm{d}\phi \\ + \frac{\Sigma}{\Delta}\mathrm{d}r^2 + \Sigma\mathrm{d}\theta^2 + \frac{(r^2+a^2)^2 - \Delta a^2\sin^2\theta}{\Sigma}\sin^2\theta\,\mathrm{d}\phi^2\,, \end{aligned} \tag{2.1}$$

where

$$\Delta = r^2 - 2Mr + Q^2 + a^2 \qquad \Sigma = r^2 + a^2\cos^2\theta\,. \tag{2.2}$$

The gauge potential is

$$A = -\frac{Qr}{\Sigma}(\mathrm{d}t - a\sin^2\theta\,\mathrm{d}\phi)\,. \tag{2.3}$$

When $Q = 0$, the Kerr-Newman solution is known as the Kerr solution; when $J = 0$ it is known as the Reissner-Nordström solution; and when both are zero, it is known as the Schwarzschild solution. In this thesis we will not be concerned with rotating black holes, and so will work only with the metric

$$\mathrm{d}s^2 = -\left(1 - \frac{2M}{r} + \frac{Q^2}{r^2}\right)\mathrm{d}t^2 + \left(1 - \frac{2M}{r} + \frac{Q^2}{r^2}\right)^{-1}\mathrm{d}r^2 + r^2\mathrm{d}\theta^2 + r^2\sin^2\theta\,\mathrm{d}\phi^2\,. \quad (2.4)$$

Throughout this thesis we will denote

$$f(r) = 1 - \frac{2M}{r} + \frac{Q^2}{r^2}\,, \quad (2.5)$$

and

$$\mathrm{d}\Omega^2 = \mathrm{d}\theta^2 + \sin^2\theta\,\mathrm{d}\phi^2\,. \quad (2.6)$$

2.1.1 Crossing the horizon

In the coordinates (t, r, θ, ϕ) above, the metric Eq. (2.4) appears to develop a singularity at a radius satisfying $f(r_+) = 0$ (at least for some choices of M and Q). This singularity corresponds to the event horizon of the black hole, but the metric is in fact well-behaved here; it is merely the coordinates which are singular at this radius.

There are several coordinate systems which *are* well-behaved across the horizon. In this thesis we will work with two such systems. In ingoing Eddington-Finkelstein coordinates (v, r, θ, ϕ), with $\mathrm{d}v = \mathrm{d}t + \mathrm{d}r/f$, the metric Eq. (2.4) takes the form

$$\mathrm{d}s^2 = -\left(1 - \frac{2M}{r} + \frac{Q^2}{r^2}\right)\mathrm{d}v^2 + 2\mathrm{d}v\,\mathrm{d}r + r^2\mathrm{d}\Omega^2\,. \quad (2.7)$$

In Painlevé-Gullstrand coordinates (t_*, r, θ, ϕ), with $\mathrm{d}t_* = \mathrm{d}t + \sqrt{1-f}\,\mathrm{d}r/f$, the metric takes the form

$$\mathrm{d}s^2 = -\left(1 - \frac{2M}{r} + \frac{Q^2}{r^2}\right)\mathrm{d}t_*^2 + 2\sqrt{\frac{2M}{r} - \frac{Q^2}{r^2}}\,\mathrm{d}t_*\,\mathrm{d}r + \mathrm{d}r^2 + r^2\mathrm{d}\Omega^2\,. \quad (2.8)$$

In both of these systems, the metric is non-singular for all $r > 0$. There is no coordinate transformation that can remove the singularity at $r = 0$, since this is a physical curvature singularity. This is not apparent by examining the Ricci scalar, which is zero everywhere (since the spacetime has traceless energy-momentum tensor). However, higher-order curvature invariants, such as $R^{\mu\nu\rho\sigma}R_{\mu\nu\rho\sigma}$, diverge at this point.

2.1.2 Extremal solutions

A priori there are no restrictions on M and Q in Eq. (2.4). However, for $|Q| > M$ we note that $f(r)$ is positive for all $r > 0$, so that in fact there is no horizon. The physical singularity at $r = 0$ is hence *naked*, and since one cannot predict what emerges from a spacetime singularity, one cannot predict the late-time behaviour of the system anywhere in spacetime. In fact, dynamical formulation of such a singularity is ruled out by the weak cosmic censorship conjecture, which has been proved in some specific cases, and is supported by a body of numerical evidence.

For $|Q| = M$ the solution suffers no such issues, however, with a horizon at $r_+ = M$. Such a black hole is termed *extremal*. The near-horizon geometry is qualitatively different from the $|Q| < M$ case, however, since $f'(r_+)$ is zero in the extremal case and non-zero otherwise. In particular, whilst the near-horizon geometry of non-extremal Reissner-Nordström spacetime looks like (2D) Rindler spacetime, that of an extremal black hole looks like (2D) anti-de Sitter spacetime.

Extremal black holes are particularly interesting in the context of supergravity theories, in which they play the role of non-perturbative solitonic states. In theories with extended supersymmetry, the *BPS bound* requires that the mass of any massive state in the theory is at least as large as the central charge in the supersymmetry algebra, which in certain cases is the gauge charge of the state. This constraint on the spectrum of the theory both ensures that weak cosmic censorship holds, and implies that extremal black holes are the lightest states compatible with a given charge, and hence are absolutely stable.

2.1.3 Penrose diagrams

Written out concretely in terms of coordinates, the metrics discussed above give information about how the geometry of spacetime is locally curved. However, coordinates are always only valid in a particular patch of the full spacetime, and do not give any insight into its causal or global topological structure.

Penrose diagrams provide a useful way to visualise the spacetime as a whole, and

to understand the behaviour of null paths in the spacetime. An understanding of null paths is necessary to determine which regions can influence or be influenced by which other regions — that is, to determine the spacetime's causal structure.

Penrose diagrams are most useful when the spacetime has spherical symmetry, such that the important features of the spacetime are captured by a two-dimensional submanifold M_2 with metric g_2. Formally, a Penrose diagram is a compact region of the plane endowed with the two-dimensional Minkowski metric, which differs from the original spacetime (M_2, g_2) by a conformal transformation. Points at infinity in the original spacetime (or on the boundary of it) are mapped to parts of the boundary of this Penrose diagram by the conformal transformation. Crucially, since two conformally related metrics share the same null geodesics, the behaviour of light in the Penrose diagram must match that of the original spacetime. Since null geodesics in the Penrose diagram are straight lines at 45 degrees, the causal structure of the original spacetime becomes easy to understand.

In Figure 2.1 we give the Penrose diagrams for 4D Minkowski spacetime and for Schwarzschild spacetime. For 4D Minkowski spacetime, suppressing the angular directions yields 2D Minkowski spacetime without any modification. However, we nevertheless perform a conformal transformation in order to bring the points at infinity in the original spacetime to a finite distance in the Penrose diagram. The boundaries labelled $\mathcal{I}^+$ and $\mathcal{I}^-$, termed past and future null infinity respectively, represent the points at infinity reached by following null geodesics.

We see from the Penrose diagram for Schwarzschild spacetime that the region with $r < 2M$ is causally disconnected from future null infinity — no signal from this region can reach an observer outside of it. We also see that this region doesn't have the structure of the interior of a ball, as we might naively expect. Indeed, at a fixed moment of time the volume of space 'inside' the horizon is infinite; the singularity $r = 0$ is not a place but rather a moment of time, to the future of all observers. Thus the interior of a black hole is better thought of as a causally disconnected patch of the universe, infinite in spatial extent but terminating in finite time.

For completeness we mention that there exists a larger spacetime, known as

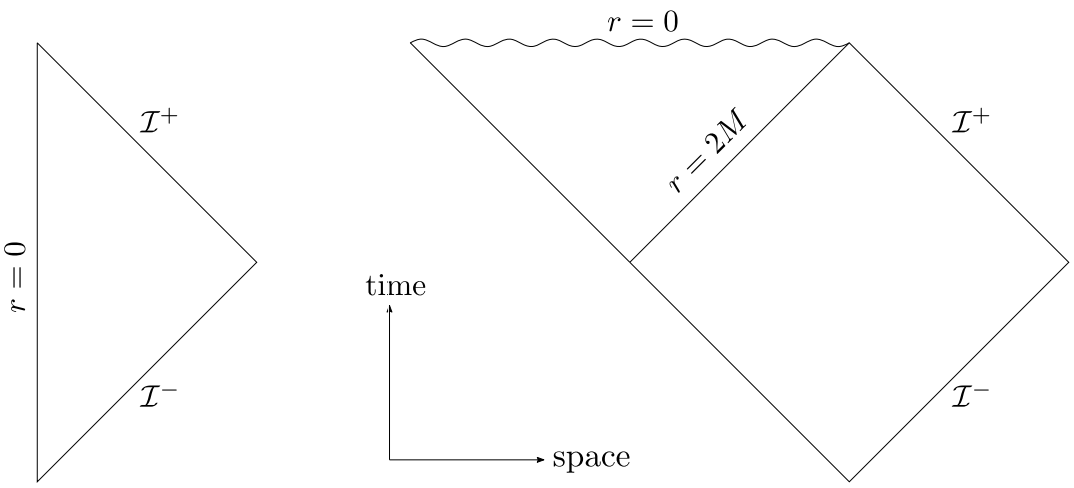

Figure 2.1: The Penrose diagrams for 4D Minkowski spacetime (left) and Schwarzschild spacetime (right).

Kruskal spacetime, which contains the Schwarzschild solution as a submanifold. This is the unique analytic spacetime which both contains Schwarzschild spacetime and which is not contained within a larger spacetime itself. We give the Penrose diagram for Kruskal spacetime in Figure 2.2. The metrics in Eqs. (2.7) and (2.8) cover the two regions of Schwarzschild spacetime illustrated in Figure 2.1, corresponding to the regions labelled I and II in Figure 2.2. In *outgoing* Eddington-Finkelstein coordinates (u, r, θ, ϕ), with $\mathrm{d}u = \mathrm{d}t - \mathrm{d}r/f$, the Schwarzschild metric takes the form

$$\mathrm{d}s^2 = -\left(1 - \frac{2M}{r} + \frac{Q^2}{r^2}\right)\mathrm{d}u^2 - 2\mathrm{d}u\,\mathrm{d}r + r^2\mathrm{d}\Omega^2\,. \tag{2.9}$$

The metric in this coordinate system is also non-singular for all $r > 0$, but the region $r < 2M$ is not the same as that in Figure 2.1. Instead, these coordinates cover regions I and IV of Kruskal spacetime. Indeed, we can define so-called Kruskal coordinates in terms of the Eddington-Finkelstein coordinates u and v by

$$U = -\exp(-u/4M)\,, \tag{2.10}$$

$$V = \exp(v/4M)\,. \tag{2.11}$$

In Kruskal coordinates (U, V, θ, ϕ) the metric takes the form

$$\mathrm{d}s^2 = -\frac{32M^3 \exp(-r/2M)}{r}\mathrm{d}U\,\mathrm{d}V + r^2\mathrm{d}\Omega^2\,. \tag{2.12}$$

These coordinates cover all four patches of Kruskal spacetime:

region I	$U < 0, V > 0$
region II	$U > 0, V > 0$
region III	$U > 0, V < 0$
region IV	$U < 0, V < 0$.

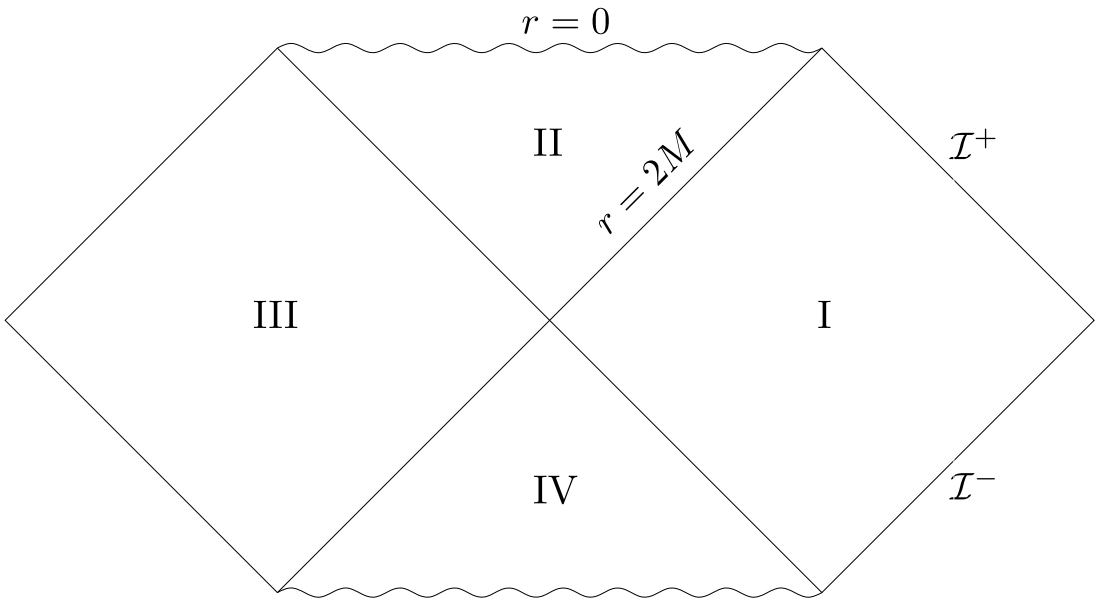

Figure 2.2: The Penrose diagram for Kruskal spacetime. Region I corresponds to the ordinary exterior of the black hole; region II corresponds to the black hole interior. Regions III and IV are unphysical, and correspond to time-reversed copies of regions I and II respectively.

2.2 Black hole thermodynamics, entropy and information theory

The event horizon, defined as the boundary of the black hole interior, has many remarkable properties. Since the metric is well-behaved at the horizon, a freely falling

observer that passes through the horizon should not be able to perform any local experiments to detect its presence. Nevertheless, to an observer at infinity, the horizon appears as a surface with physical properties such as temperature and entropy. In this section we discuss the origin of these properties.

Two classical properties of an event horizon are its area and its surface gravity. The area of the horizon of a Reissner-Nordström black hole is $4\pi r_+^2$. One can show [37] that for a stationary, analytic, asymptotically flat black hole spacetime, there exists a Killing vector field ξ which is normal to the horizon. Since the normal to a null hypersurface satisfies $\xi^2 = 0$ (on the surface itself), there exists a function κ such that

$$\nabla_a(\xi^2) = -2\kappa\xi_a \tag{2.13}$$

on the horizon. The function κ is called the *surface gravity* of the event horizon. The surface gravity of a Reissner-Nordström black hole is

$$\kappa = \frac{\sqrt{M^2 - Q^2}}{(M + \sqrt{M^2 - Q^2})^2}\,, \tag{2.14}$$

which is constant by virtue of the symmetries of the spacetime.

2.2.1 The laws of black hole mechanics

There are various formulae relating the area, surface gravity, and energy of a black hole spacetime that are collectively known as the laws of black hole mechanics [38]. These are as follows:

The zeroth law: the surface gravity κ is constant on the event horizon of a black hole satisfying the dominant energy condition.

The first law: for two Kerr-Newman black hole solutions differing from each other by a small amount,

$$\frac{\kappa}{8\pi}\,\mathrm{d}A = \mathrm{d}M - \Omega\,\mathrm{d}J - \Phi\,\mathrm{d}Q\,, \tag{2.15}$$

where Ω and Φ are respectively the angular velocity and electric potential of the horizon: $\Omega = MJ/(M^2 r_+^2 + J^2)$ and $\Phi = Q/r_+$.

The second law: the area of the event horizon does not decrease over time, for a strongly asymptotically predictable spacetime satisfying the null energy condition.

The second law, or black hole area theorem, has several implications. For example, consider the merging of two Schwarzschild black holes, with masses M_1 and M_2, to form a single black hole of mass M_3. In this process, energy may be released in the form of gravitational waves, and in principle this can be used to do work. However, the area theorem places a limit on just how much work can be done. Since the area of a Schwarzschild black hole is proportional to its mass squared, the second law implies

$$M_3 \geq \sqrt{M_1^2 + M_2^2}\,. \tag{2.16}$$

The efficiency of the process is given by $\eta = (M_1 + M_2 - M_3)/(M_1 + M_2)$. One can show that the maximum efficiency compatible with the bound Eq. (2.16) occurs when $M_1 = M_2$. In this case,

$$\eta = 1 - 1/\sqrt{2}\,. \tag{2.17}$$

The existence of an upper limit on the amount of energy that can be usefully extracted from a system of black holes, and the monotonically increasing nature of the black hole area, is highly reminiscent of a thermodynamic system. Indeed, though the laws of black hole mechanics are derived entirely within the framework of classical general relativity, they strongly resemble the corresponding laws of thermodynamics:

The zeroth law: two thermodynamic systems in thermal equilibrium with a third are in thermal equilibrium with each other. There hence exists a notion of temperature which is constant throughout the combined system.

The first law: for two systems in thermodynamic equilibrium characterised by an energy and an entropy, differing from each other by a small amount,

$$T\,\mathrm{d}S = \mathrm{d}E - \mathrm{d}W\,, \tag{2.18}$$

where W is the work required to take the first system to the second.

The second law: the entropy of an isolated system does not decrease over time.

The three laws of black hole mechanics thus correspond exactly to the laws of thermodynamics if we identify the area of the horizon with the entropy, and the surface gravity with the temperature (omitting constants of proportion):

$$\begin{aligned} T &\leftrightarrow \kappa\,, \\ S &\leftrightarrow A\,. \end{aligned} \tag{2.19}$$

In [38] this resemblance was considered nothing more than a close analogy, with the correspondence Eq. (2.19) not representative of anything physical. However, it is now believed that in fact the laws of black hole mechanics *are* the laws of thermodynamics, as applied to black holes. In particular, it is believed that black holes have an intrinsic thermodynamic entropy and temperature. In the rest of this section, we will discuss the physical meaning of black hole entropy; in the following sections we will outline the sense in which black holes have a temperature.

2.2.2 Entropy

Entropy is a measure of the lack of knowledge we have about a system. Given a probability distribution $\{P_n\}$ on the space of states n accessible to the system, we define the (Shannon) entropy by

$$S = -\sum_n P_n \ln P_n\,. \tag{2.20}$$

If we have complete knowledge about the system — that is, we know $P_m = 1$ for some m and $P_n = 0$ otherwise — then the entropy is zero. Conversely, the entropy is maximised when $P_n = 1/W$ for all states n, where W is the total number of accessible states. In this latter case, we have the least possible information about the system, and the entropy is given by

$$S = \ln W\,, \tag{2.21}$$

which is Boltzmann's expression for the entropy.

When matter, or information, falls into a black hole, it becomes inaccessible to any observer outside the black hole. Thus, the observer's knowledge of the state of the system is decreased, and the entropy of the system should thus be greater. Since a black hole gets larger as matter and information fall into it, we can suppose there is some monotonic relation between a black hole's size and its entropy. We here outline an argument due to Bekenstein [39] that the black hole entropy should be proportional to its area, as opposed to its volume, say.

The idea is that for a particle to 'fit' inside a black hole, it must be smaller than it. Thus for a black hole with mass M and Schwarzschild radius R, the infalling particle must have energy at least $1/R$. The minimum increase in the radius of the black hole is then $\mathrm{d}R \sim \mathrm{d}M \sim 1/R$, and hence

$$\mathrm{d}A \sim 1\,. \tag{2.22}$$

Crucially, the minimum increase in area is independent of the size of the black hole. Likewise, the minimum loss of information caused by this process is also of order unity, independent of the size of the black hole. It is hence natural to postulate that the black hole entropy should be proportional to its area.

Within classical general relativity, we thus see that it is natural to associate an entropy to a black hole as a measure of the amount of inaccessible information that has fallen into it. However, if black holes are to be truly thermodynamic objects, they must also have a temperature. Thus it must be possible to establish a thermal equilibrium between a black hole and, say, a gas of photons, wherein the black hole emits photons at precisely the rate it absorbs them. This is in direct contradiction with the statement that nothing can emerge from behind the event horizon of a black hole, and appears to arrest the entire programme to identify the laws of black hole mechanics with those of thermodynamics. It was not until the discovery of Hawking [4, 5], that black holes *do* emit particles when quantum mechanical effects are taken into consideration, that the notion of black holes as thermodynamic objects became inescapable. We derive the result of Hawking in the following sections. Here, we state the key result that in the semiclassical limit, a black hole radiates as a black

body with temperature given by

$$T = \frac{\kappa}{2\pi}\,. \tag{2.23}$$

This relation, and the requirement that the first law of black hole mechanics match that of thermodynamics, fixes the constant of proportion in the relation between entropy and area:

$$S = \frac{A}{4}\,. \tag{2.24}$$

2.2.3 The information problem

Quantum mechanically, a system for which we have incomplete information (that is, for which we only know the state with some probability) is described as being in a *mixed state*. Mixed states arise naturally when our system is composed of two subsystems, and we only have access to one of them. Classically, arbitrarily precise measurements of one system should lead to arbitrarily complete information about that system. However, in quantum mechanics, it is possible for the two subsystems to be entangled, such that it is impossible to obtain complete information about one system without knowledge of the other. For example, the pure state

$$|\psi\rangle = \frac{1}{\sqrt{2}}|a\rangle|\uparrow\rangle + \frac{1}{\sqrt{2}}|b\rangle|\downarrow\rangle\,, \tag{2.25}$$

where $|a\rangle$ and $|b\rangle$ belong to an inaccessible Hilbert space, appears to us as a mixed state; the best we can say is that the particle is equally likely to be spin-up or spin-down. Note that this is very different from the state given by an equal superposition of spin-up and spin-down; in that case, we can find some other direction in space with respect to which the particle is definitely spin-up. Time evolution in quantum mechanics is such that pure states evolve to pure states, and never to mixed states. In the language of density matrices, the purity of a state is quantified by the trace of ρ^2, with $\mathrm{tr}(\rho^2) = 1$ if and only if the state is pure. The fact that pure states remain pure states can then be attributed to the unitarity of time-evolution:

$$\mathrm{tr}(\rho^2) \to \mathrm{tr}(U\rho U^\dagger U\rho U^\dagger) = \mathrm{tr}(\rho^2)\,. \tag{2.26}$$

If these same principles are to apply to black holes, the increase of entropy that occurs as information is hidden behind the horizon does not correspond to evolution from a pure to a mixed state, but rather to the entanglement of the black hole exterior with the interior, in such a way that information only *appears* to be lost to an observer who has access only to the black hole exterior.

However, we know from Hawking that black holes shrink, by radiating particles with a thermal spectrum. Though the analysis does not apply in the strong-gravity regime that inevitably occurs in the final stage of evaporation, it seems reasonable to assume that this evaporation process continues, in some manner, until the black hole ceases to exist. This poses a great puzzle: if there is no black hole interior, there is no 'hidden subsystem' that the exterior could be entangled with. Thus, the mixed state we observe outside the black hole is in fact a mixed state of the entire system. The formation and evaporation of a black hole has hence led to the evolution of a pure state to a mixed state, in contradiction with the principles of quantum mechanics.

The black hole information puzzle is not resolved. We here briefly outline the three most commonly proposed resolutions; though none of these are entirely satisfactory, recent work points to the second resolution as being the most promising.

Resolution 1: simply, the principles of quantum mechanics are wrong. It may simply be that unitary time evolution does not apply to black holes, and some modified form of quantum mechanics is needed to accurately describe them. However, the presence of unitarity-violating effects at the Planck scale will nevertheless feed down to physics at lower energies, and there are strong constraints on such effects [40]. Moreover, it is known [41] that any linear evolution equation which allows the density matrix to evolve from a pure to a mixed state must violate either locality or energy-momentum conservation.

Resolution 2: the Hawking radiation exterior to a black hole is in fact eventually described by a pure state, which depends in some way on the information inside the black hole. This requires information from inside the horizon to be communicated to the particles outside of it. Moreover, this process must be occurring even when the black hole is large, and the relevant energies are small, such that we cannot simply

appeal to Planck-scale physics to explain the communication. This follows from the fact that the entanglement entropy of the black hole, equal to that of the external radiation, can never exceed the coarse-grained value $A/4$.

Resolution 3: the black hole never completely evaporates. Since the final stage of evaporation cannot be studied using known semiclassical methods, it seems reasonable to postulate that the black hole never completely disappears, and that the information which fell into the black hole remains inside some Planck-scale 'remnant'. However, since an arbitrary amount of information can have fallen into the black hole throughout its lifetime, there must be infinitely many species of final state remnant to account for this. This appears to lead to a variety of catastrophes, including the infinite entropic favourability of stellar decay to remnants, the infinite pair production rate for such remnants, and the renormalisation of Newton's constant to zero [42].

2.3 Aspects of quantum field theory

In this section we review two mechanisms for the production of particles within the framework of quantum field theory.

2.3.1 Particle production by a time-dependent background

In [43] it was shown that particle production can occur in the vacuum state when there is a time-dependent background metric. We review the argument here for the case of a scalar field. In a time-independent background, there exists a Killing vector field K corresponding to time translations. We can always find solutions to the field equations which are eigenfunctions of K:

$$K\phi = -i\omega\phi\,. \tag{2.27}$$

We classify the solutions with $\omega > 0$ as positive energy solutions, and those with $\omega < 0$ as negative energy solutions. We can always choose a set of positive frequency solutions ϕ_ω such that $\{\phi_\omega, \bar{\phi}_\omega | \, \omega > 0\}$ is a basis for the space of solutions[1], orthog-

[1]In general there will be many independent solutions for each eigenvalue ω. However, for simplicity of notation, we shall assume there is just one.

onal with respect to some inner product $\langle \cdot, \cdot \rangle$. In the quantum theory, we define annihilation operators a_ω associated to each positive frequency solution, such that the quantum field Φ can be decomposed as

$$\Phi(x) = \sum_{\omega>0} \phi_\omega(x) a_\omega + \text{h.c.}\,, \tag{2.28}$$

where we take the quantum field to be Hermitian. The annihilation operators appearing in Eq. (2.28) can be extracted by taking an inner product:

$$a_\omega = \langle \Phi, \phi_\omega \rangle\,. \tag{2.29}$$

These operators define the entire Hilbert space of the theory. In particular, the vacuum is defined to be the state annihilated by all such operators. The one-particle states are defined by acting on the vacuum with the conjugate creation operators. We hence see that the notion of 'particle' is intimately tied to the way we decompose our space of classical solutions into two subspaces, and this in turn depends on what we mean by 'energy'.

Now suppose that our background is time-dependent, but time-independent at early times and late times. In both asymptotic regions, there is a Killing vector field — denote them by K and L respectively — though they are unrelated to one another. Hence the late-time energy eigenstates ψ, which satisfy

$$L\psi = -i\nu\psi\,, \tag{2.30}$$

are *a priori* unrelated to the early-time energy eigenstates ϕ. Correspondingly, what is meant by the vacuum at early times and late times will be different.

An eigenstate of the late-time Killing vector field can be decomposed in terms of the eigenstates of the early-time Killing vector field:

$$\psi_\nu = \sum_\omega \left(\alpha_\omega \phi_\omega + \beta_\omega \bar{\phi}_\omega\right). \tag{2.31}$$

The late time annihilation operators are thus given by

$$b_\nu = \left\langle \Phi, \sum_\omega (\alpha_\omega \phi_\omega + \beta_\omega \bar{\phi}_\omega) \right\rangle \tag{2.32}$$

$$= \sum_\omega \left(\bar{\alpha}_\omega a_\omega + \bar{\beta}_\omega a_\omega^\dagger\right). \tag{2.33}$$

If the system is in the vacuum state as judged by the early-time observer, the expected number of particles in the mode ν at late time is

$$N_\nu = \langle 0|b_\nu^\dagger b_\nu|0\rangle = \sum_{\omega\,\omega'} \bar{\beta}_\omega \beta_{\omega'} \langle 0|a_\omega a_{\omega'}^\dagger|0\rangle = \sum_\omega |\beta_\omega|^2 \,, \tag{2.34}$$

which is non-zero in general.

2.3.2 Particle production by an unstable background

The mechanism for particle production discussed above rests on the differing notions of what is meant by 'particle' at different points in time. The quantum state of the system $|0\rangle$ does not change. There is a more conventional picture of particle production, in which the background state of the system $|\psi\rangle$ is not an energy eigenstate, and indeed unstable towards decay into particles.

One important example of this is the Schwinger mechanism [44], whereby a strong electric field decays into charged particle-antiparticle pairs. Here we sketch a derivation of this effect. In outline, we take the path integral for QED and integrate out the electron to yield an effective theory for the electromagnetic field. One discovers that the resulting Lagrangian has an imaginary part, indicating that the corresponding Hamiltonian is not Hermitian, and the theory not unitary. Of course, this is to be expected, since in QED it is possible for configurations of photons to evolve into configurations including electrons and positrons, but this is not possible in our effective theory. The imaginary part of the Lagrangian is directly related to the decay rate of the electric field configuration. See [45] for an account of this material.

The effective action for the electromagnetic field $\Gamma[A]$ is defined implicitly by

$$\int DA\, \exp(i\Gamma[A]) = \int DAD\bar{\psi}D\psi\, \exp(iS_{\mathrm{QED}}[A,\bar{\psi},\psi])\,. \tag{2.35}$$

From this definition, one can show that for a constant electromagnetic field, the effective action is given by the integral of the Euler-Heisenberg Lagrangian [46]:

$$\mathcal{L}_{\mathrm{EH}} = -\frac{1}{4}F^{\mu\nu}F_{\mu\nu} - \frac{q^2}{32\pi^2}\int_0^\infty \frac{\mathrm{d}s}{s}\, e^{-sm^2}\left(\frac{\mathrm{Re}\,\cosh(qsX)}{\mathrm{Im}\,\cosh(qsX)}F^{\mu\nu}\tilde{F}_{\mu\nu} - \frac{4}{q^2s^2} - \frac{2}{3}F^{\mu\nu}F_{\mu\nu}\right), \tag{2.36}$$

where q is the charge of the electron and

$$X^2 = \frac{1}{2}F^{\mu\nu}F_{\mu\nu} + \frac{i}{2}F^{\mu\nu}\tilde{F}_{\mu\nu}\,, \tag{2.37}$$

with

$$F^{\mu\nu}F_{\mu\nu} = 2(B^2 - E^2)\,, \tag{2.38}$$

$$F^{\mu\nu}\tilde{F}_{\mu\nu} = 4B\cdot E\,. \tag{2.39}$$

The imaginary terms in this Lagrangian arise from the poles in the hyperbolic cosine. Specialising to the case of zero magnetic field, one finds

$$\mathcal{L}_{\rm EH} = \frac{1}{2}E^2 - \frac{1}{8\pi^2}\int_0^\infty \frac{{\rm d}s}{s^3}\, e^{-sm^2}\left((qsE)\cot(qsE) - 1 + \frac{1}{3}(qsE)^2\right)\,, \tag{2.40}$$

from which we identify poles in the integrand at $s_n = n\pi/qE$.

The probability that a given electric field configuration described by the state $|\psi\rangle$ remains unchanged after a time T is

$$P = |\langle\psi|e^{-iHT}|\psi\rangle|^2 = e^{2\,{\rm Im}\,(H)T}|\langle\psi|\psi\rangle|^2 = e^{-2\,{\rm Im}\,(\Gamma)}\,, \tag{2.41}$$

and hence the rate of decay of the configuration per unit volume is

$$r = 2\,{\rm Im}\,(\Gamma)/VT = 2\,{\rm Im}\,\mathcal{L}_{\rm EH}\,. \tag{2.42}$$

Evaluating the contribution of the poles in the integrand in Eq. (2.40) to the imaginary part of $\mathcal{L}_{\rm EH}$, one finds this decay rate is given by

$$r = \frac{q^2E^2}{4\pi^3}\sum_{n=1}^{\infty}\frac{1}{n^2}\exp\left(-\frac{n\pi m^2}{qE}\right)\,. \tag{2.43}$$

2.4 Hawking radiation

In this section, we explain the sense in which black holes have a temperature proportional to their surface gravity. In particular, we show that the quantum field theoretic phenomena discussed above, when considered in the context of a black hole background, lead to the creation of particles with a precisely thermal spectrum, characterised by the temperature in Eq. (2.23).

There are in fact several ways of understanding that black holes have a natural intrinsic temperature. Due to the theoretical importance of the result, we present three different derivations of the phenomenon. The original derivation, due to Hawking, considers the behaviour of quantum fields on the time-dependent background corresponding to stellar collapse. Using the ideas outlined in Section 2.3.1, one can show that at late times there is a non-zero particle number in the vacuum.

The second derivation, due to Gibbons and Hawking [47], involves the Euclidean path integral for the gravitational field in the absence of any matter. A Euclidean path integral for a quantum field theory, with periodic boundary conditions in imaginary time, defines the statistical mechanics of that theory. One can show that in a black hole background, there is only one choice of period for which the metric is non-singular; this period corresponds to the inverse temperature of the black hole.

The third derivation, due to Wilczek and Parikh [48], involves the tunnelling of point particles through the horizon. Classically such a trajectory is forbidden, of course, but we can nevertheless consider the action for such a process in the quantum theory. One can show that the tunnelling action takes the form of a Boltzmann factor, from which the temperature of the black hole can be extracted. Further discussion can be found in [49–51].

2.4.1 Derivation 1: Scattering of classical waves

Consider the quantum theory of a free massless scalar field defined on a fixed but time-dependent background geometry, corresponding to gravitational collapse to form a black hole. We suppose that the system is in the vacuum state as defined by an early-time observer, and wish to compute the number of particles as seen by a late-time observer. Following Section 2.3.1, we thus wish to determine how late-time energy eigenstates decompose into early-time energy eigenstates.

For an observer at future null infinity, the natural notion of time is Schwarzschild time, or equivalently the outgoing Eddington-Finkelstein coordinate u. We can hence take the Killing vector field to be $L = \partial/\partial t|_r = \partial/\partial u|_r$, whose eigenfunctions are

outgoing null plane waves:

$$\psi_\nu(u) = \exp(-i\nu u)\,. \tag{2.44}$$

For an observer at past null infinity, the natural notion of time is also Schwarzschild time, or equivalently the ingoing Eddington-Finkelstein coordinate v. We can hence take the Killing vector field to be $K = \partial/\partial t|_r = \partial/\partial v|_r$, whose eigenfunctions are ingoing null plane waves:

$$\phi_{\omega'}(v) = \exp(-i\omega' v)\,. \tag{2.45}$$

Since these functions are only solutions to the field equations in the asymptotic future and past respectively, we need to evolve the functions in Eq. (2.45) forwards in time, through the collapsing background, in order to compare them with late-time solutions in Eq. (2.44). In the geometric optics approximation, points of constant phase of the ingoing waves follow null geodesics. Those null geodesics which reach arbitrarily late times pass arbitrarily close to the horizon. See Figure 2.3.

If there were no matter present, the ingoing wave would pass through the origin and reach late time as an outgoing wave, the time evolution captured simply by $v \to u$. In the black hole background, however, we note from Eq. (2.12) that the metric is proportional to $\mathrm{d}U\,\mathrm{d}V$ near to the horizon. Two ingoing geodesics which differ by a fixed value of v at early time thus differ, near to the horizon, not by a fixed value of u but by a fixed value of U. Thus the original ingoing waves have time-dependence in the asymptotic future of the form

$$\phi_\omega(U) = \exp(-i\omega U)\,. \tag{2.46}$$

The relation between the two coordinates u and U is (cf. Eq. (2.10))

$$u = -4M\ln(-U/2M)\,. \tag{2.47}$$

The decomposition in Eq. (2.31) relevant to our purposes is thus[2]

$$\psi_\nu(u) = \int_0^\infty \mathrm{d}\omega\left(\alpha_\omega e^{-i\omega U} + \beta_\omega e^{i\omega U}\right). \tag{2.48}$$

[2]The coefficients α_ω and β_ω will be different for each choice of frequency ν, but we omit further ν subscripts to avoid clutter.

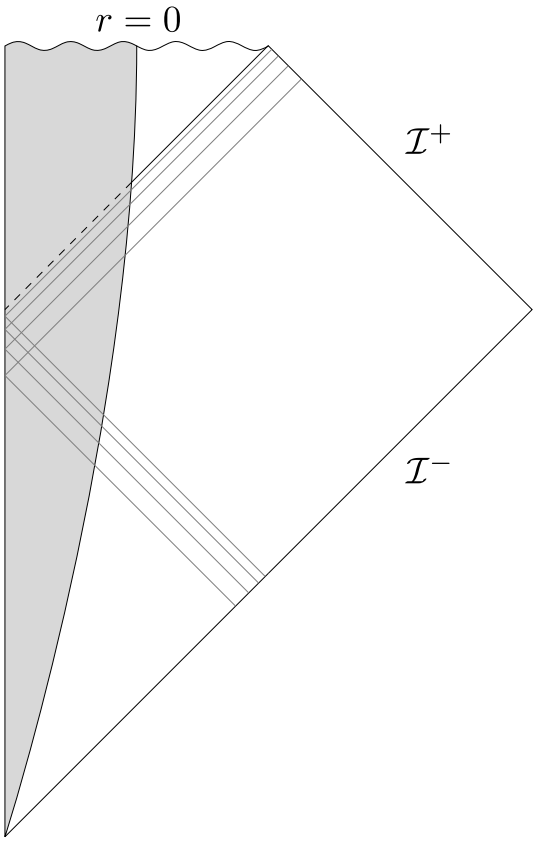

Figure 2.3: The Penrose diagram for spherically symmetric collapse to form a black hole. The shaded region corresponds to the infalling matter. In grey are shown the null geodesics followed by points of constant phase of an ingoing wave.

Standard Fourier theory tells us that

$$\alpha_\omega = \frac{1}{2\pi}\int_{-\infty}^{0} \mathrm{d}U\, \exp(i\omega U + 4Mi\nu \ln(-U/2M))\,, \tag{2.49}$$

$$\beta_\omega = \frac{1}{2\pi}\int_{-\infty}^{0} \mathrm{d}U\, \exp(-i\omega U + 4Mi\nu \ln(-U/2M))\,. \tag{2.50}$$

To make progress, consider the integral

$$I = \frac{1}{2\pi}\int_{-\infty}^{\infty} \mathrm{d}U\, \exp(i\omega U + 4Mi\nu \ln(-U/2M))\,, \tag{2.51}$$

which differs from α_ω purely in terms of the limits of integration. The integrand is an analytic function of U. The factor $\exp(i\omega U)$ tempts us to close the contour of integration in the upper-half complex U plane; if the integrand is sufficiently well-

behaved at infinity, Jordan's lemma will guarantee $I = 0$. In fact the integrand does not vanish sufficiently quickly at infinity, but this is an artefact of using non-normalisable functions ϕ_ω in our basis. A more rigorous analysis using a basis of wavepackets reproduces the same results, and so we will proceed to take $I = 0$.

One needs to take care with the logarithm in Eq. (2.51), since its argument is sometimes negative. Since we must close the contour of integration in the upper-half plane, we choose the branch cut for the logarithm to run along the negative imaginary axis. This in turn fixes $\ln(-1)$ to be $+i\pi$. We hence have

$$0 = I = \frac{1}{2\pi}\int_{-\infty}^{0} \mathrm{d}U\, \exp(i\omega U + 4Mi\nu \ln(-U/2M)) + \frac{1}{2\pi}\int_{0}^{\infty} \mathrm{d}U\, \exp(i\omega U + 4Mi\nu \ln(U/2M) - 4M\pi\nu)\,. \quad (2.52)$$

By changing variables $U \to -U$ in the second integral, we discover

$$0 = \alpha_\omega + \exp(-4M\pi\nu)\beta_\omega\,. \quad (2.53)$$

There is a normalisation condition on the coefficients α_ω and β_ω which arises from the requirement that the late-time creation operators in Eq. (2.32) obey the same canonical commutation relations as the early-time operators. This is

$$\sum_\omega \left(|\alpha_\omega|^2 - |\beta_\omega|^2\right) = 1\,. \quad (2.54)$$

Using Eqs. (2.53) and (2.54), the expected number of particles seen by the late-time observer, as determined by Eq. (2.34), is

$$N_\nu = \sum_\omega |\beta_\omega|^2 = \frac{1}{\exp(8M\pi\nu) - 1}\,. \quad (2.55)$$

Thus, the number of particles produced in the mode ν is given precisely by the Planck distribution, where the temperature is related to the black hole mass by

$$T = \frac{1}{8\pi M} = \frac{\kappa}{2\pi}\,. \quad (2.56)$$

This is the famous result of Hawking.

2.4.2 Derivation 2: The Euclidean path integral

The partition function for a quantum theory of gravity can be written, formally, as

$$Z = \int Dg \, \exp(-S) \,, \tag{2.57}$$

where we take S to be the Euclidean Einstein-Hilbert action with boundary term:

$$S = -\frac{1}{16\pi} \int_M \mathrm{d}^d x \sqrt{\det g} \, \mathcal{R} + \frac{1}{8\pi} \int_{\partial M} \mathrm{d}^{d-1} x \sqrt{\det h} \, K \,. \tag{2.58}$$

In the path integral we integrate only over metrics which are periodic in imaginary time. To understand the constraints on this period, it is sufficient to restrict to the class of such metrics which are spherically-symmetric and time-independent [52]:

$$\mathrm{d}s^2 = e^{2\Phi(r)} \mathrm{d}\tau^2 + e^{2\Lambda(r)} \mathrm{d}r^2 + r^2 \mathrm{d}\Omega^2 \,. \tag{2.59}$$

Suppose there is some radius r_+ at which $e^{2\Phi(r)}$ vanishes. This will correspond to the event horizon in the Lorentzian continuation of this geometry. We rewrite the metric in the vicinity of this radius, with $e^{\Phi} \simeq (e^{\Phi})'(r - r_+)$ and $\rho = e^{\Lambda(r_+)}(r - r_+)$, as

$$\mathrm{d}s^2 = ((e^{\Phi})' e^{-\Lambda}|_{r=r_+})^2 \rho^2 \mathrm{d}\tau^2 + \mathrm{d}\rho^2 + r^2 \mathrm{d}\Omega^2 \,. \tag{2.60}$$

Written in terms of the coordinates (ρ, τ), this metric closely resembles the flat metric on the plane, with τ playing the role of the angular coordinate. To avoid a conical singularity at the origin, however, we must take the period of τ to be such that[3]

$$\beta (e^{\Phi})' e^{-\Lambda}|_{r=r_+} = 2\pi \,. \tag{2.61}$$

One can compute the surface gravity of the metric Eq. (2.59). It is precisely the combination of metric factors appearing in the above equations:

$$\kappa = (e^{\Phi})' e^{-\Lambda}|_{r=r_+} \,. \tag{2.62}$$

The period of τ corresponds to the inverse temperature of the system. Thus we conclude that

$$T = \frac{\kappa}{2\pi} \,, \tag{2.63}$$

[3]One could argue that the singularity could also be removed by simply omitting it from the manifold. This results in a manifold which is not geodesically complete on any spacelike hypersurface, and there are certain grounds for excluding these manifolds from the path integral.

in agreement with the original derivation of Hawking.

In the above we consider a theory of pure gravity. To understand how the temperature we found translates into the thermal behaviour of matter in a black hole background, consider a field theory defined in Kruskal spacetime. The Euclidean path integral over fields defined on the entire spacetime gives rise to a vacuum state $|0\rangle$ known as the Hartle-Hawking state:

$$\langle \Phi | 0 \rangle = \int^{\Phi} D\phi \, \exp(-S[\phi]) \, . \tag{2.64}$$

The state as seen by an observer in region I, who has no access to region III, is a reduced density matrix given by tracing out states in region III:

$$\rho_I = \mathrm{tr}_{\mathrm{III}} |0\rangle\langle 0| \, . \tag{2.65}$$

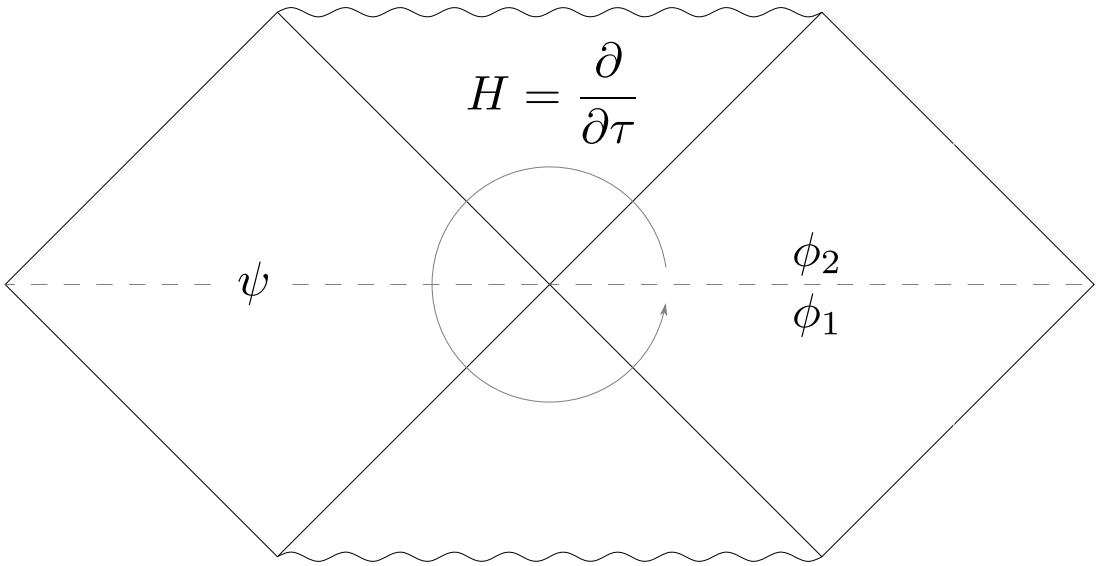

Figure 2.4: The path integral that describes the transition from the vacuum to the state $|\phi_1 \, \psi\rangle$ and subsequently from the state $|\phi_2 \, \psi\rangle$ to the vacuum. When summed over ψ, the path integral describes a transition from ϕ_2 to ϕ_1, where the Hamiltonian that generates the evolution corresponds to translation in Euclidean time.

From the path integral one can show that performing this trace amounts to evolving around Kruskal spacetime in the angular coordinate $\theta = \kappa\tau$ by an angle 2π:

$$\langle\phi_1|\rho_I|\phi_2\rangle = \sum_{\psi}\langle\phi_1\,\psi|0\rangle\langle 0|\phi_2\,\psi\rangle = \int_{\phi_2}^{\phi_1} D\phi\,\exp\left(-\int_0^{2\pi}\mathrm{d}\theta\,L[\phi]\right)\,, \tag{2.66}$$

with $\int \mathrm{d}\theta\, L = S$. This yields a density matrix which is precisely thermal:

$$\rho_I = \exp(-\beta H)\,, \tag{2.67}$$

where $\beta = 2\pi/\kappa$ and H is the Hamiltonian associated to translations in Euclidean time τ. But this is precisely the Euclidean continuation of the Hamiltonian corresponding to translations in Schwarzschild time, which is physically the energy measured by an observer at infinity. We hence find that fields in this background have thermal behaviour characterised by the temperature $T = \kappa/2\pi$.

2.4.3 Derivation 3: Tunnelling through the horizon

There is a heuristic picture of Hawking radiation that is not apparent in the previous derivations. This picture involves the production of a particle-antiparticle pair at the horizon, with the particle escaping to infinity and the antiparticle falling into the black hole. In order to conserve energy, the antiparticle needs to have negative energy, which at first glance appears to be problematic. However, defining energy as the projection of the 4-momentum p in the direction of the Killing vector field $K = \partial/\partial v|_r$ (with v the Eddington-Finkelstein coordinate appearing in Eq. (2.7)),

$$E = -p\cdot K\,, \tag{2.68}$$

we learn that this is not in fact a problem. In particular, whilst K is timelike outside the horizon, and thus E corresponds to a measure of energy, inside the horizon K is spacelike, and thus the antiparticle does not have negative energy, but rather negative spatial momentum. The physical energy of the antiparticle is in fact positive.

To understand quantitatively the rate at which this process produces particle-antiparticle pairs, we examine the dynamics of a classical particle moving freely in a black hole background. The action for such a particle is

$$S = \int p_\mu \mathrm{d}x^\mu \qquad p_\mu = g_{\mu\nu}\frac{\mathrm{d}x^\nu}{\mathrm{d}\sigma}\,, \tag{2.69}$$

where σ is an affine parameter along the worldline of the particle, chosen so that p^μ coincides with the physical 4-momentum of the particle. For a massive particle, this requires that $\mathrm{d}\sigma = \mathrm{d}\tau/m$, with τ the proper time. We can consider the action associated with motion from just inside to just outside the horizon. Quantum mechanically, this will give rise to a tunnelling probability Γ

$$\Gamma \sim \exp(-2\,\mathrm{Im}\,S)\,, \tag{2.70}$$

According to the Planck law, particles with frequency ω should be radiated at a rate with exponential dependence $\Gamma \sim \exp(-\omega/T)$. We can hence read off the temperature at which the black hole radiates according to

$$T = \frac{\omega}{2\,\mathrm{Im}\,S}\,. \tag{2.71}$$

We will study the process in Painlevé-Gullstrand coordinates, Eq. (2.8). The time coordinate t_*, just as for Schwarzschild time, corresponds to the time measured by a stationary observer at infinity. The radial dynamics of massless particles in Schwarzschild spacetime are determined by the equations

$$\left(1 - \frac{2M}{r}\right)\dot{t}_*^2 - 2\sqrt{\frac{2M}{r}}\,\dot{r}\dot{t}_* - \dot{r}^2 = 0\,, \tag{2.72}$$

$$\left(1 - \frac{2M}{r}\right)\dot{t}_* - \sqrt{\frac{2M}{r}}\,\dot{r} = \omega\,. \tag{2.73}$$

The second equation is the geodesic equation corresponding to the time-independence of the metric; in terms of the momentum defined in Eq. (2.69), it can be written $p_{t_*} = \omega$, and so ω has the interpretation of the energy of the particle as measured at infinity.

We wish to consider the trajectory of an outgoing particle. No classical outgoing trajectory which crosses the horizon exists, of course. However, the analytic continuation of an outgoing trajectory with $r > 2M$ backwards across the horizon will give rise to an imaginary term in our action, just as expected for classically forbidden motion, and this term represents the tunnelling amplitude. Eq. (2.72) can be factorised to yield, for an outgoing particle, the equation

$$\frac{\mathrm{d}r}{\mathrm{d}t_*} = 1 - \sqrt{\frac{2M}{r}}\,. \tag{2.74}$$

We then have

$$\operatorname{Im} S = \operatorname{Im} \int \omega \, \mathrm{d}t_* + \operatorname{Im} \int p_r \, \mathrm{d}r \tag{2.75}$$

$$= \operatorname{Im} \int \left(\sqrt{\frac{2M}{r}} \, \dot{t}_* + \dot{r} \right) \mathrm{d}r \, . \tag{2.76}$$

Using Eqs. (2.73) and (2.74) we can eliminate $\dot{t}_*$ and $\dot{r}$ to yield:

$$\operatorname{Im} S = \operatorname{Im} \int \frac{\omega}{1 - \sqrt{2M/r}} \, \mathrm{d}r \, . \tag{2.77}$$

The integrand has a pole at $r = 2M$, the horizon. Choosing the prescription to integrate clockwise around this pole (into the upper-half complex-r plane), we find

$$\operatorname{Im} S = 4\pi M \omega \, , \tag{2.78}$$

giving $T = 1/8\pi M$, as expected.

2.4.4 Greybody factors

Though black holes radiate as objects with temperature $T = \kappa/2\pi$, they do not behave as perfect black bodies. A particle incident upon the black hole has some probability to be reflected off the non-uniform gravitational field, dependent on the particle's frequency. The rate of absorption of particles onto a black hole is hence reduced, and if the black hole is to be in thermal equilibrium with the surrounding bath of particles, the rate of emission must be reduced by the same factor. Equivalently, there is some probability that a particle emitted by the black hole is reflected back into the horizon. Eq. (2.55) thus reads more precisely

$$N_\omega = \frac{\mathcal{A}(\omega)}{\exp(\omega/T) - 1} \, , \tag{2.79}$$

where $\mathcal{A}$ is the absorption probability. By standard scattering arguments we can relate this to the cross-section for the capture process:

$$\sigma = \frac{\pi \mathcal{A}}{\omega^2} \, . \tag{2.80}$$

In the context of thermal radiance this cross-section is known as a *greybody factor*. Taking σ to be the cross-sectional area A of the object reproduces the usual Planck law for a perfect black body:

$$P = \int \frac{\mathrm{d}\omega}{2\pi}\, \omega N_\omega = \frac{A}{2\pi^2} \int \mathrm{d}\omega\, \frac{\omega^3}{\exp(\omega/T) - 1}\,, \tag{2.81}$$

with P the total energy radiated per unit time. At high energies, for which the absorption process can be analysed in terms of point particles, the cross-section asymptotes to a constant. This constant is the absorption area of the black hole, larger than its geometric cross-section on account of the gravitational attraction of the black hole, but on the same order of magnitude. For lower energies the cross-section is generically very different from the geometric cross-section. Understanding the behaviour of these greybody factors for different types of emitted particle and different types of black hole will be a central theme of this thesis.

2.5 Higher dimensions

Thus far we have restricted attention purely to the $(3+1)$-dimensional case relevant to our universe. General relativity in other dimensions has some unique features. We mention in passing that in lower dimensions, gravity is non-dynamical. In particular, in two spatial dimensions, the Riemann tensor contains as many independent components as there are Einstein equations, and so Einstein's equations completely determine the metric. When there is no matter present, there is also no curvature, and hence the gravitational field can transmit no information. In one spatial dimension, one can show that every metric has vanishing Einstein tensor. This can be seen as a consequence of the conformal invariance of the Einstein tensor in two dimensions, combined with the fact that every two-dimensional metric is conformal to the flat metric. In one spatial dimension, therefore, gravity cannot be described by the conventional Einstein equations.

In dimensions greater than four, gravity behaves in a qualitatively similar manner to four dimensions. In Chapter 5 we will consider black hole solutions in higher dimensions, in the context of the ADD model [53]. We defer a description of the behaviour

of these black holes until then, and here briefly summarise the basic ingredients of theories with large extra dimensions.

2.5.1 Large extra dimensions

The existence of extra compact spatial dimensions is an appealing explanation for the observed weakness of gravity relative to the other fundamental forces. Informally, the force of gravity is weaker because it is 'diluted' amongst these extra dimensions. More formally, in the case that the geometry of the extra dimensions is independent of ours (spacetime is an 'unwarped product'), the gravitational action can be written

$$S = \frac{M_*^{2+n}}{16\pi} \int \mathrm{d}^{4+n}x \sqrt{-\det g} \left(\mathcal{R}_4 + \mathcal{R}_n\right) , \tag{2.82}$$

where M_* is the fundamental Planck scale, $\mathcal{R}$ is the Ricci scalar, and n is the number of extra dimensions. Neglecting the second term, we can perform the integral over the extra spatial dimensions to generate an effective 4D action. If R denotes the size of the extra dimensions, we find the relation

$$M_P^2 \sim M_*^{2+n} R^n \, . \tag{2.83}$$

It is hence possible for the fundamental Planck scale M_* to be far lower than the 4D Planck scale, if the extra dimensions are sufficiently large.

Naturally, experiments exist that probe the Standard Model up to around 1 TeV. This corresponds to far smaller distance scales than the size of the extra dimensions required give rise to a weak-scale fundamental Planck mass. Thus the particles of the Standard Model must not notice these extra dimensions — they must be localised to a brane. Naturally one should ask *why* the Standard Model should be localised to a brane within higher-dimensional space. A number of mechanisms have been proposed for this, involving the confining of particles within a potential well or topological defect in higher-dimensional space [54, 55]. It is also natural in the context of type II string theories, in which branes occur with gauge theories automatically localised to them.

The spectrum of these theories hence consists of the Standard Model along with a graviton propagating in $(4+n)$ dimensions. From a four-dimensional point of view, a

graviton with non-zero momentum in the direction of the extra dimensions appears as a particle with mass equal to this momentum. If these extra dimensions are compact, the possible momenta are quantized, and the spectrum hence consists of a tower of so-called Kaluza-Klein modes, with the massless 4D graviton corresponding to a zero-momentum mode.

We briefly mention that there do exist other massless modes, arising from the symmetries of the extra dimensions, such as the moduli fields which describe the dimensions' size. For both phenomenological and theoretical reasons such fields must by some mechanism gain a mass: this evades the significant experimental implications of additional massless particles, and stabilises the size and shape of the extra dimensions. See [56] for a review. We will make the important assumption that the mechanism by which these moduli are stabilised does not substantially alter the nature of the solutions to Einstein's equations. In particular, we will assume that the higher-dimensional Schwarzschild metric is still a valid description of a black hole, at least in the case its radius is much smaller than the size of the extra dimensions.

3

Hawking Radiation of Extended Objects

3.1 Introduction

As discussed in Chapter 2, there has been much research into the precise spectrum of Hawking radiation since its discovery in 1974. In particular, there have been detailed studies of the rate of emission of particles of different masses and spins, for black holes charged and uncharged, spinning and static, and in different dimensions.

All such studies, however, assume the emitted particles are pointlike. In nature, of course, many particles are extended objects. Bound states of QCD, for instance, have finite size. Solitons, such as monopoles in gauge theories or Q-balls in scalar field theories, are not pointlike either. Even non-composite particles, such as fundamental strings or even black holes themselves, can have finite extent.

In this chapter we study the effects of the extended nature of such objects on the temperature of the black hole and the precise spectrum of emission. The finite size of these objects modifies their interaction with the gravitational field; in particular, they are subject to tidal forces. We expect that these forces may alter the process of tunnelling through the horizon, as well as the subsequent evolution of the particles in the black hole background. For small black holes, such as the primordial black holes that may have existed in the early universe [24], these tidal forces should be large enough as to modify the spectrum of emission. To study this, we first determine the effective field equations describing the dynamics of extended objects, with the tidal

forces manifesting themselves through an additional potential term in the equations of motion. We then solve these equations with appropriate boundary conditions to extract the absorption probabilities and greybody factors. We restrict attention to uncharged and non-rotating black holes, and consider only spinless emitted particles.

This chapter is divided into five sections. In Section 2, we discuss the general theory that determines the motion of extended objects in curved spacetimes. In particular, we establish an expansion of the action in powers of the spacetime curvature, that we truncate to lowest order. In Section 3, we compute the temperature of a black body that radiates extended objects, and show that it coincides with the usual Hawking temperature. In Section 4 we numerically compute the greybody factors associated with emission of such particles, with analytic results possible in the high-mass regime. Finally, in Section 5, we discuss the results, and mention the implications for various finite size particles we observe, or hypothesise to exist, in nature.

3.2 Theory of extended objects

We will study the dynamics of extended objects in a background gravitational field by approximating them as point particles with some *effective action* that is a modification of the typical relativistic point-particle action. All the effects of tidal forces on the body can be captured in a systematic fashion through terms coupling to the curvature of the metric. If we assume the extended object is spherical, the problem of writing down terms compatible with rotational symmetry, worldline reparametrization invariance and general coordinate invariance is straightforward [57]. Expanding in powers of the Riemann tensor, the first few terms in such an effective action are

$$S = -m \int \mathrm{d}\tau - c_1 \int \mathrm{d}\tau \, \mathcal{R} - c_2 \int \mathrm{d}\tau \, \mathcal{R}_{\mu\nu} \dot{x}^\mu \dot{x}^\nu + \cdots \tag{3.1}$$

where c_1, c_2 are constants, $\mathcal{R}_{\mu\nu}$ is the Ricci tensor, and $\mathcal{R}$ the Ricci scalar. For Schwarzschild spacetime, which will be the case we consider in this chapter, $\mathcal{R}$ and $\mathcal{R}_{\mu\nu}$ are zero. The lowest-order non-vanishing terms in the action are thus constructed from two powers of the Riemann tensor. Contracting these with the 4-velocity in every

possible fashion leads us to the effective action[1]

$$S = -\int \mathrm{d}\tau \Big(m + c\, E_{\mu\nu} E^{\mu\nu} + c'\, B_{\mu\nu} B^{\mu\nu} \Big) \,, \tag{3.2}$$

where

$$E_{\mu\nu} = R_{\mu\alpha\nu\beta} \dot{x}^\alpha \dot{x}^\beta \,, \tag{3.3}$$

$$B_{\mu\nu} = \epsilon_{\mu\alpha\beta\gamma} R^{\alpha\beta}{}_{\delta\nu} \dot{x}^\gamma \dot{x}^\delta \,. \tag{3.4}$$

The constants c, c' have dimensions of volume and are assumed to depend on the size of the object; we discuss this dependence in Section 3.5. Assuming purely radial motion, we find for Schwarzschild spacetime that[2] $B_{\mu\nu} = 0$. Eq. (3.2) then becomes

$$S = -\int \mathrm{d}\tau \left(m + c\, \frac{6M^2}{r^6} \left(\left(1 - \frac{2M}{r} \right) \dot{t}_*^2 - 2\sqrt{\frac{2M}{r}}\, \dot{t}_* \dot{r} - \dot{r}^2 \right)^2 \right) \,. \tag{3.5}$$

We note that such objects no longer move on geodesics; the deviation from geodesic motion is due to the aforementioned tidal forces.

3.3 Hawking temperature for extended objects

In Section 2.4.3 we presented a derivation of the Hawking temperature for massless pointlike particles moving in Schwarzschild spacetime. We here present a derivation along these lines first for pointlike particles with non-zero mass, and then subsequently for extended objects, and show that the temperature in both cases agrees with the usual Hawking formula $T = 1/8\pi M$, as expected from the zeroth law.

3.3.1 Case $m > 0$

For massive point particles, which follow geodesics, the dynamics are governed by

$$\left(1 - \frac{2M}{r} \right) \dot{t}_*^2 - 2\sqrt{\frac{2M}{r}}\, \dot{t}_* \dot{r} - \dot{r}^2 = 1 \,, \tag{3.6}$$

$$\left(1 - \frac{2M}{r} \right) \dot{t}_* - \sqrt{\frac{2M}{r}}\, \dot{r} = \omega \,. \tag{3.7}$$

[1] There are several other terms one could conceivably write down, involving eight, six, two, or zero powers of the 4-velocity. These either vanish identically, vanish in Schwarzschild spacetime, or reduce to one of the terms in Eq. (3.2).

[2] We emphasise that for more general motion, $B_{\mu\nu}$ is not zero.

Using these equations to solve for p_r is somewhat more complicated than in the massless case, but essentially the same. Taking Eq. (3.7) and substituting for $\dot{r}$ into Eq. (3.6) yields a quadratic equation in $\dot{t}_*$ which we can solve:

$$\dot{t}_*^2 \left(\frac{r}{2M} - 1\right) - \dot{t}_* \left(\frac{\omega r}{M}\right) + \left(\frac{r\omega^2}{2M} + 1\right) = 0\,. \tag{3.8}$$

We find

$$\left(1 - \frac{2M}{r}\right) \dot{t}_* = \omega \pm \sqrt{\frac{2M}{r}} \sqrt{\omega^2 - 1 + \frac{2M}{r}}\,, \tag{3.9}$$

$$\dot{r} = \pm \sqrt{\omega^2 - 1 + \frac{2M}{r}}\,. \tag{3.10}$$

From here we compute the imaginary part of the action thus:

$$\operatorname{Im} S = \operatorname{Im} \int p_r \,\mathrm{d}r \tag{3.11}$$

$$= \operatorname{Im} \int \left(\sqrt{\frac{2M}{r}}\, \dot{t}_* + \dot{r}\right) \mathrm{d}r \tag{3.12}$$

$$= \operatorname{Im} \int \left(\frac{\dot{r} + \omega\sqrt{2M/r}}{1 - 2M/r} + \dot{r}\right) \mathrm{d}r\,. \tag{3.13}$$

Taking the positive sign for $\dot{r}$ and substituting yields

$$\operatorname{Im} S = \operatorname{Im} \int \left(\frac{\sqrt{\omega^2 - 1 + 2M/r} + \omega\sqrt{2M/r}}{1 - 2M/r}\right) \mathrm{d}r\,. \tag{3.14}$$

Finally we integrate around the pole at $r = 2M$ to extract the imaginary part. As in the massless case, we find

$$\operatorname{Im} S = 4\pi M\omega\,, \tag{3.15}$$

which yields $T = 1/8\pi M$ by Eq. (2.71).

3.3.2 Case $c > 0$

In order to calculate the tunnelling rate for particles of finite size, we first need to determine the modifications to the equations of motion that result from the additional term in the action, before substituting these back into the action. Matters are simplified greatly for radial motion; using the standard normalisation of the 4-velocity,

the action is simply

$$S = -\int \mathrm{d}\tau \left(m + c\,\frac{6M^2}{r^6} \right) =: -m \int \mathrm{d}\tau\, \lambda(r)\,. \tag{3.16}$$

As per usual, we can use the 4-velocity normalisation in place of the equation of motion for $r(\tau)$, leaving us with only one equation to determine. The t_*-independence of the effective action makes this relatively simple (cf. Eq. (3.7)):

$$\omega = \left(\left(1 - \frac{2M}{r} \right) \dot{t}_* - \sqrt{\frac{2M}{r}}\, \dot{r} \right) \lambda(r)\,. \tag{3.17}$$

The manipulations of the previous section proceed here as before, but with ω replaced everywhere by $\omega/\lambda(r)$. We thus compute

$$\mathrm{Im}\, S = \mathrm{Im} \int \lambda(r) p_{t_*}\, \mathrm{d}t_* + \mathrm{Im} \int \lambda(r) p_r\, \mathrm{d}r\,. \tag{3.18}$$

The first term has no imaginary part. The second term is given by

$$\mathrm{Im} \int \lambda(r) p_r\, \mathrm{d}r = \mathrm{Im} \int \lambda(r) \left(\frac{\sqrt{(\omega/\lambda)^2 - 1 + 2M/r} + (\omega/\lambda)\sqrt{2M/r}}{1 - 2M/r} \right) \mathrm{d}r\,. \tag{3.19}$$

At the pole, the factors of $\lambda(2M)$ cancel, yielding

$$\mathrm{Im}\, S = 4\pi M \omega\,, \tag{3.20}$$

as before.

3.4 Greybody factors

We have found that a Schwarzschild black hole with mass M radiates extended objects at the Hawking temperature T. We next wish to find the exact rate at which such objects are radiated. That is to say, we wish to determine the greybody factors discussed in Section 2.4.4. Decomposing the absorption probability into angular momentum modes, for massive particles Eq. (2.80) becomes

$$\sigma = \frac{\pi}{k^2} \sum_\ell (2\ell + 1) \mathcal{A}_\ell\,, \tag{3.21}$$

where ℓ is the partial wave number and k is the particle's momentum, given by $k = \sqrt{\omega^2 - m^2}$. We will calculate the quantities $\mathcal{A}_\ell$ by solving the field equations for

the relevant particle in the black hole background, imposing purely ingoing boundary conditions at the horizon, corresponding to total absorption.

We will be interested exclusively in the low-momentum regime, $kM \ll 1$. This corresponds to the wavelength of the particle being much larger than the Schwarzschild radius of the black hole. Analytic results for both massless and massive particles are well-known in this regime [16]. Furthermore, the greybody factor in the low-momentum regime will be determined by the $\ell = 0$ partial wave, for which there is a great simplification of the tidal terms in the action, seen in Eq. (3.16).

For point particles, an analytic expression for the greybody factor in the regime where the de Broglie and Compton wavelengths of the particle are much larger than the Schwarzschild radius of the black hole (that is, $\omega M \ll 1$) was found in [15]:

$$\sigma(k) = 32\pi^2 M^3 \frac{(2k^2+m^2)\sqrt{k^2+m^2}}{k^2}\left(1-\exp\left(-2\pi M\frac{2k^2+m^2}{k}\right)\right)^{-1}. \tag{3.22}$$

For low-momenta massive particles, this becomes

$$\sigma(k) \simeq \frac{32\pi^2 M^3 m^3}{k^2}\,. \tag{3.23}$$

In the low-energy massless case, the limiting behaviour is rather different. Taking the $m = 0$, $k \to 0$ limit of Eq. (3.22), we have

$$\sigma(k) \simeq 16\pi M^2\,. \tag{3.24}$$

3.4.1 Effective field theory of extended objects

Recall that the action for a radially infalling extended object can be written

$$S = -\int \mathrm{d}\tau \left(m + c\,\frac{6M^2}{r^6}\right). \tag{3.25}$$

Though the action in principle contains four powers of the velocity, for radial motion these appear precisely in the combination of the 4-velocity to the fourth power (for more general motion this is not the case). We note that this amounts to the action for a relativistic point particle, but with a position-dependent *effective mass*

$$\mu(r) = m + c\,\frac{6M^2}{r^6}\,. \tag{3.26}$$

The corresponding classical field theory that describes spinless coherent collections of these particles is thus the Klein-Gordon theory with such an effective mass:

$$\mathcal{L} = -\frac{1}{2}(\partial_\mu \phi)(\partial^\mu \phi) - \frac{1}{2}\mu(r)^2\phi^2 \,. \tag{3.27}$$

We can formalise this correspondence as follows. First note that we can introduce an einbein $e(x)$ into the particle action to modify it thus[3]:

$$S = \frac{1}{2}\int \mathrm{d}\sigma \left(e^{-1} g_{\mu\nu}\dot{x}^\mu \dot{x}^\nu - e\mu(r)^2\right) \,. \tag{3.28}$$

Upon quantizing this theory of a point particle we find the effective action [58]

$$\Gamma[g_{\mu\nu}] = \frac{1}{2}\mathrm{tr}\ln(\nabla^2 - \mu(r)^2) \,, \tag{3.29}$$

which is precisely the effective action of the Klein-Gordon theory Eq. (3.27). The classical equation of motion derived from this Lagrangian is simply

$$g^{\mu\nu}\nabla_\mu\nabla_\nu\phi - \mu(r)^2\phi = 0 \,. \tag{3.30}$$

3.4.2 Solving the equations of motion

It remains to solve Eq. (3.30) subject to appropriate boundary conditions. We will restrict our analysis to the $\ell = 0$ partial wave solution of this equation, since it is derived from the assumption of radial particle motion. In Schwarzschild coordinates, we decompose our field ϕ as

$$\phi(x) = e^{-i\omega t}R(r) \,. \tag{3.31}$$

Then Eq. (3.30) reads

$$\frac{1}{r^2}\left(1-\frac{2M}{r}\right)\partial_r\left(r^2\left(1-\frac{2M}{r}\right)\partial_r\right)R(r) - \mu(r)^2\left(1-\frac{2M}{r}\right)R(r) + \omega^2 R(r) = 0 \,. \tag{3.32}$$

We can simplify this equation using the tortoise radial coordinate r_*:

$$r_* = r + 2M\ln\left(\frac{r}{2M} - 1\right) \qquad \Longrightarrow \qquad \frac{\mathrm{d}r_*}{\mathrm{d}r} = \left(1-\frac{2M}{r}\right)^{-1} \,. \tag{3.33}$$

[3]Indeed, this is the more appropriate action one should use for massless particles.

Then the equation of motion becomes, with $S = rR$ [59],

$$-\frac{\mathrm{d}^2 S}{\mathrm{d}r_*^2} + V(r)S = \omega^2 S \qquad \text{with} \qquad V(r) = \left(\mu(r)^2 + \frac{2M}{r^3}\right)\left(1 - \frac{2M}{r}\right), \quad (3.34)$$

where r is implicitly a function of r_*. To calculate the absorption probability, we impose purely *ingoing* boundary conditions at the horizon. When $r = 2M$, this equation becomes that of a simple harmonic oscillator, with solution

$$R(r_*) = A_+ \exp(i\omega r_*) + A_- \exp(-i\omega r_*)\,. \quad (3.35)$$

Ingoing boundary conditions correspond to $A_+ = 0$. At large distances, the effects of the tidal terms are negligible. In the massless case, the solutions are spherical Bessel functions, whilst the long-range $2M/r$ term in the massive case yields Coulomb wavefunction solutions. In the far-field region these have the asymptotic form [60]:

$$R(r) = \frac{B_+}{r}\exp(ikr - i\eta\ln(2kr) + i\theta) + \frac{B_-}{r}\exp(-ikr + i\eta\ln(2kr) - i\theta)\,, \quad (3.36)$$

where $\eta = -M(2k^2 + m^2)/2k$ and θ is an unimportant constant phase.

Starting with boundary conditions at the horizon, we numerically integrate Eq. (3.34) out to large r to extract the reflection coefficient, given by the squared ratio of the magnitudes of B_+ and B_-. The absorption probability we desire is then simply

$$\mathcal{A} = 1 - \left|\frac{B_+}{B_-}\right|^2, \quad (3.37)$$

and from here the greybody factor can be computed according to Eq. (3.21).

3.4.3 Results

We present in this section the results of the numerical simulations. We first consider the regime where the mass and energy of the particle are small, in the sense that $\omega M \ll 1$ and $mM \ll 1$. Thereafter we consider the large mass ($mM \gg 1$) case.

3.4.3.1 Low mass emission

The effect of the finite size of the object is always to reduce the greybody factor σ. We plot in Figure 3.1 the behaviour of the greybody factor as a function of momentum

k, in both the massive and massless case. In particular, we find that, irrespective of the wavelength of the particle, the effect of the tidal terms is to reduce the absorption probability by a constant factor which we call $X(c)$:

$$X(c) = \frac{\sigma(c)}{\sigma(0)}\,. \tag{3.38}$$

We find that for small c, $X(c)$ is equal to one, as expected, whilst for large c, $X(c)$ tends to zero, suppressing the greybody factor:

$$X(0) = 1\,, \tag{3.39}$$

$$\lim_{c\to\infty} X(c) = 0\,. \tag{3.40}$$

We wish to know how this quantity behaves as a function of the parameters m and M. We find that as a function of the dimensionless ratio

$$s = \frac{c}{M^3}\,, \tag{3.41}$$

the quantity $X(s)$ is independent of the masses m and M. The form of $X(s)$ as a function of s is plotted in Figure 3.2.

We can understand this scaling relation by rewriting Eq. (3.30) in terms of a dimensionless radius $\rho = r/M$ (and its corresponding tortoise coordinate). We have

$$-\frac{\mathrm{d}^2 S}{\mathrm{d}\rho_*^2} + \left(\left(mM + \frac{6c}{M^3\rho^6}\right)^2 + \frac{2}{\rho^3}\right)\left(1 - \frac{2}{\rho}\right) S = \omega^2 M^2 S\,. \tag{3.42}$$

The dimensionless parameters in this equation are mM, ωM and c/M^3. The effective mass is a rapidly decaying function of ρ, and so we expect the short distance behaviour to depend only on c/M^3, and the large distance behaviour on m and ω. In principle, these parameters could be combined in a complicated way when we match in the intermediate regime. However, for small masses and energies, the absorption probability is expected to be very small (cf. Eqs. (3.21), (3.22) and (3.24)). Equivalently, the coefficients B_+ and B_- in (3.36) are almost equal and opposite. The matching of the two solutions in the intermediate regime thus amounts to a single continuity condition, relating the size of the small r solution (which depends only on

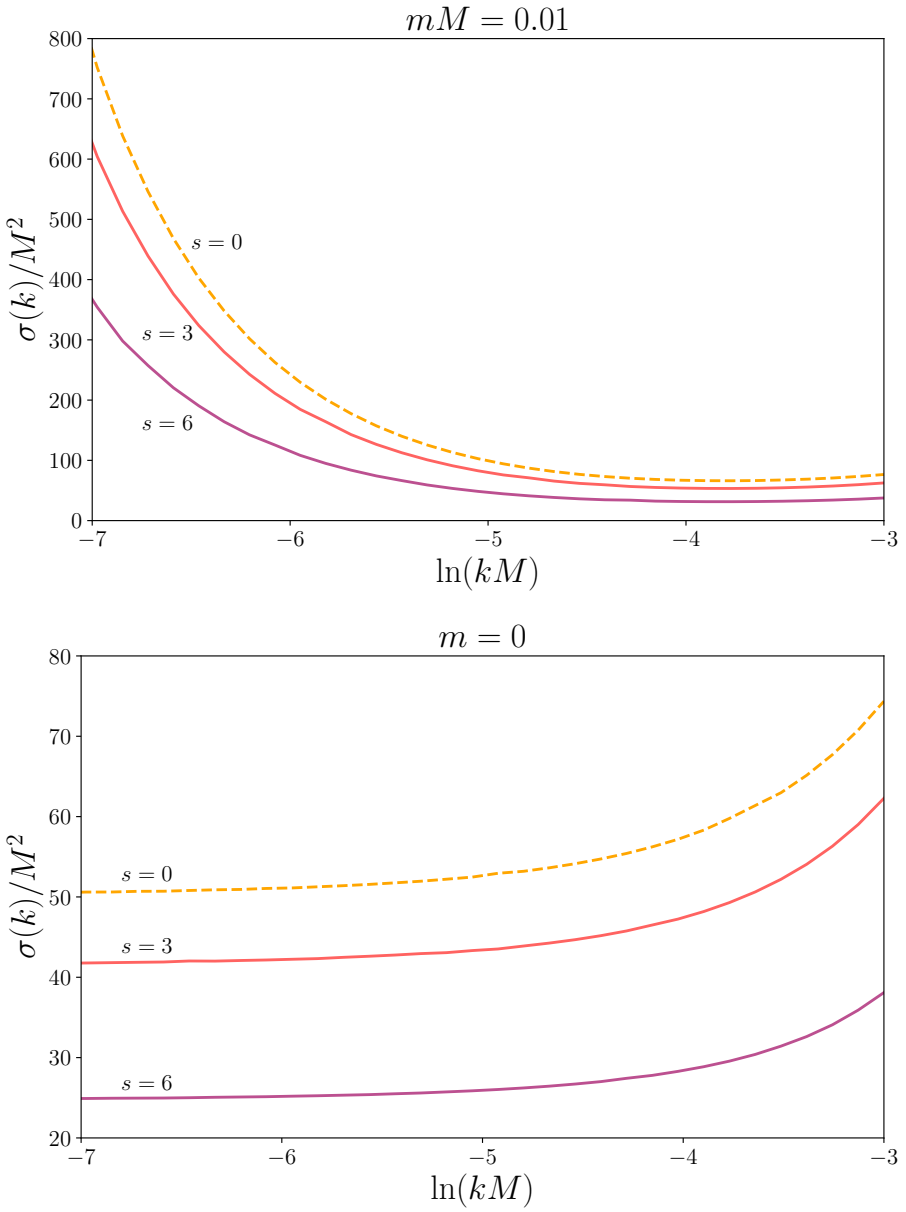

Figure 3.1: Cross-section σ against momentum k, for three choices of $s = c/M^3$. In the upper panel we plot σ in the low-mass regime, and in the lower panel the massless cross-section. One sees that the tidal terms reduce the value of the cross-section by a factor independent of momentum k. One also observes the $1/k^2$ asymptotic dependence of the massive cross-section, in contrast to the constant limiting value of the massless cross-section.

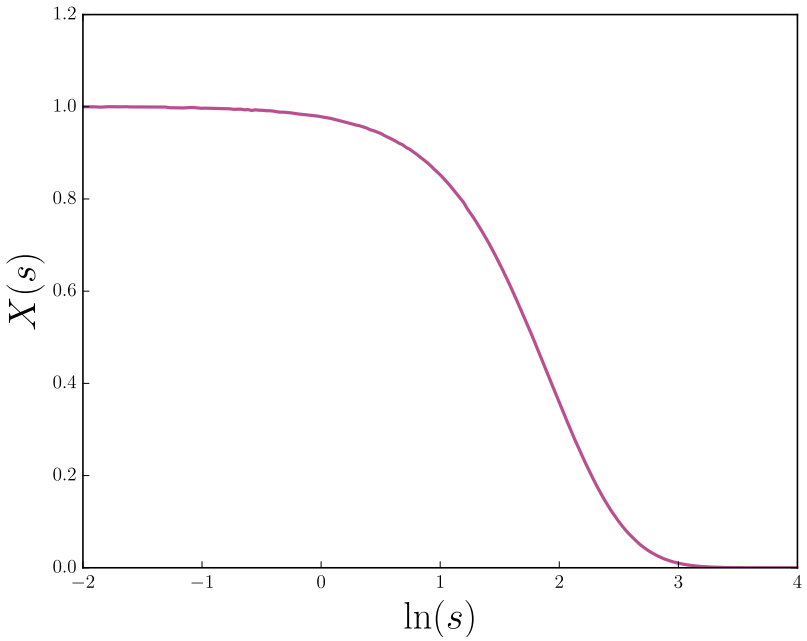

Figure 3.2: The absorption cross-section (normalised to the point-particle cross-section) $X(s)$ against s, the strength of the tidal terms. Independent of the wavelength of the particle, the cross-section is reduced by a factor which becomes smaller as s increases, reaches $1/2$ at around $s_{1/2} \simeq 5.9$, and eventually becomes exponentially small.

c/M^3) and the size of the large r solution (which depends only on mM and ωM). This explains the factorisation of the cross-section into the product of the point-particle cross-section and the tidal effects.

The point at which the greybody factor is reduced to half, $s_{1/2}$, is given by

$$s_{1/2} \simeq 5.9\,. \tag{3.43}$$

We find that beyond this point, the tail of the function $X(s)$ is well-modelled by an exponential. Numerically we determine that

$$X(s) \sim \exp(-s/s_0) \qquad \text{with} \qquad s_0 \simeq 3.3\,. \tag{3.44}$$

We can understand the above functional form, as well as the independence of $X(s)$ and the masses m and M, by examining the effective potential that the particle moves in.

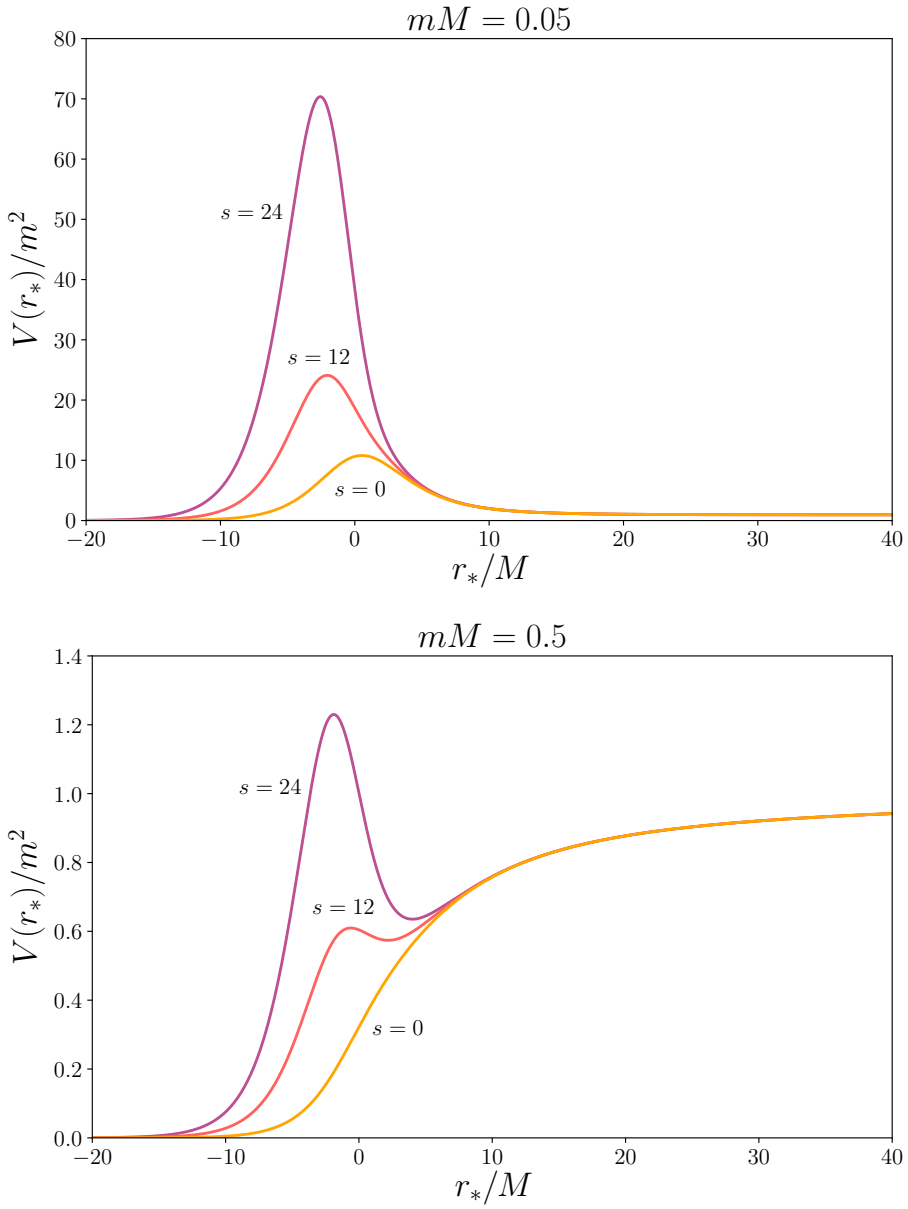

Figure 3.3: The effective potential $V(r_*)$ from Eq. (3.34) against r_*, for three choices of s, characterising the strength of the tidal term. In the upper panel is this potential in the low-mass regime, and in the lower panel the potential with a mass close to the critical mass $m_c \simeq 0.385/M$. The effect of the tidal terms is to either produce or enhance a potential barrier through which the particle must tunnel, thereby reducing the probability of emission.

Eq. (3.34) resembles the 1D Schrödinger equation for a particle moving in a potential well. For the particle at infinity to reach the horizon, it must tunnel through a potential barrier, which exists for all values of c for sufficiently light particles. We plot this effective potential for certain values of s in Figure 3.3. We hence expect the absorption probability to have an exponential suppression of the form

$$\mathcal{A} \sim \exp\left(-2\int \mathrm{d}r_* \sqrt{V(r;c)-\omega^2}\right) =: \exp\left(-2I(c)\right) . \tag{3.45}$$

For small m, ω, we find

$$I(c) \simeq \int_2^\infty \mathrm{d}\rho \sqrt{\left(\left(\frac{6c}{M^3\rho^6}\right)^2 + \frac{2}{\rho^3}\right)\left(1-\frac{2}{\rho}\right)^{-1}} . \tag{3.46}$$

We see that this integral depends on c only through the dimensionless parameter c/M^3. Furthermore, numerical evaluation of this integral as a function of c shows that it remains roughly constant until around $c/M^3 \sim 5$, and then rises approximately linearly, with gradient $1/3.3 \simeq 1/s_0$. This explains the exponential suppression of the absorption probability. We plot this integral against s on the left of Figure 3.4.

3.4.3.2 High mass emission

In the high-mass regime, the restriction $kM \ll 1$ corresponds to consideration of only non-relativistic particles. We can understand the behaviour of the absorption probability in this regime by considering once again the behaviour of the effective potential. It was shown for point particles in [61] that for m greater than a critical value $m_c \simeq 0.385/M$, the effective potential becomes a monotonically increasing function of r. Above this mass, therefore, there should be a large enhancement of the absorption cross-section due to the disappearance of a barrier to tunnel through. However, for a sufficiently large tidal term, the potential once more develops a barrier, and we expect exponential suppression of the cross-section.

For large m we find a simple analytic relation for the value of $s = c/M^3$ at which this barrier develops:

$$s_1 \simeq \frac{1}{2}\left(\frac{3}{2}\right)^{11} mM . \tag{3.47}$$

This relation is remarkably well borne out by numerical simulations for $mM \gtrsim 1$. We can again examine the integral $I(c)$ of our effective potential in the regime where s is greater than s_1, and a barrier exists. As before, the integral depends linearly on the value of s, and so we expect exponential suppression of the cross-section for s above s_1. The gradient is approximately $1/3.3$ as before, independent of the masses m and M. Thus

$$X(s) \sim \exp((s - s_1)/s_0) \qquad \text{with} \qquad s_0 \simeq 3.3\,. \tag{3.48}$$

We plot the barrier integral against s on the right of Figure 3.4.

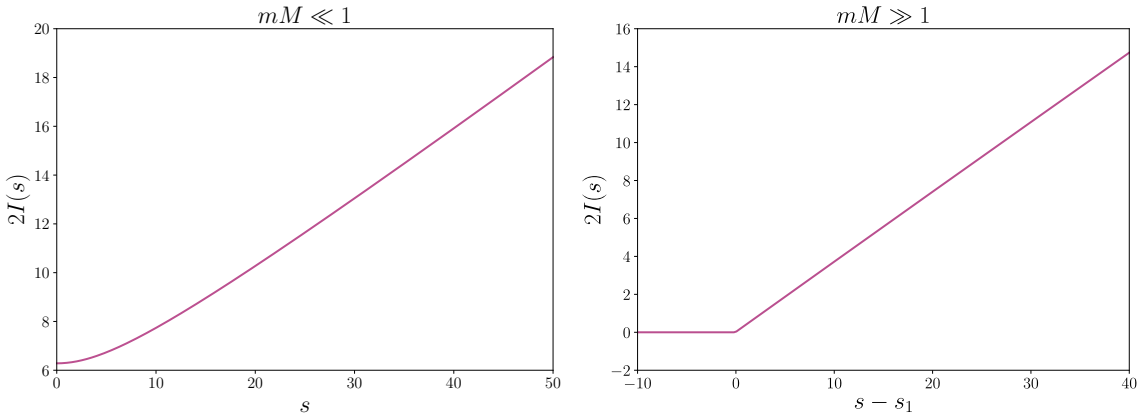

Figure 3.4: The barrier integral $I(s)$ defined by Eq. (3.45) against s. On the left is this function in the low-mass regime, and on the right the high-mass regime. For large s the behaviour is linear, indicating an exponential dependence of the cross-section on s. In the high-mass regime, this linear behaviour only starts above a critical value s_1, given by Eq. (3.47).

3.5 Discussion

We have found that Hawking radiation of spatially extended objects always occurs at a lower rate to that of the corresponding pointlike objects, at least for scalar particles in the low-momentum regime. It is interesting to ask whether this effect is significant for extended objects in nature, such as protons, strings, or GUT monopoles. To estimate this, we need to find some relation between the physical size of these objects

and the corresponding parameter c in the action.

In the following we reinstate the Planck mass M_P. The parameter c has dimensions of volume. For a given object, there are three characteristic length scales: its Compton radius $1/m$, its gravitational radius m/M_P^2, and its physical size d. For highly gravitationally-bound objects (we can consider the possibility of black holes radiating black holes themselves), the physical size is on the order of the gravitational radius, and a matching calculation indicates that $c \sim M_P^2 d^5$ [57]. For non-gravitational objects, we expect d and $1/m$ to be the only relevant scales. However, we also expect the effects of the tidal forces to be well-behaved in the massless limit[4], implying no dependence on the Compton wavelength: $c \sim d^3$.

We compute in Table 3.1 the value of the black hole mass M (in Planck units) that results in an order two-fold suppression of the emission rate for various (hypothetical) extended objects in nature.

Object	Mass m	Size d	M/M_P
Massless String Excitation	0	10^{-35} m	1
Proton	1 GeV	10^{-15} m	10^{20}
GUT Monopole	10^{16} GeV	10^{-31} m	10^{4}
Micro BH	m	m/M_P^2	m/M_P

Table 3.1: Black hole mass M such that the emission rate is approximately halved relative to the point-particle case, for various extended objects.

Finally, we must discuss the limitations of this analysis. Firstly, by reducing the theory of extended objects to an effective theory involving couplings to the curvature, we implicitly assume the object is rigid. For non-rigid objects, the point-particle approximation is inappropriate. However, this analysis should be valid whenever there is a sufficiently large mass gap in the spectrum of the extended object. For sufficiently low energies, we can expect the particle to remain in its ground state, and hence behave as a rigid object. We should also expect that for very large curvatures,

[4]For many extended objects, such as protons and GUT monopoles, the Compton and physical radii are comparable, so this argument is unnecessary.

it is not sufficient to take only the first term in the expansion of the action, and that higher-order terms become relevant.

Secondly, we have restricted attention to the long wavelength regime. In this regime the effects on the spectrum are dominated by s-wave radiation, for which there is a large simplification of the effective action. Further, we took the emitted particles to be spinless, which led us to an effective theory of a scalar field. We refer the analysis of higher spins and higher partial waves to future work.

Thirdly, we have only considered radiation from Schwarzschild black holes. It would be worthwhile to consider how finite size effects modify the spectrum of rotating or charged black holes, or of black holes in different spacetime dimensions. For charged black holes radiating charged objects, for instance, there will be forces on the object as it escapes to infinity due to inhomogeneities in the electric field as well as those in the gravitational field, which would likely give rise to a rich range of phenomena. However, even emission of pointlike particles from charged black holes has an intricate structure — we discuss this in the following chapter.

4

Tunnelling of Charged Particles from Black Holes

4.1 Introduction

We have so far in this thesis considered the creation of particles by uncharged non-rotating black holes, as discovered by Hawking. Particle creation in another context, namely that by a static *electric* field, had been understood a quarter of a century earlier, with the work of Schwinger [44]. Since it is possible for a black hole to be electrically charged, we expect that black holes can lose mass and charge through this process also.

Whilst there has been a wealth of research into the spectrum of radiation of uncharged particles from black holes, for which Schwinger pair production is irrelevant, and into the nature of Schwinger pair production outside a charged black hole, with thermal effects ignored [62], there has not been such detailed analysis of the interplay of the two effects — of the entirety of emission from a hot electrically charged black hole. Where both processes are considered, it is usually as applied to *different* species of particle — that is, one considers Hawking radiation of photons, say, and Schwinger production of electrons [63].

In this chapter, we clarify how the total rate at which a charged black hole emits a particular species of charged particle is determined by both production processes. Not only is it interesting in its own right to understand the nature of radiation in the general case, it is important in understanding how black hole decay behaves in certain

theoretically interesting limits. The weak gravity conjecture [64], for instance, which loosely speaking states that $q > m$ for some particle in the spectrum of any consistent quantum theory of gravity, is motivated in large part by arguments involving the decay of extremal black holes. We thus wish to understand precisely how black hole radiation behaves in the limit that the black hole charge, or indeed the emitted particle's charge, tends to its mass.

This chapter is divided into five sections. In Section 2, we review the energetics of charged black holes and discuss the general theory of Schwinger pair production in flat spacetime. In Section 3, we take account of both Hawking radiation and Schwinger pair production to give an exact formula for the rate at which charged black holes lose energy (or indeed some other quantity), in terms of transmission coefficients that can be calculated, at least in principle, by solving a differential equation. In Section 4 we provide approximate formulae for these transmission coefficients in terms of tunnelling integrals, as well as an interpretation of black hole decay as a two-stage tunnelling process. Finally, in Section 5, we summarise our results.

We will use the terms 'boson' and 'fermion' to mean spin-0 and spin-1/2 particles respectively; we will not consider particles of spin $s \geq 1$ in this chapter.

4.2 Preliminary theory

4.2.1 Energetics of a charged black hole

A charged non-rotating four-dimensional black hole is described by the Reissner-Nordström metric Eq. (2.4):

$$\mathrm{d}s^2 = -\left(1 - \frac{2M}{r} + \frac{Q^2}{r^2}\right)\mathrm{d}t^2 + \left(1 - \frac{2M}{r} + \frac{Q^2}{r^2}\right)^{-1}\mathrm{d}r^2 + r^2\mathrm{d}\Omega^2\,, \tag{4.1}$$

where Q is the charge of the black hole and M is its total (ADM) energy. There is an event horizon at $r_+ = M + \sqrt{M^2 - Q^2}$ and a singularity at $r = 0$. The electromagnetic potential outside the black hole is

$$A = -\frac{Q}{r}\,\mathrm{d}t\,. \tag{4.2}$$

We can consider the energy M of a charged black hole to have two contributions: one, from the mass energy stored inside the hole itself, M_{irr}, and two, from the energy stored in the electric field outside the black hole, U:

$$M_{\text{irr}} \coloneqq \frac{r_+}{2} = \frac{1}{2}M + \frac{1}{2}\sqrt{M^2 - Q^2}\,, \tag{4.3}$$

$$U \coloneqq \frac{1}{8\pi}\int E^2\,\mathrm{d}V = \frac{Q^2}{2r_+} = \frac{Q^2}{2M + 2\sqrt{M^2 - Q^2}}\,. \tag{4.4}$$

One can check that $M_{\text{irr}} + U = M$. Since the area of the black hole is a monotonic function of its irreducible mass, the classical area theorem $\mathrm{d}A \geq 0$ corresponds to

$$\mathrm{d}M_{\text{irr}} \geq 0\,. \tag{4.5}$$

In other words, we can classically extract energy only from the external field of the black hole, and never from its irreducible mass. By extracting energy in such a way that $\mathrm{d}M_{\text{irr}} = 0$, we find that the maximum energy that can be extracted from a charged black hole is U, after which point the charge is reduced to zero. The field energy U can constitute up to half of the total energy of the black hole.

If a black hole emits a particle of charge q and energy ω, the first law of black hole mechanics Eq. (2.15) reads

$$\mathrm{d}M = \frac{\kappa}{8\pi}\,\mathrm{d}A + \Phi\,\mathrm{d}Q\,, \tag{4.6}$$

$$-\omega = \frac{\sqrt{M^2 - Q^2}}{8\pi r_+^2}\,\mathrm{d}A - \frac{qQ}{r_+}\,, \tag{4.7}$$

where κ is the surface gravity and $\Phi = Q/r_+$ is the electric potential at the horizon. We see that emission is divided into two qualitatively different regimes: one, where $\omega \leq q\Phi$, which is classically allowed ($\mathrm{d}A \geq 0$), and one, $\omega > q\Phi$, which is not, ($\mathrm{d}A < 0$). In fact particles with energies greater than qQ/r_+ *can* be radiated when quantum effects are taken into consideration; this is precisely Hawking radiation.

Note that one needs to take care with this equation when the black hole is extremal, that is, when $M = Q$. Then the surface gravity vanishes and Eq. (4.7) appears to read

$$\omega = q\,. \tag{4.8}$$

That is, the black hole can only emit particles of energy q. This is false, on account that A is not a differentiable function of M, Q at $M = Q$. Informally, $\mathrm{d}A$ becomes infinite for small perturbations about extremality.

In this case, we know that ω cannot be larger than q, for this would result in a super-extremal black hole and an associated naked singularity. Considering the finite change in horizon radius $\Delta r_+ = M - \omega + \sqrt{(M-\omega)^2 - (M-q)^2} - M$, one can show that the area of the black hole increases for all $\omega < q$, provided the black hole is sufficiently heavy.

4.2.2 Hawking radiation of uncharged particles

Hawking's calculation applies to a charged black hole just as to an uncharged one. The spectrum of radiation is precisely that which one would expect from a thermodynamic black body at a temperature given by $T_{\mathrm{BH}} = \kappa/2\pi$. For a Reissner-Nordström black hole this temperature is (cf. Eq. (2.14))

$$T_{\mathrm{BH}} = \frac{\sqrt{M^2 - Q^2}}{2\pi r_+^2}\,, \tag{4.9}$$

and the total rate of energy loss is (cf. Eq. (2.81))

$$-\frac{\mathrm{d}M}{\mathrm{d}t} = \frac{g}{2\pi^2}\int_m^\infty \mathrm{d}\omega\, \frac{\omega^2 k}{\exp(\omega/T_{\mathrm{BH}}) \mp 1}\sigma(\omega)\,, \tag{4.10}$$

where g is the number of degrees of freedom of the particle and k is its momentum, $k = \sqrt{\omega^2 - m^2}$. The upper sign in the denominator corresponds to bosons and the lower sign to fermions. The rate at which the black hole loses some other quantity, such as charge, can be found by replacing one factor of ω inside the integral by the quantity of interest.

We saw in Eqs. (3.23) and (3.24) that for Hawking radiation from a Schwarzschild black hole, the greybody factor $\sigma(\omega)$ has only polynomial dependence on k in the low-energy limit, asymptoting to a constant at high energies. However, as we will find, for charged particles this greybody factor can be exponentially sensitive to ω, resulting in large suppression of radiation in parts of the emission spectrum.

In Figure 4.1 we give a crude plot of the regions in parameter space in which we expect Hawking radiation and Schwinger pair production to be important (or indeed energetically possible). In particular, we expect Hawking radiation to become important when the temperature of the black hole exceeds the mass of the particle, and the Schwinger effect to become important when the electrostatic force on the particle at the horizon exceeds its mass squared. Order one factors are ignored. See [65] for a two-dimensional slice of this diagram.

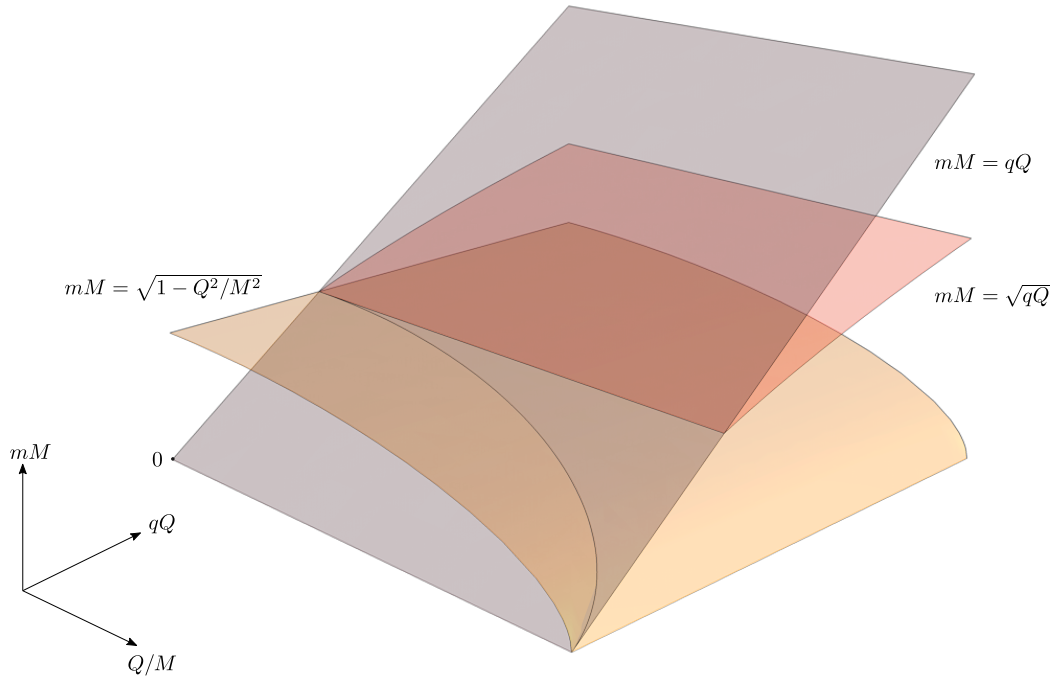

Figure 4.1: A plot of the regions in parameter space in which the two emission processes are important. On the three axes are plotted the mass of the emitted particle, the charge of the emitted particle, and the mass-to-charge ratio of the black hole. Beneath the orange surface, Hawking radiation is appreciable. Beneath the grey plane, Schwinger pair production is possible. Beneath the red surface, Schwinger pair production is appreciable. Here Q/M ranges between zero and one, whilst the other two quantities range between zero and three.

4.2.3 Schwinger production in flat spacetime

It was shown by Schwinger [44] that a static electric field configuration is quantum mechanically unstable towards decay into a pair of charged particles. We gave a quantum field theoretic derivation of this in Section 2.3.2. Energetically, the sum of the kinetic energies of the two particles must equal the change in potential energy between their positions, less the change in field energy stored in the electric field:

$$q\Delta\Phi - \Delta U = \omega_1 + \omega_2 \,. \tag{4.11}$$

In the case that the electric field remains unchanged, this puts a bound on the strength of the electric field required for the process to be energetically possible:

$$q\Delta\Phi > 2m \,. \tag{4.12}$$

To understand the rate at which this process happens, we need to examine the field equations governing the behaviour of charged matter in an electric field. We will restrict attention to 1+1 dimensions for simplicity.

In flat spacetime, the equation governing the behaviour of spin-0 charged particles in a static electric field $E(x)$ is the Klein-Gordon equation:

$$-D^\mu D_\mu \phi + m^2\phi = \left[\left(\frac{\partial}{\partial t} - iqA_t\right)^2 - \frac{\partial^2}{\partial x^2} + m^2\right]\phi = 0 \,, \tag{4.13}$$

where $\partial_x A_t = E(x)$ (so $-qA_t$ is the potential energy). For spin-1/2 particles, the relevant equation is the Dirac equation:

$$\not{D}\psi - m\psi = \left[\gamma^0\left(\frac{\partial}{\partial t} - iqA_t\right) + \gamma^1\frac{\partial}{\partial x} - m\right]\psi = 0 \,. \tag{4.14}$$

We can square this to give

$$-\not{D}\not{D}\psi + m^2\psi = \left[\left(\frac{\partial}{\partial t} - iqA_t\right)^2 - \frac{\partial^2}{\partial x^2} + m^2 + q\sigma^{\mu\nu}F_{\mu\nu}\right]\psi = 0 \,. \tag{4.15}$$

We can always choose σ^{01} to be diagonal, with diagonal elements $\pm i/2$, so that it measures spin along the x-axis. We thus find that each component ψ_i of the

fermion obeys an equation very similar to the bosonic equation, but with an additional imaginary term representing the coupling of the spin to the electric field:

$$\left[\left(\frac{\partial}{\partial t} - iqA_t\right)^2 - \frac{\partial^2}{\partial x^2} + m^2 - iq\sigma E\right]\psi_i = 0\,, \tag{4.16}$$

with $\sigma = \pm 1$. We note that for $\sigma = 0$ this reduces to Eq. (4.13). Substituting the time-dependence $\exp(-i\omega t)$ into Eq. (4.16), the system reduces to a Schrödinger-like equation, corresponding to motion in the effective potential

$$V_{\text{eff}} = m^2 - (\omega + qA_t)^2 - iq\sigma E\,. \tag{4.17}$$

We require V_{eff} to be negative at $x = \pm\infty$ for asymptotic plane wave solutions to exist. Taking $A_t(-\infty)$ to be zero by convention, we find from the energetic condition $\omega + m < q\Delta\Phi = -qA_t(\infty)$ that $\omega + qA_t$ is positive on the asymptotic left and negative on the asymptotic right. Hence there must be a point at which $\omega + qA_t = 0$, and hence $\operatorname{Re} V_{\text{eff}} = m^2 > 0$. We thus see that Eq. (4.16) describes motion in a potential with a barrier.

It was shown by Nikishov [66] that the mean number of particles produced by the field can be found by examining the scattering of plane waves off this potential barrier. In particular, if R is the reflection coefficient, the mean number of particles produced is

$$n = \pm(R - 1)\,, \tag{4.18}$$

where the upper sign refers to bosons and the lower sign to fermions. Ordinarily R would be less than unity, but we will find that for bosons it is greater than unity, ensuring n is always positive.

The quantity in Eq. (4.18) represents the amplification of a flux of particles incident on the electric field, a measure of the rate of stimulated emission. Indeed, the fact that the rate of *spontaneous* emission is dictated by the rate of stimulated emission is reminiscent of the case of emission and absorption of photons by atoms. There is a simple argument due to Einstein that these rates are related in a direct way. Here we give an analogue schematic argument.

Denote a state with a given electric field and n particle pairs by $|n\rangle$. The probability that the electric field produces another particle pair is given by $P_1 = A + nB$, where A is the coefficient of spontaneous emission and B the coefficient of stimulated emission, the probability being proportional to the number of pairs. The probability that the resulting state $|n+1\rangle$ decays back to the original configuration is dictated by a stimulated absorption rate $P_2 = (n+1)B'$. Since energy is conserved in Schwinger pair production, these two states should have the same energy, and so equal populations when in thermal equilibrium. Thus equilibrium demands of us that $P_1 = P_2$:

$$A + nB = (n+1)B' \,, \tag{4.19}$$

and for this equation to hold for any n, we must have $A = B = B'$. Hence the rate of stimulated emission is equal to that of spontaneous emission. We note that for bosons, this is equivalent to the well-known result in quantum mechanics that the probability for a system to decay to a state with n bosons is enhanced by a factor of $(n+1)$ relative to the probability to decay to a state with zero bosons. Such an argument is briefly outlined for rotating black holes in [67].

4.2.3.1 Boundary conditions: an outgoing wave

There is an important subtlety in the setup of this scattering problem. The boundary condition dictated by causality is that there are both ingoing and outgoing waves on one side of the potential barrier, with only an outgoing wave on the other side.

However, what is the nature of an outgoing wave on the right-hand side (say) of the potential barrier? It is tempting to say that the solution at infinity should go as $\exp(ikx)$, as opposed to $\exp(-ikx)$. That is, would we write $\phi_L = \tilde{A}\exp(ikx) + \tilde{B}\exp(-ikx)$ and $\phi_R = \tilde{C}\exp(ikx)$. This represents a positive flux towards the right, but is not correct. The reason is that the particle on the right has energy $\omega + qA_t(\infty)$, which is *negative*. For the particle to be moving in the positive direction, its group velocity must be positive. With negative energy, it is hence also necessary that the particle have negative momentum, and so the correct boundary condition to impose is that the wave on the right has the form $\exp(-ikx)$. In the above and the following,

any momenta denoted by k are *implicitly positive*. This argument applies equally to bosons and fermions.

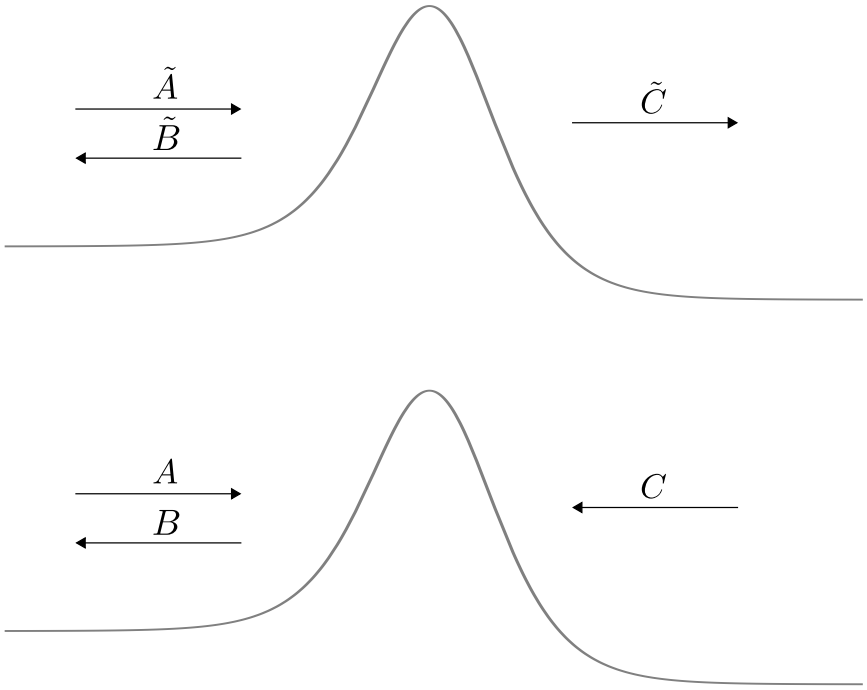

Figure 4.2: The naive (upper) and physical (lower) setup of fluxes.

We'll define the transmission T and reflection R coefficients by

$$T = |C/A|^2 \,, \tag{4.20}$$

$$R = |B/A|^2 \,, \tag{4.21}$$

and denote their naive counterparts with a tilde. We make the observation that the physical setup of fluxes is simply the time-reversal of the naive setup, provided we exchange the ingoing and reflected waves. This allows us to relate

$$\tilde{R} = \frac{1}{R} \,. \tag{4.22}$$

It will transpire that with the physical setup of fluxes, the reflection coefficient will be greater than unity for bosons, and less than unity for fermions (as we might expect from the Pauli exclusion principle). With the naive setup, the reflection coefficient

is instead greater than unity for fermions — this is the result known as the Klein paradox. The resolution of the 'paradox' lies in the very fact that particle-antiparticle pairs can be produced by the electric field [68], but we make pains to note that, despite the original formulation of the paradox, it is in fact *bosons* which are amplified upon incidence with a strong electric field, not fermions.

4.2.3.2 Flux conservation

To relate the reflection and transmission coefficients for the above problem, we need to understand the relevant flux conservation equations. For bosons, there is an obvious conserved current,

$$J_b(\phi) = i\phi\partial_x\phi^* - i\phi^*\partial_x\phi\,, \tag{4.23}$$

which is conserved in the sense that $\partial_x J_b = 0$. For the naive boundary conditions described above, this gives the conservation law

$$k_L|\tilde{A}|^2 - k_L|\tilde{B}|^2 = k_R|\tilde{C}|^2\,. \tag{4.24}$$

For fermions, the fact that the effective potential in Eq. (4.16) is complex means this quantity is not conserved. In this case, we must instead use the conservation of the underlying Dirac current

$$J_f(\psi) = \bar{\psi}\gamma^1\psi\,. \tag{4.25}$$

In the asymptotic regions $x = \pm\infty$, the solutions to the Dirac equation are plane waves. Writing $\Omega = \omega + qA_t$, and labelling the components of ψ by ψ_i, we have

$$J_f(\psi) \propto \frac{1}{\Omega}\sum_i J_b(\psi_i)\,. \tag{4.26}$$

Since Ω is negative on the asymptotic right, we see that though a particle on the left with spatial dependence $\exp(ikx)$ corresponds to positive flux, a particle on the right with spatial dependence $\exp(ikx)$ corresponds to negative flux. For the naive boundary conditions, this conservation law becomes

$$\frac{k_L}{\Omega_L}|\tilde{A}|^2 - \frac{k_L}{\Omega_L}|\tilde{B}|^2 = \frac{k_R}{\Omega_R}|\tilde{C}|^2\,, \tag{4.27}$$

where we note the term on the right-hand side is negative. In the simplest case that $k_L = k_R$, the two naive conservation equations Eqs. (4.24) and (4.27) reduce to

$$|\tilde{A}|^2 - |\tilde{B}|^2 = |\tilde{C}|^2 \,, \tag{4.28}$$

$$|\tilde{A}|^2 - |\tilde{B}|^2 = -|\tilde{C}|^2 \,. \tag{4.29}$$

In terms of the physical setup of fluxes, the right-hand sides of Eqs. (4.24) and (4.27) obtain an additional minus sign. Dividing through by $|A|^2$, the physical conservation laws can be written:

$$KT \coloneqq \frac{k_R}{k_L} T = R - 1 \qquad \text{bosons} \,, \tag{4.30}$$

$$KT \coloneqq \left| \frac{k_R \Omega_L}{k_L \Omega_R} \right| T = 1 - R \qquad \text{fermions} \,, \tag{4.31}$$

where we denote by K the positive prefactors involving ratios of momenta. We can relate the naive and physical transmission coefficients using the relation $\tilde{R} = 1/R$:

$$T = \frac{\tilde{T}}{1 - K\tilde{T}} \qquad \text{bosons} \,, \tag{4.32}$$

$$T = \frac{\tilde{T}}{1 + K\tilde{T}} \qquad \text{fermions} \,. \tag{4.33}$$

From here we find that the mean number n of particles produced in the mode ω, given by $n = \pm(R - 1) = KT$, is

$$n_b = \frac{K\tilde{T}}{1 - K\tilde{T}} \qquad \text{bosons} \,, \tag{4.34}$$

$$n_f = \frac{K\tilde{T}}{1 + K\tilde{T}} \qquad \text{fermions} \,. \tag{4.35}$$

4.2.3.3 A point particle perspective

In [69] and [62] an alternative argument is given for the relation between the two transmission probabilities above. An equivalent argument is also given in more detail in [70]. The idea is that $K\tilde{T} = P$ corresponds to the *relative* probability of producing a single particle pair, in the sense that the probability of producing a state with n pairs is the product of P and the probability of producing a state with $n - 1$ pairs. Denoting by N the probability of producing no particles, we can fix N by demanding

that the sum of all probabilities is unity. For bosons, an arbitrary number of particles can be produced, and so

$$N(1 + P + P^2 + \cdots) = 1 \qquad \Longrightarrow \qquad N = 1 - P\,. \tag{4.36}$$

We can then straightforwardly compute the expected number of particles produced:

$$n_b = N(P + 2P^2 + 3P^3 + \cdots) = \frac{NP}{(1-P)^2} = \frac{P}{1-P}\,. \tag{4.37}$$

For fermions, the argument is similar. The probability of producing no particles is N, and of producing one particle is NP. Producing two or more particles is forbidden. For the probabilities to add to unity, we hence need

$$N = \frac{1}{1+P}\,. \tag{4.38}$$

The expected number of particles produced is then simply

$$n_f = NP = \frac{P}{1+P}\,. \tag{4.39}$$

We see that Eqs. (4.37) and (4.39) are precisely the relations from the previous subsection between $\tilde{T}$ and T.

4.3 Total rate of radiation

The phenomenon whereby particles incident on an electric field can have amplified reflected flux applies equally to the electric field outside a black hole. In this context, the amplification is known as *superradiance*. See [71] for further discussion. Just as in the flat spacetime case, this gives rise to the possibility of spontaneous production of charged particle pairs outside the horizon, in addition to the thermal production of those same particles. In this section, we give formulae for the total rate of emission from a black hole, accounting for both of these processes.

We can rewrite the greybody factor in the Hawking formula Eq. (4.10) in terms of the reflection coefficient for waves incident on the black hole as in Eq. (3.21):

$$\sigma(\omega) = \frac{\pi}{k^2}\sum_{\ell}(2\ell+1)(1-R_\ell)\,. \tag{4.40}$$

We see that the Hawking radiation formula Eq. (4.10) contains this same $(1-R)$ factor that determines the Schwinger pair production rate Eq. (4.18). This amplification factor can be attributed to the transmission of the wave out through the resulting electric field, corresponding to the Schwinger process.

As well as altering the nature of the reflection coefficient R, the presence of an electric field also modifies the thermal factors appearing in Eq. (4.10). The exact rate of radiation from a black hole is thus

$$-\frac{\mathrm{d}M}{\mathrm{d}t} = \frac{g}{2\pi^2}\int_m^\infty \mathrm{d}\omega\, \frac{\omega^2 k\sigma(\omega)}{\exp((\omega-q\Phi)/T_{\mathrm{BH}})\pm 1}\,. \tag{4.41}$$

We can then trade the reflection coefficients R_ℓ appearing in Eq. (4.40) for transmission coefficients using Eqs. (4.30) and (4.31):

$$\sigma(\omega) = (\omega-q\Phi)\frac{\pi}{k^3}\sum_\ell (2\ell+1)T_\ell \qquad \text{bosons}\,, \tag{4.42}$$

$$\sigma(\omega) = \frac{\pi\omega}{k^3}\sum_j (2j+1)T_j \qquad \text{fermions}\,. \tag{4.43}$$

Substituting these results into Eq. (4.41), we find that the exact rate that a black hole loses energy through emission of charged bosons is

$$-\frac{\mathrm{d}M}{\mathrm{d}t} = \frac{g}{2\pi}\sum_\ell (2\ell+1)\int_m^\infty \mathrm{d}\omega\, \frac{\omega^2}{k^2}(\omega-q\Phi)\frac{T_\ell}{\exp((\omega-q\Phi)/T_{\mathrm{BH}})-1}\,. \tag{4.44}$$

Expressed in terms of the transmission factor, we can resolve a possible objection with Eq. (4.41). Note that although the denominator in the Bose-Einstein distribution gives rise to a simple pole at $\omega = q\Phi$, this is cancelled by the factor $(\omega - q\Phi)$ coming from the flux conservation equation. When the black hole is extremal, this factor will ensure that the rate of radiation at $\omega = q\Phi$ is zero, in contrast to the claims of [63], which suggests that energies close to $q\Phi$ dominate the total emission integral on account that T_ℓ is largest there. Likewise, this extra flux factor ensures the integrand is everywhere positive. For fermions, the exact rate of emission is

$$-\frac{\mathrm{d}M}{\mathrm{d}t} = \frac{g}{2\pi}\sum_j (2j+1)\int_m^\infty \mathrm{d}\omega\, \frac{\omega^3}{k^2}\frac{T_j}{\exp((\omega-q\Phi)/T_{\mathrm{BH}})+1}\,. \tag{4.45}$$

We note that at zero temperature, the exponential factors becomes step functions that are zero for $\omega > q\Phi$, and the resulting expressions are precisely those one expects for

radiation occurring solely due to the Schwinger mechanism:

$$-\frac{\mathrm{d}M}{\mathrm{d}t} = \frac{g}{2\pi}\sum_{\ell}(2\ell+1)\int_{m}^{q\Phi}\mathrm{d}\omega\,\frac{\omega^2}{k^2}(q\Phi-\omega)T_\ell \qquad \text{bosons}\,, \tag{4.46}$$

$$-\frac{\mathrm{d}M}{\mathrm{d}t} = \frac{g}{2\pi}\sum_{j}(2j+1)\int_{m}^{q\Phi}\mathrm{d}\omega\,\frac{\omega^3}{k^2}T_j \qquad \text{fermions}\,. \tag{4.47}$$

These formulae are simply the black hole analogues of Eq. (4.18), correctly accounting for the phase-space and flux factors.

In Section 4.4.4 we will justify the formulae Eqs. (4.44) and (4.45) as arising from a combined process of tunnelling through both the horizon and the electric field. In the rest of this section, we describe how to calculate this transmission coefficient, firstly by setting up the relevant differential equation, and then by defining the appropriate boundary conditions.

4.3.1 The boson equation

The equation governing a charged bosonic particle in this background is the Klein-Gordon equation:

$$-D^\mu D_\mu\phi + m^2\phi = 0\,. \tag{4.48}$$

Taking our field ϕ to have time-dependence $\exp(-i\omega t)$ and angular-dependence that of spherical harmonics, this becomes

$$-\frac{f}{r^2}\frac{\mathrm{d}}{\mathrm{d}r}\left(r^2 f\frac{\mathrm{d}}{\mathrm{d}r}\right)\phi + f\left(m^2+\frac{\ell(\ell+1)}{r^2}\right)\phi - \left(\omega-\frac{qQ}{r}\right)^2\phi = 0\,. \tag{4.49}$$

To simplify this equation, we define a tortoise coordinate r_* by

$$\frac{\mathrm{d}r_*}{\mathrm{d}r} = 1/f\,, \tag{4.50}$$

and rescale our field (cf. Section 3.4.2)

$$\Psi = r\phi\,. \tag{4.51}$$

In terms of these new quantities, our equation becomes

$$-\frac{\mathrm{d}^2\Psi}{\mathrm{d}r_*^2} + \left(1-\frac{2M}{r}+\frac{Q^2}{r^2}\right)\left(m^2+\frac{\ell(\ell+1)}{r^2}+\frac{2M}{r^3}-\frac{2Q^2}{r^4}\right)\Psi - \left(\omega-\frac{qQ}{r}\right)^2\Psi = 0\,. \tag{4.52}$$

We have reduced the Klein-Gordon equation to a simple ODE — indeed, as in Eq. (4.16), this is a Schrödinger-like equation, with an effective potential that has two pieces; one due to the gravitational field, and one due to the electromagnetic field. We plot the form of this potential for a typical choice of the various parameters in Figure 4.3 in Section 4.4.2.

4.3.2 The fermion equation

The equation governing a charged fermion in this background is the Dirac equation:

$$\not{D}\psi = \gamma^\mu(\nabla_\mu - iqA_\mu)\psi = \gamma^\mu(\partial_\mu + \Omega_\mu - iqA_\mu)\psi = m\psi\,, \tag{4.53}$$

where Ω_μ is the spin-connection. As in Eq. (4.15), we can diagonalise this equation in spinor space by squaring it — we discuss this in detail in Appendix 4.A. Note that the equations governing the behaviour of spin-1/2 particles in a black hole background were analysed in detail by Teukolsky [72]. However, these apply to massless particles, which is not appropriate for our purposes, and also make use of the Newman-Penrose formalism [73], which is more machinery than is necessary for analysing our spherically symmetric problem. After appropriate manipulations and field redefinitions, the Dirac equation can also be cast in the form of a Schrödinger-like equation, where each component satisfies

$$\begin{aligned} -\frac{\mathrm{d}^2\Psi}{\mathrm{d}r_*^2} + \left(1 - \frac{2M}{r} + \frac{Q^2}{r^2}\right)\left(m^2 + \frac{(j+1/2)^2}{r^2} - i\sigma\frac{qQ}{r^2}\right)\Psi \\ - \left(\omega - \frac{qQ}{r}\right)^2\Psi + \left(\frac{M}{r^2} - \frac{Q^2}{r^3}\right)\left(\frac{\mathrm{d}}{\mathrm{d}r_*} + i\sigma\left(\omega - \frac{qQ}{r}\right)\right)\Psi = 0\,, \end{aligned} \tag{4.54}$$

with $\sigma = \pm 1$ denoting the sign of the spin of the fermion and j, the total angular momentum quantum number, taking on the values $j = k + 1/2$ for any non-negative integer k.

4.3.3 Boundary conditions: ingoing at the horizon

As we discussed in Section 3.4, the appropriate boundary condition to impose in solving the transmission problem is that the wave is purely ingoing at the black hole

horizon. However, we also saw in Section 4.2.3.1 that there were some subtleties in defining the direction of a wave when an electric potential is present. In this section we explicitly clarify the nature of the boundary conditions.

The field equation for both bosons and fermions at the horizon is simply[1]

$$-\frac{\mathrm{d}^2\Psi}{\mathrm{d}r_*^2} = (\omega - qQ/r_+)^2\Psi\,. \tag{4.55}$$

The general solution there is given by

$$\Psi = C\exp(-i\Omega r_*) + D\exp(i\Omega r_*)\,, \tag{4.56}$$

where $\Omega = \omega - qQ/r_+$. When Ω is positive, and the emission corresponds purely to Hawking radiation, there is no difficulty: an ingoing wave corresponds to one with $D = 0$. On the other hand, when $\Omega < 0$, it is the second term which represents a wave with ingoing momentum, and so we might be tempted to claim that $C = 0$ is the appropriate boundary condition.

However, as argued in Section 4.2.3.1, we must take care to note that since the energy of the wave is also negative, a negative momentum would give rise to a positive group velocity, i.e., an outgoing wave. The correct physical boundary condition is hence a wave with outgoing momentum. Thus, irrespective of the value of ω relative to $q\Phi$, the correct boundary condition to impose is that, at the horizon,

$$\Psi = C\exp(-i\Omega r_*)\,. \tag{4.57}$$

At infinity, both field equations reduce to

$$-\frac{\mathrm{d}^2\Psi}{\mathrm{d}r_*^2} = (\omega^2 - m^2)\Psi = k^2\Psi\,, \tag{4.58}$$

with general solution

$$\Psi = A\exp(-ikr_*) + B\exp(ikr_*)\,. \tag{4.59}$$

The transmission coefficient T is then defined simply by $|C/A|^2$ for bosons, and for fermions by $\sum_i |C_i|^2 / \sum_i |A_i|^2$, where the index labels the spinor component.

[1]This is not obvious from the fermion equation Eq. (4.54), but can be seen by returning to the first-order Dirac equation. See Eq. (4.101) in Appendix 4.A.

4.4 Radiation as tunnelling

In this section we discuss how the emission of charged particles from charged black holes can be viewed as a tunnelling process, whereby the particle tunnels both through the horizon of the black hole (corresponding to Hawking radiation) and the electric field outside it (corresponding to Schwinger pair production). In Section 2.4.3 we presented a picture of tunnelling of uncharged particles through the horizon in Schwarzschild spacetime. We here present an analogous derivation for charged particles moving in the background of a Reissner-Nordström black hole.

4.4.1 Tunnelling through the horizon

In Painlevé-Gullstrand coordinates, defined for a charged black hole by $\mathrm{d}t_* = \mathrm{d}t + \sqrt{1-f}/f\,\mathrm{d}r$, the metric takes the form

$$\mathrm{d}s^2 = -\left(1 - \frac{2M}{r} + \frac{Q^2}{r^2}\right)\mathrm{d}t_*^2 + 2\sqrt{\frac{2M}{r} - \frac{Q^2}{r^2}}\,\mathrm{d}t_*\,\mathrm{d}r + \mathrm{d}r^2\,. \tag{4.60}$$

The equations of motion analogous to Eq. (2.72) and Eq. (2.73) are

$$g^{\mu\nu}p_\mu p_\nu = -m^2\,, \tag{4.61}$$

$$P_{t_*} \coloneqq p_{t_*} + qA_{t_*} = -\omega\,, \tag{4.62}$$

where p_μ is defined as in Eq. (2.69). We can eliminate p_{t_*} from these equations to determine an expression for p_r (assuming purely radial motion as before):

$$p_r = \frac{1}{f}\sqrt{1-f}(\omega + qA_{t_*}) + \frac{1}{f}\sqrt{(\omega + qA_{t_*})^2 - fm^2}\,. \tag{4.63}$$

Since the action for a charged particle involves the canonical momentum P_μ, and hence the gauge potential, we need to understand the behaviour of this potential at the horizon. In the usual coordinates, $A = -Q/r\,\mathrm{d}t$. Unlike the metric, however, this is legitimately singular at the horizon, on account that the form $\mathrm{d}t$ is singular there but the prefactor $-Q/r$ is well-behaved. This is not a problem however, but merely an indication that we are working in a singular gauge. We can perform a singular gauge transformation that makes A smooth everywhere (for $r > 0$) — for instance,

choosing the gauge function to be precisely the difference between the coordinates t_* and t, we find

$$A = -\frac{Q}{r}\,\mathrm{d}t_*\,. \tag{4.64}$$

Since A is now well-defined and real everywhere, it doesn't contribute an imaginary part to the tunnelling action. We need only worry about the contribution of p_r. Thus

$$\mathrm{Im}\,S = \mathrm{Im}\int P_\mu \mathrm{d}x^\mu = \mathrm{Im}\int p_\mu \mathrm{d}x^\mu = 2\pi\,\mathrm{Res}\left(\frac{1}{f}\right)(\omega - qQ/r_+)\;, \tag{4.65}$$

where Res indicates the residue of the pole at $r = r_+$. We thus have a tunnelling probability of the form

$$\exp(-2\,\mathrm{Im}\,S) = \exp(-(\omega - q\Phi)/T_{\mathrm{BH}})\,, \tag{4.66}$$

where T_{BH} is precisely the temperature in Eq. (4.9):

$$1/T_{\mathrm{BH}} = 4\pi\,\mathrm{Res}\left(\frac{1}{f}\right) \quad\Longrightarrow\quad T_{\mathrm{BH}} = \frac{\sqrt{M^2 - Q^2}}{2\pi r_+^2}\,. \tag{4.67}$$

The factor in Eq. (4.66) is precisely the Boltzmann factor for a particle with energy ω in an electric potential Φ.

To determine the mean number of particles produced as a result of this tunnelling process, we can use the arguments of Section 4.2.3.3 that relate tunnelling probabilities to the expected number of particles produced:

$$n_b = \frac{P}{1-P} \qquad \text{bosons}\,, \tag{4.68}$$

$$n_f = \frac{P}{1+P} \qquad \text{fermions}\,. \tag{4.69}$$

Treating the quantity $\exp(-2\,\mathrm{Im}\,S)$ as the relative probability P of producing a particle outside the horizon, the expected number of particles produced is

$$n_b = \frac{1}{\exp((\omega - q\Phi)/T_{\mathrm{BH}}) - 1} \qquad \text{bosons}\,, \tag{4.70}$$

$$n_f = \frac{1}{\exp((\omega - q\Phi)/T_{\mathrm{BH}}) + 1} \qquad \text{fermions}\,. \tag{4.71}$$

These are none other than the usual Bose-Einstein and Fermi-Dirac distributions.

4.4.2 Tunnelling through the electric field

We have already established that the mean number of particles emitted by the black hole depends on the transmission coefficient T for fields with ingoing boundary conditions at the horizon. In general, determining this transmission coefficient requires us to numerically solve the field equations discussed in Section 4.3 (see, for example, [74]). However, we can find approximate expressions for T using the WKB method. A similar analysis was performed in [75] and [76] for the flat spacetime case. See also [62] for a discussion in the context of black holes.

To the lowest level of approximation, the WKB method implies

$$K\tilde{T} = \exp(-2S)\,, \tag{4.72}$$

where S is a tunnelling integral defined explicitly below. In fact, as shown in [77], a more accurate form of the transmission coefficient is given by

$$K\tilde{T} = \frac{1}{\exp(2S) \pm 1}\,, \tag{4.73}$$

where the upper sign refers to bosons and the lower sign to fermions, and where the result applies to the naive transmission problem. Though the WKB analysis only applies when S is large, and though these two expressions agree to first order in $\exp(-2S)$, the second expression is useful because it happens to coincide with the *exact* form of the transmission probability in the flat space constant-field case — this occurs because the relevant field equation reduces to the Schrödinger equation for a particle moving in an (inverted) harmonic oscillator, a system for which higher-order WKB corrections vanish.

Combining this more exact formula with the relations between the naive and correct forms of the transmission coefficient Eqs. (4.32) and (4.33), we find that the WKB approximation gives us the deceptively simple

$$KT = \exp(-2S)\,, \tag{4.74}$$

for both bosons and fermions. The tunnelling integrals are

$$S = \int \sqrt{\left(1 - \frac{2M}{r} + \frac{Q^2}{r^2}\right)\left(m^2 + \frac{\ell(\ell+1)}{r^2} + \frac{2M}{r^3} - \frac{2Q^2}{r^4}\right) - \left(\omega - \frac{qQ}{r}\right)^2}\, \mathrm{d}r_* \,, \tag{4.75}$$

for bosons and

$$S = \int \sqrt{\left(1 - \frac{2M}{r} + \frac{Q^2}{r^2}\right)\left(m^2 + \frac{(j+1/2)^2}{r^2}\right) - \left(\omega - \frac{qQ}{r}\right)^2}\, \mathrm{d}r_* \,, \tag{4.76}$$

for fermions[2]. In Figure 4.3 we plot the effective potential appearing underneath the square root in these equations, in the large m limit.

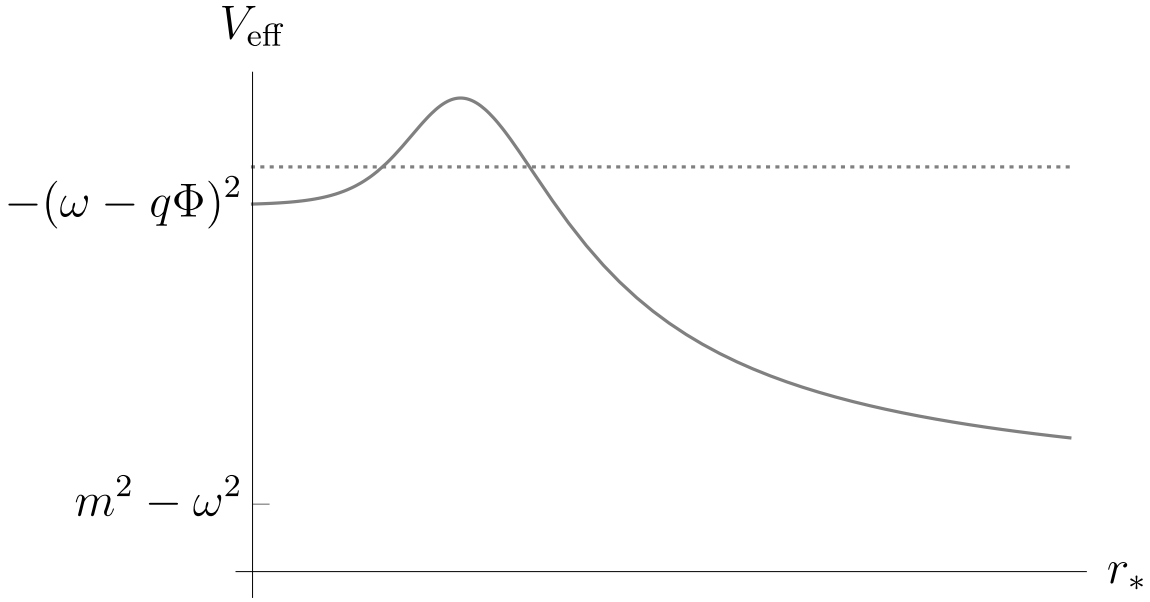

Figure 4.3: The tunnelling barrier, as defined by the function under the square root in Eq. (4.77), for an illustrative choice of ω. The dotted line represents the zero of energy — tunnelling occurs through the region in which the potential lies above this line. The barrier asymptotes to $-k^2 = m^2 - \omega^2$.

We note that Eq. (4.74) is not applicable when the particle momentum is in any region of space small — in particular, it does not apply as $\omega \to q\Phi$. In that limit, $KT \to 0$ for bosons on account that the momentum factor $(\omega - q\Phi)$ appearing in K goes to zero there.

[2]We refer to Appendix 4.A for a derivation of this result.

4.4.3 The large m limit: particles

The tunnelling integrals discussed above are difficult to evaluate in general. However, they simplify greatly in the limit that the Compton wavelength of the particle is much less than the radius of the black hole, $mM \gg 1$. In this case, the tunnelling integral reduces both for fermions and bosons to

$$S = \int \sqrt{\left(1 - \frac{2M}{r} + \frac{Q^2}{r^2}\right) m^2 - \left(\omega - \frac{qQ}{r}\right)^2}\, \mathrm{d}r_* \,. \tag{4.77}$$

In the limit that the black hole is much larger than the wavelength of the particle, we expect to be able to understand the emission from a point particle perspective, without reference to field equations. Indeed, we note that a radially moving relativistic point particle in our black hole background has dispersion relation

$$g^{\mu\nu} p_\mu p_\nu = -m^2 \quad \Longrightarrow \quad \frac{1}{f}\left(\omega - \frac{qQ}{r}\right)^2 - f p_r^2 = m^2 \,. \tag{4.78}$$

The radial momentum p_r is hence imaginary between the two radii r_1, r_2 determined by solving Eq. (4.78) with $p_r = 0$. The action for a particle moving from the horizon to infinity thus acquires an imaginary part given by

$$\mathrm{Im}\, S = \int_{r_1}^{r_2} |p_r(r)|\, \mathrm{d}r = \int_{r_1}^{r_2} \sqrt{\left(1 - \frac{2M}{r} + \frac{Q^2}{r^2}\right) m^2 - \left(\omega - \frac{qQ}{r}\right)^2}\, \mathrm{d}r_* \,. \tag{4.79}$$

This is precisely the integral in Eq. (4.77). We plot in Figure 4.4 the two radii r_1, r_2 for different choices of energy ω. The two energies $\omega = qQ/r \pm m\sqrt{f}$ which solve Eq. (4.78) with $p_r = 0$ can be thought of as the edges of 'positive' and 'negative' energy bands in a traditional Dirac sea picture. The process of tunnelling from the filled lower band out to the other band, producing a particle and a corresponding hole, coincides with the usual physical picture of Schwinger pair production.

The integral Eq. (4.77) was analysed in [63] for $\omega < qQ/r_+$. It is given by

$$\mathrm{Im}\, S = \frac{\pi m^2}{k(k+\omega)} \left(qQ - (\omega - k)M\right) \,, \tag{4.80}$$

where $k = \sqrt{\omega^2 - m^2}$. We can see from Figure 4.4, however, that there is also a region of imaginary radial momentum for some energies $\omega > qQ/r_+$. This tunnelling barrier

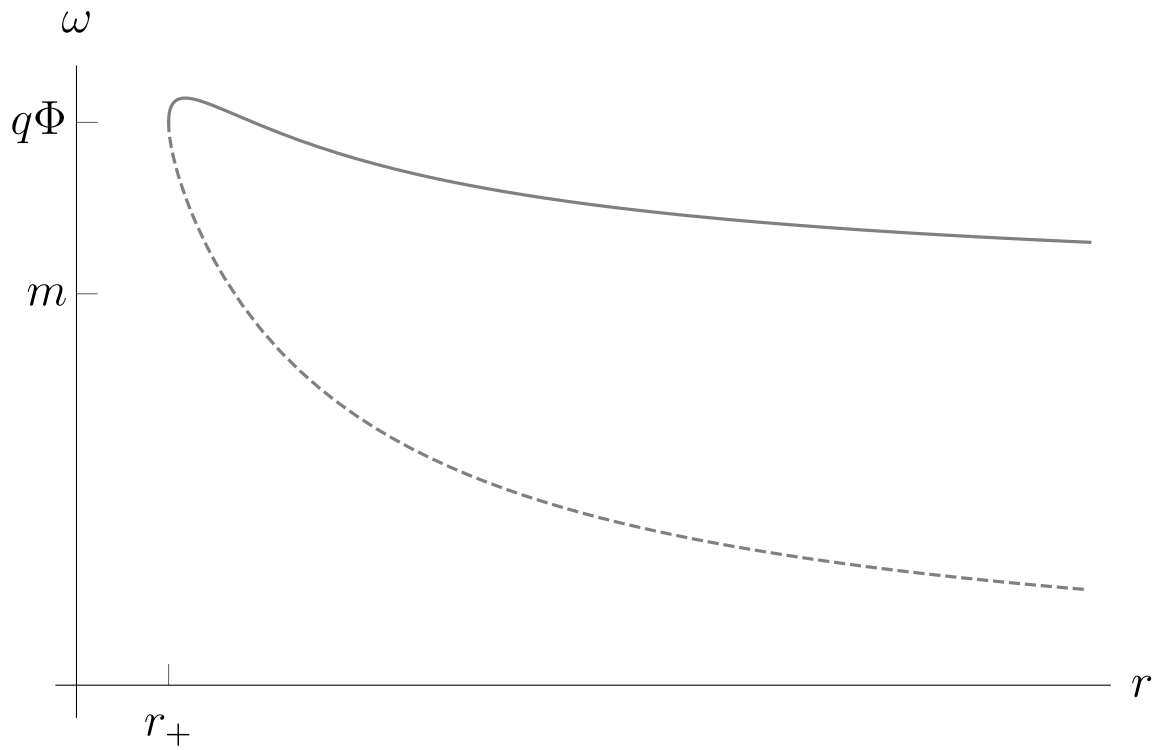

Figure 4.4: The region in the ω–r plane in which there exists a tunnelling barrier, in the large m limit. The dotted line corresponds to energies less than $q\Phi$ — in this regime, there is always a barrier to emission. For a small range of energies greater than $q\Phi$, however, there also exists a barrier to tunnelling.

would be unimportant if the only emission process were Schwinger pair production, since particles with energies greater than qQ/r_+ would not be emitted. However, Hawking emission is of course possible for particles with energy greater than qQ/r_+, and the rate of such emission will hence be suppressed by an additional tunnelling exponential. We find that the maximum energy for which a barrier exists is

$$\omega_{\max} = m^2\sqrt{\frac{M^2-Q^2}{Q^2(q^2-m^2)}} + \frac{q}{Q}\frac{q^2Q^2-m^2M^2}{M(q^2-m^2)+q\sqrt{(q^2-m^2)(M^2-Q^2)}}\,, \tag{4.81}$$

and that the radii r_1, r_2 coincide at the value

$$r_{\max} = M\frac{\alpha^2-Q^2}{\alpha^2-M^2} + \alpha\sqrt{M^2-Q^2}\,\frac{\sqrt{\alpha^2-Q^2}}{\alpha^2-M^2}\,, \tag{4.82}$$

where $\alpha = qQ/m$. For particles with energies in the range $qQ/r_+ < \omega < \omega_{\max}$, the

tunnelling integral is given by

$$\mathrm{Im}\, S/\pi = \frac{\omega q Q - 2\omega^2 M + m^2 M}{k} + \frac{qMQ + \omega Q^2 - 2\omega M^2}{\sqrt{M^2 - Q^2}}\,. \tag{4.83}$$

We emphasise the qualitative result that, at least in the point-particle limit, there will be an additional exponential suppression of radiation with energy less than $\omega_{\max}$, as compared to the spectrum predicted by the thermal distributions.

4.4.4 A combined tunnelling process

We have so far seen how both the thermal distribution factors and the transmission coefficients appearing in Eqs. (4.44) and (4.45) can be calculated by treating emission as a tunnelling process. In this final section, we use the reasoning of Section 4.2.3.3 to provide an interpretation of the total emission rate, which involves the product of these two factors, as a combined process of tunnelling, through the horizon and subsequently the electric field.

We view emission as a two-stage process. Firstly, the particle tunnels through the horizon. For particles with $\omega > q\Phi$, the resultant particle is real (in that it has positive energy at the horizon) and can escape to infinity. For particles with negative energy at the horizon, we can view this tunnelling process as readjusting the particle numbers in the Dirac sea outside the horizon. Particles in this Dirac sea can then tunnel through the electric field to infinity. We will frame the analysis in terms of density matrices for notational ease, although these need only be thought of as describing probability distributions.

For fermions this picture is clearer. The tunnelling action $P_H = \exp(-(\omega - q\Phi)/T_{\mathrm{BH}})$ describes the probability of producing one particle in the Dirac sea *relative* to producing none. Denoting particles in the Dirac sea with a bar, this yields the density matrix (the subscript h standing for horizon)

$$\rho_h = N_H|\bar{0}\rangle\langle\bar{0}| + N_H P_H|\bar{1}\rangle\langle\bar{1}|\,, \tag{4.84}$$

where $N_H = 1/(1 + P_H)$ ensures the probabilities sum to unity. Only the state in which there is a particle in the Dirac sea can tunnel to become a real particle at

infinity. As before, the relative probability of this process is $P_S = K\tilde{T}$. Hence the density matrix at infinity is

$$\rho_\infty = N_H|\bar{0}\rangle\langle\bar{0}| + N_H P_H N_S|\bar{1}\rangle\langle\bar{1}| + N_H P_H N_S P_S|1\rangle\langle 1|\,, \tag{4.85}$$

where $N_S = 1/(1+P_S)$. The mean number of particles detected is then simply

$$n_f = \mathrm{tr}(n\rho_\infty) = N_H N_S P_H P_S = \frac{1}{1+\exp((\omega - q\Phi)/T_{\mathrm{BH}})}\frac{K\tilde{T}}{1+K\tilde{T}}\,, \tag{4.86}$$

where n is the number operator that counts particles at infinity. This is precisely the factor appearing in Eq. (4.45).

For bosons, the picture is somewhat murkier, on account that there is no simple description of the bosonic vacuum in terms of a Dirac sea of negative energy particles. However, such interpretations have been proposed, as in [78], for instance. In such a picture, the negative energy bosonic states can contain any *negative* number of particles, with the vacuum corresponding to the state with negative one particles per mode. Denoting a state with $-n$ particles by $|\bar{n}\rangle$, for continuity with the fermionic notation, we can view the process of tunnelling through the horizon as repopulating these negative energy states thus:

$$\rho_h = N_H\Big(|\bar{1}\rangle\langle\bar{1}| + \frac{1}{P_H}|\bar{2}\rangle\langle\bar{2}| + \frac{1}{P_H^2}|\bar{3}\rangle\langle\bar{3}| + \cdots\Big)\,, \tag{4.87}$$

where $N_H = 1 - 1/P_H$. When thermal effects are absent, the system is described by the vacuum state $|\bar{1}\rangle$, and this state can lead to production of an arbitrary number of charged particles at infinity. In particular, the probability for n particles to be produced is given by a geometric distribution with relative probability P_S:

$$|\bar{1}\rangle\langle\bar{1}| \to N_S\Big(|0\rangle\langle 0| + P_S|1\rangle\langle 1| + P_S^2|2\rangle\langle 2| + \cdots\Big)\,, \tag{4.88}$$

where $N_S = 1 - P_S$. We next ask what the resulting state at infinity is for the doubly-occupied state $|\bar{2}\rangle$, after tunnelling through the electric field. If each 'particle' in this state is independent of the other, we expect the resulting probability distribution to be the sum of two independent geometric distributions with the same mean.

Likewise, we expect the state $|\bar{n}\rangle$ to tunnel to a state described by n independent geometric distributions. The sum of independent and identical geometric distributions is described by the negative binomial distribution. In particular, we have

$$|\bar{n}\rangle\langle\bar{n}| \to (1-P_S)^n \sum_{k=0}^{\infty} \binom{n+k-1}{k} P_S^k \, |k\rangle\langle k| \,. \tag{4.89}$$

Combining this tunnelling process with the horizon tunnelling process in Eq. (4.87) gives the density matrix at infinity in the bosonic case:

$$\rho_\infty = N_H \sum_{n=1}^{\infty} P_H^{1-n} (1-P_S)^n \sum_{k=0}^{\infty} \binom{n+k-1}{k} P_S^k \, |k\rangle\langle k| \,. \tag{4.90}$$

From here, as before, we can calculate the expected number of particles detected at infinity. One finds

$$n_b = \mathrm{tr}(n\rho_\infty) = \frac{1}{1-\exp((\omega - q\Phi)/T_{\mathrm{BH}})} \frac{K\tilde{T}}{1-K\tilde{T}} \,, \tag{4.91}$$

which is precisely the factor appearing in Eq. (4.44).

The probability distribution given in Eq. (4.90) thus reproduces the mean number of particles produced by the black hole. We note, however, that this picture of tunnelling also provides distinct predictions for the variance, skewness and higher moments of the distribution of number of particles produced.

4.5 Discussion

We have given exact formulae for the rate of emission of charged particles from charged black holes, taking care to define the differential equations that govern this process, the appropriate boundary conditions for those differential equations, and to specify precisely the phase-space and flux factors appropriate to massive particles for which $\omega \neq k$. Concrete expressions for the transmission coefficients have been given in the point-particle limit, and in particular we have found that for particles with energy below ω_{max}, given in Eq. (4.81), emission rates from black holes will be exponentially suppressed relative to energies above it. In addition to justifying the formulae for the average number of particles received at infinity, we have also given the expected

probability distribution for the number of these particles, in a given mode. This provides new predictions for, e.g., the uncertainty in the number of particles received.

We have restricted attention to non-rotating black holes in this work. We note, however, that rotating black holes have many similar properties to charged black holes — in particular, there is a region of energies for which flux directed onto the black hole is reflected with larger amplitude, as alluded to in Section 1.1. In terms of point particles, this process goes by the name of the Penrose process [79]. Quantum mechanically, we thus expect a rotating black hole to spontaneously emit spinning particles (in such a way as to reduce its angular momentum), although it is not clear what the appropriate flat spacetime analogue of this process would be. It would be interesting in future work to examine how such spontaneous emission could also be viewed as a tunnelling process, this time through a vacuum spacetime, but one with a more non-trivial gravitational field structure.

It is known that any black hole in nature with appreciable charge will very quickly neutralise by accreting oppositely charged species onto it [65]. A theoretical understanding of charged black hole emission is thus not directly relevant to astrophysics or cosmology. In the following chapter we thus consider black holes whose evaporation *can* have substantial effects on the evolution of the universe.

4.A The Dirac equation in RN spacetime

Using Latin indices a, b to denote a normalised basis aligned with the (t, r, θ, ϕ) coordinate system, we define our gamma matrices by

$$\{\gamma^a, \gamma^b\} = 2\eta^{ab}\,. \tag{4.92}$$

We can choose, for instance,

$$\gamma^0 = i\begin{pmatrix} 0 & 0 & 1 & 0 \\ 0 & 0 & 0 & 1 \\ 1 & 0 & 0 & 0 \\ 0 & 1 & 0 & 0 \end{pmatrix} \qquad \gamma^1 = i\begin{pmatrix} 0 & 0 & 1 & 0 \\ 0 & 0 & 0 & -1 \\ -1 & 0 & 0 & 0 \\ 0 & 1 & 0 & 0 \end{pmatrix}, \tag{4.93}$$

to ensure that σ^{01} is diagonal:

$$-i\sigma^{01} = \frac{1}{2}\gamma^0\gamma^1 = \frac{1}{2}\mathrm{diag}(1, -1, -1, 1)\,. \tag{4.94}$$

The curved spacetime Dirac equation, in the presence of an electromagnetic field, is

$$\not{D}\psi = \gamma^\mu(\nabla_\mu - iqA_\mu)\psi = \gamma^\mu(\partial_\mu + \Omega_\mu - iqA_\mu)\psi = m\psi\,, \tag{4.95}$$

where Ω_μ is the spin connection. Further discussion can be found in [80]. We will first rewrite this equation in the case $A_\mu = 0$, restoring the electric field later. In terms of the tortoise coordinate defined by Eq. (4.50), and writing ∂_* to mean $\partial/\partial r_*$, the Dirac equation can be written explicitly as

$$\gamma^\mu\partial_\mu\psi + \frac{1}{2}\left(\frac{\gamma^1}{\sqrt{f}}\left(\frac{2}{r} - \frac{3M}{r^2} + \frac{Q^2}{r^3}\right) + \gamma^2\frac{\cot\theta}{r}\right)\psi = m\psi\,, \tag{4.96}$$

with

$$\gamma^\mu\partial_\mu = \frac{\gamma^0}{\sqrt{f}}\partial_t + \frac{\gamma^1}{\sqrt{f}}\partial_* + \frac{\gamma^2}{r}\partial_\theta + \frac{\gamma^3}{r\sin\theta}\partial_\phi\,. \tag{4.97}$$

Naively squaring this equation yields the second-order form

$$\left(\nabla_S^2 + 2\Omega\cdot\partial + \Omega^2 + \nabla_\mu\Omega^\mu\right)\psi = m^2\psi\,, \tag{4.98}$$

where ∇_S^2 is the scalar Laplacian. Explicitly, the operator on the left-hand side is

$$\begin{aligned}&\frac{1}{f}\left(-\partial_t^2 + \partial_*^2\right) + \frac{2}{r}\partial_* + \frac{L_S^2}{r^2} - \frac{1}{4f}\left(\frac{M}{r^2} - \frac{Q^2}{r^3}\right)^2 - \frac{f}{2r^2} - \frac{\cot^2\theta}{4r^2}\\ &- \frac{2}{f}\left(\frac{M}{r^2} - \frac{Q^2}{r^3}\right)i\sigma^{01}\partial_t + \frac{\sqrt{f}}{r^2}i\sigma^{12}(\cot\theta + 2\partial_\theta) + \frac{2\cot\theta}{r^2\sin\theta}i\sigma^{23}\partial_\phi + \frac{2\sqrt{f}}{r^2\sin\theta}i\sigma^{13}\partial_\phi\,,\end{aligned} \tag{4.99}$$

where L_S^2 is the usual angular momentum operator in quantum mechanics. This unwieldy equation is not only non-diagonal in spinor space, unlike its flat space counterpart, but it does not reduce to the wave equation at the horizon or spatial infinity. We instead first perform the following field redefinition (see [81], for instance)

$$\Psi = rf^{1/4}\sqrt{\sin\theta}\,\psi\,, \tag{4.100}$$

which vastly simplifies the first-order equation Eq. (4.96):

$$\gamma^\mu\partial_\mu\Psi = m\Psi\,. \tag{4.101}$$

One can always choose the spinors to be eigenfunctions of the angular operator

$$L\Psi \coloneqq \left(\partial_\theta + \frac{\partial_\phi}{\sin\theta}\right)\Psi = -i\lambda\gamma^0\gamma^1\Psi\,, \tag{4.102}$$

where the eigenvalue λ satisfies $\lambda^2 = (j+1/2)^2$. Since the particle has spin half, the total angular momentum j can be any half-integer, and so λ^2 can be any positive square integer. Multiplying Eq. (4.101) through by $\sqrt{f}$ and squaring gives

$$\left(-\partial_t^2 + \partial_*^2\right)\Psi = f\left(m^2 + \frac{\lambda^2}{r^2}\right)\Psi + \gamma^1\partial_*\left(m\sqrt{f} + \frac{i\lambda\sqrt{f}}{r}\gamma^0\gamma^1\right)\Psi\,. \tag{4.103}$$

We can further simplify this equation by substituting in the first-order form:

$$\left(-\partial_t^2 + \partial_*^2\right)\Psi_i = f\left(m^2 + \frac{\lambda^2}{r^2}\right)\Psi_i + \left(\frac{M}{r^2} - \frac{Q^2}{r^3}\right)(\partial_* - \sigma\partial_t)\Psi_i + \frac{i\lambda f^{3/2}}{r^2}(\gamma^0\Psi)_i\,, \tag{4.104}$$

where $\sigma = \pm 1$ is the sign of the spin of the fermion. The final term in this equation is the only one which is not diagonal in spinor space. Since we will be analysing this equation using the WKB method, and since this term is sub-leading both to the second derivative terms, which go as ω^2, and to the first derivative terms, which go as ω, we will henceforth ignore this term.

Reintroducing the electromagnetic potential yields a broadly similar equation. There is an additional spin-field coupling (morally the $\sigma^{\mu\nu}F_{\mu\nu}$ term in Eq. (4.15)):

$$\begin{aligned}-\left(\partial_t + \frac{iqQ}{r}\right)^2\Psi_i + \partial_*^2\Psi_i = f\left(m^2 + \frac{(j+1/2)^2}{r^2}\right)\Psi_i \\ + \left(\frac{M}{r^2} - \frac{Q^2}{r^3}\right)\left(\partial_* - \sigma\left(\partial_t + \frac{iqQ}{r}\right)\right)\Psi_i - i\sigma f\frac{qQ}{r^2}\Psi_i\,.\end{aligned} \tag{4.105}$$

As we discuss in Appendix 4.B, to leading order in the WKB approximation, we can simplify this equation to

$$\left(\omega - \frac{qQ}{r}\right)^2\Psi_i + \frac{\mathrm{d}^2\Psi_i}{\mathrm{d}r_*^2} = f\left(m^2 + \frac{(j+1/2)^2}{r^2}\right)\Psi_i\,, \tag{4.106}$$

where we've substituted the time-dependence $\exp(-i\omega t)$.

For completeness, we give the relation between the tortoise coordinate r_* and the original radial coordinate r. For non-extremal black holes we have

$$r_* = r - \frac{2M^2 - Q^2}{2\sqrt{M^2 - Q^2}}\ln\left(\frac{r - M + \sqrt{M^2 - Q^2}}{r - M - \sqrt{M^2 - Q^2}}\right) + M\ln\left(\frac{r^2 - 2Mr + Q^2}{4M^2}\right)\,, \tag{4.107}$$

whilst for extremal black holes we have instead

$$r_* = r + 2M\ln\left(\frac{r - M}{M}\right) - \frac{M^2}{r - M}\,. \tag{4.108}$$

4.B The WKB solution

Here we provide a quick review of the WKB solution of an ordinary differential equation. See [82] for a general overview and [77] for more technical information. Suppose we have an equation of the form

$$\frac{\mathrm{d}^2 y}{\mathrm{d}x^2} + U(x)\frac{\mathrm{d}y}{\mathrm{d}x} + V(x) = 0\,, \tag{4.109}$$

where $V(x)$ is in some sense large, say of order μ^2. Then we try a solution of the form

$$y = \exp(iW(x))\,, \tag{4.110}$$

and expand $W = \mu W_0 + W_1 + \cdots$ and $V = \mu^2 V_0 + \mu V_1 + \cdots$ and $U = U_0 + \cdots$ in powers of μ. The leading and next-to-leading order equations read:

$$-\mu^2 (W_0')^2 + \mu^2 V_0 = 0\,, \tag{4.111}$$

$$i\mu W_0'' - 2\mu W_0' W_1' + i\mu U_0 W_0' + \mu V_1 = 0\,. \tag{4.112}$$

The zeroth-order equation is solved by

$$W_0 = \pm \int \sqrt{V_0}\,\mathrm{d}x =: \int k\,\mathrm{d}x\,, \tag{4.113}$$

and hence the first-order equation becomes

$$2W_1' = i\frac{k'}{k} + iU_0 + \frac{V_1}{k}\,. \tag{4.114}$$

If V_1 is imaginary and U_0 and k are real, this will mean W_1 is pure imaginary, and so the first-order equation dictates how the amplitude of the wave varies with position. For illustration, we can consider the Dirac equation above with $\lambda = q = 0$ for simplicity. Then

$$V_0 = \omega^2 - fm^2\,, \tag{4.115}$$

$$V_1 = -\frac{i\omega\sigma}{2f}\frac{\mathrm{d}f}{\mathrm{d}r_*}\,, \tag{4.116}$$

$$U_0 = -\frac{1}{2f}\frac{\mathrm{d}f}{\mathrm{d}r_*}\,. \tag{4.117}$$

Consider $\sigma = -1$ — we know from Eq. (4.101) that a wave with this spin must be outgoing at the horizon, which corresponds to taking $k > 0$. In this case we can in fact solve Eq. (4.114) for W_1:

$$2W_1 = i \ln k - \frac{i}{2} \int \mathrm{d}r_* \, \frac{1}{f} \frac{\mathrm{d}f}{\mathrm{d}r_*} \left(1 - \frac{\omega}{k}\right) . \tag{4.118}$$

Rewriting k in terms of $f(r_*)$ leaves us with an integral we can perform analytically:

$$2W_1 = i \ln k - \frac{i}{2} \int \mathrm{d}f \, \frac{1}{f} \left(1 - \frac{1}{\sqrt{1 - fm^2/\omega^2}}\right) \tag{4.119}$$

$$= i \ln k - i \ln \left(1 + \sqrt{1 - fm^2/\omega^2}\right) . \tag{4.120}$$

Our WKB solution thus becomes

$$\psi(r_*) \propto \left(\frac{\omega + k(r_*)}{k(r_*)}\right)^{1/2} \exp\left(i \int^{r_*} \mathrm{d}r_* \sqrt{\omega^2 - f(r_*)m^2}\right) . \tag{4.121}$$

We note that the additional complications introduced by the presence of the terms V_1 and U_0 have unimportant quantitative consequences — since the wavenumber k lies in the range $0 < k(r_*) < \omega$, the numerator of the amplitude can vary by at most a factor of $\sqrt{2}$ over the domain of interest. We can hence find a good approximation to the transmission amplitude by retaining only zeroth-order terms in the WKB expansion.

5

Primordial Black Hole Constraints with Large Extra Dimensions

5.1 Introduction

In Chapter 1 we claimed that primordial black holes (PBHs) were a compelling solution to the dark matter problem, being naturally cold, dark, and consistent with the framework of known physics. For this reason a great deal of work has been done in understanding the astrophysical and cosmological consequences of a large PBH background; for many choices of PBH mass, strict constraints exist on the fraction of dark matter they could constitute. See [83] for a review.

Many of these constraints, in particular those applying to smaller mass PBHs (in the mass range 10^{10} g to 10^{17} g), are due to the effects of the Hawking radiation these black holes emit. It is therefore interesting to consider how modifying the nature of Hawking evaporation modifies the constraints on the density of primordial black holes in the universe.

In this chapter, we consider how the dominant constraints on the density of small PBHs — those from the extragalactic gamma ray background (EGB) — differ in the scenario that black holes can radiate into higher dimensions. The nature of gravity on short scales is not well established: whilst Coulomb's law (or its quantum field theoretic generalisation) is known to apply down to distances of order 10^{-18} m, Newton's law of gravity has only been tested on scales of order several microns. Consequently, it is consistent for there to exist extra large spatial dimensions, and

being extraordinarily compact objects, even black holes as heavy as 10^{17} g could be sensitive to these dimensions.

Most new physics, involving the introduction of extra degrees of freedom available for black holes to radiate, would result in little reduction in detectable evaporation products and at best modest weakening of existing constraints. The motivation for studying extra-dimensional evaporation is the critical fact that higher-dimensional black holes, if smaller than the size of the extra dimensions, are significantly *colder* than their 4D counterparts, for a given fixed mass. These PBHs are thus expected to produce fewer evaporation products, and thus be subject to weaker constraints, than ordinary 4D black holes.

This chapter is divided into five sections. In Section 2 we review the latest constraints on the PBH density across the entire range of masses. In Section 3 we discuss the behaviour of black holes in theories with large extra dimensions, and explain how the evaporation rate is modified in such a way as to substantially modify the nature of all constraints on low-mass PBHs. In Section 4 we present the main result of our analysis, the modified constraints on the PBH density arising from the extragalactic photon background, for several choices of the number of extra dimensions. Finally, in Section 5, we discuss the modifications we expect to occur to other constraints on the PBH density.

5.2 Existing primordial black hole constraints

Constraints on the density of primordial black holes can be divided into two classes: constraints from the gravitational effects of the black holes themselves, and constraints from the particles they produce through Hawking evaporation. Since the total rate of energy loss is less for larger black holes, these evaporative constraints exist only for PBHs of mass less than about 10^{17} g. Conversely, gravitational effects of PBHs are typically negligible for black holes below this mass.

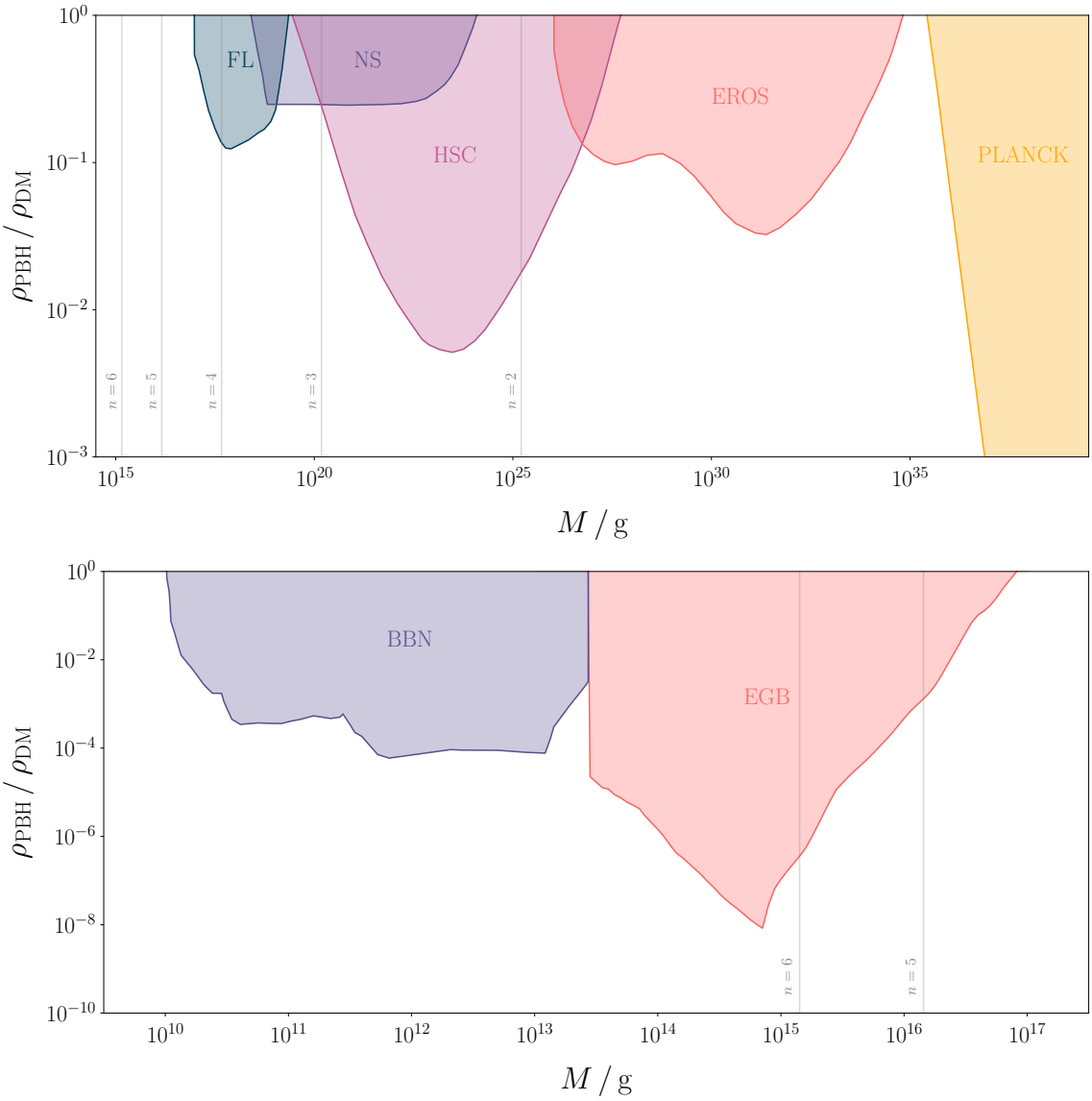

Figure 5.1: Constraints on the PBH density (at formation) as a fraction of the dark matter density. Shaded regions are excluded. In the upper panel are those constraints arising from the gravitational influence of the black holes, adapted from [84]; from left to right the constraints arise from femtolensing experiments (FL), capture by neutron stars (NS), microlensing experiments (HSC and EROS), and effects on the CMB (PLANCK). The vertical grey lines indicate the mass M_c at which the black hole radius is equal to the size of the extra dimensions, as discussed in Section 5.3. In the lower panel are those constraints arising from the effects of the PBH evaporation products; the constraints from BBN are taken from [25] and those from the EGB we have reproduced ourselves.

5.2.1 Gravitational constraints

The constraints on the PBH density for masses above around 10^{17} g are illustrated in the upper panel of Fig 5.1. Perhaps the most important of these come from lensing experiments. For small black holes, the wave nature of electromagnetic radiation is significant, and gravitational lensing around the black hole can give rise to an interferometry pattern in the received radiation (termed *femtolensing*) [85][1]. For larger black holes this interference is not detectable, though gravitational lensing can nevertheless result in the apparent magnification of stars passing behind them (termed *microlensing*) [87, 88].

There also exist astrophysical effects associated with the collision and subsequent capture of primordial black holes by compact objects such as neutron stars and white dwarfs. In some mass ranges, such collisions would result in the destruction of these objects; the number density of existing neutron stars and white dwarfs hence places mild bounds on the density of primordial black holes [89, 90].

For large black holes, of order 10^{35} g and larger, strict constraints arise from the effects of these PBHs on the CMB. In particular, the accretion of primordial gas around the black holes and subsequent injection of energy into the background plasma would be detectable through its influence on the angular distribution of temperature and polarization of the CMB. Data from Planck strongly constrains this scenario [91].

5.2.2 Evaporative constraints

For masses below about 10^{17} g, all constraints on the PBH density are due to the effects of black hole evaporation. The dominant constraints come from the effects on big bang nucleosynthesis (BBN) and the size of the extragalactic gamma ray background (EGB). In [25] a comprehensive analysis of these constraints was performed. Injection of high-energy particles during BBN can cause dissociation of heavier isotopes and induce extra interconversion of protons and neutrons, the extent of which is strictly constrained by the known abundances of the light elements. Constraints

[1] These results have been called into question by [86].

on black holes that have not fully evaporated today arise from the extragalactic photon background. Continual evaporation of PBHs over the course of the universe's history would have converted a considerable quantity of energy into photons (primarily gamma rays), and this would be observable in the EGB. These constraints are illustrated in the lower panel of Figure 5.1.

The constraints from the extragalactic photon background are of most relevance here, so we shall endeavour to explain the qualitative form of the constraints. Assuming the black holes are formed very early in the universe, there exists some mass M_0 such that they are disappearing today. For black holes much larger than this, incomplete evaporation occurs, and thus not all of the energy in the black holes is converted into Standard Model particles. Since the lifetime of a black hole scales approximately like the cube of its mass, a black hole need not be much heavier than M_0 before its lifetime is far longer than the age of the universe and only a small fraction of its energy is converted to photons. The constraints hence weaken as M is increased above M_0.

For masses smaller than M_0, the black holes have completely disappeared by today. Though the total energy released by the black holes is the same for all such M, the smaller the black holes, the earlier they disappeared, and hence the greater the redshifting of the photons they produced. The energy contributed to the photon background today hence decreases as M is decreased below M_0, and the constraints weaken. One needs to take a little more care than this — smaller black holes emit predominantly higher-energy radiation, and the constraints on the size of the photon background are stricter at higher energy. However, sufficient redshifting of frequency occurs that in fact the dominant constraints on small black holes come from the soft end of the gamma ray background.

For black holes smaller than about 10^{13} g, complete evaporation has occurred before photon decoupling. Such radiation is hence not visible in the photon background, and so the constraints disappear completely for such black holes.

We briefly mention that there exist several other constraints of an evaporative nature, arising from annihilation of electrons with positrons emitted by the PBHs

[92,93], *galactic* gamma rays and antiprotons [94,95], and effects on CMB anisotropy [96]. Apart from over very narrow mass ranges, the constraints from BBN and the EGB are the strictest of these.

5.3 Black holes in large extra dimensions

We discussed in Section 2.5 the proposal that there exist extra large spatial dimensions as an explanation for the size of the Planck mass relative to the weak scale. If M_* is the fundamental Planck mass, n the number of extra dimensions, and R their size, the 4D Planck mass is given by Eq. (2.83):

$$M_P^2 \sim M_*^{2+n} R^n \,. \tag{5.1}$$

For $M_* = 10$ TeV, the above relation implies that $R \sim 10^{11}$ m for $n = 1$ — certainly such a large extra dimension is ruled out by gravitational experiments on the solar system scale. For $n = 2$ one finds $R \simeq 25\,\mu$m, which is consistent with current short distance tests of Newton's law [97]. In this chapter we consider $2 \leq n \leq 6$. In Section 5.4 we will describe qualitatively the nature of the constraints for n larger than this.

5.3.1 The higher-dimensional Schwarzschild solution

We next discuss the nature of black holes in this model. Black holes which are much larger in size than these extra dimensions should be insensitive to them, and behave as ordinary 4D black holes. On the other hand, black holes much smaller than these extra dimensions should be insensitive to the finiteness of the dimensions, and behave as $(4 + n)$-dimensional objects. There will be some intermediate regime in which the black hole is not adequately described by either picture. However, the crossover between the two descriptions is continuous, for one can show that there is some critical mass M_c at which the size of the extra dimensions, the 4D Schwarzschild radius of the black hole, and the $(4+n)$-dimensional radius of the black hole all approximately coincide. This critical mass is tabulated in Table 5.1. For a review of black holes in theories with large extra dimensions, see [98].

n	M_c / g
2	1.62×10^{25}
3	1.52×10^{20}
4	4.65×10^{17}
5	1.44×10^{16}
6	1.45×10^{15}

Table 5.1: The mass M_c in grams of the black hole whose Schwarzschild radius is equal to the size of the extra dimensions, for $M_* = 10$ TeV.

In $(4+n)$ dimensions the Schwarzschild metric is given by [99]

$$\mathrm{d}s^2 = -\left(1 - \left(\frac{r_h}{r}\right)^{n+1}\right)\mathrm{d}t^2 + \left(1 - \left(\frac{r_h}{r}\right)^{n+1}\right)^{-1}\mathrm{d}r^2 + r^2\mathrm{d}\Omega_{n+2}^2\,, \tag{5.2}$$

where the horizon radius is

$$r_h = \frac{1}{M_*}\left(\frac{M}{M_*}\right)^{\frac{1}{n+1}}\left(\frac{8\Gamma((n+3)/2)}{(n+2)\pi^{(n+1)/2}}\right)^{\frac{1}{n+1}}\,, \tag{5.3}$$

and the Hawking temperature of the black hole is given by

$$T = M_*\left(\frac{M_*}{M}\right)^{\frac{1}{n+1}}\left(\frac{n+1}{4\sqrt{\pi}}\right)\left(\frac{n+2}{8\Gamma((n+3)/2)}\right)^{\frac{1}{n+1}}\,. \tag{5.4}$$

The relation between radius and temperature is particularly simple:

$$T = \frac{n+1}{4\pi r_h}\,. \tag{5.5}$$

When we restrict the metric Eq. (5.2) to the brane, we find a 4D black hole solution whose geometry differs from the ordinary Schwarzschild solution. This will affect the way the black hole gravitates. Consequently, some of the aforementioned gravitational constraints will be modified in this scenario, such as those from lensing experiments, since the bending of light around a black hole is sensitive to the precise geometry. Similarly, capture of these black holes by neutron stars and white dwarfs is sensitive to the potential energy between the two objects, which depends fundamentally on the number of extra dimensions.

The above notwithstanding, it transpires that for $M_* = 10$ TeV, the critical mass describing the transition from the 4D to the $(4+n)$-dimensional picture occurs close

to the mass at which existing constraints become dominantly evaporative[2]. These critical masses are illustrated as vertical lines in Figure 5.1. Black holes larger than this critical mass behave as ordinary 4D black holes, and the existing gravitational constraints apply.

On the other hand, Eq. (5.4) shows that the temperature of a higher-dimensional black hole can differ significantly from that of a 4D Schwarzschild black hole of the same mass. Thus the rate at which it evaporates, and the energy of the particles it produces during this evaporation, can differ considerably also. We hence expect the constraints on low-mass PBHs to be substantially modified in this scenario.

5.3.2 Bulk and brane evaporation

A black hole smaller in size than the extra dimensions radiates gravitons into the bulk and Standard Model particles onto the brane. In principle these processes could occur at very different rates. However, as demonstrated in Appendix 5.A, it transpires that the rate of loss of energy for both modes of evaporation is in fact approximately equal, being given by

$$-\frac{\mathrm{d}M}{\mathrm{d}t} \sim T^2 \,. \tag{5.6}$$

The differing dependence of the temperature on mass, however, gives rise to a black hole lifetime τ that depends critically on n:

$$M_* \tau \sim \left(\frac{M}{M_*}\right)^{\frac{n+3}{n+1}} \,. \tag{5.7}$$

By considering Eqs. (5.3), (5.4) and (5.7) in conjunction with Eq. (5.1), one can see that black holes much smaller than the size of the extra dimensions are larger, cooler, and live longer than 4D black holes of the same mass [100], at least if emission involves only a single degree of freedom[3]. However, for black holes of order the size of the extra dimensions, the numerical factors in Eq. (5.4) are not insignificant, and lead to higher-dimensional black holes disappearing substantially faster.

[2]For $n > 2$ at least. For $n = 2$, M_c is appreciably larger than this.

[3]We consider the detail of the number of emitted degrees of freedom in Section 5.4.

Throughout the rest of this chapter we will take $M_* = 10$ TeV. As mentioned at the start of this section, this is approximately the bound for $n = 2$ placed on the size of the extra dimensions by measurements of the behaviour of Newton's law on short distances. However, we briefly mention here that there are several other constraints on the size of M_*. Firstly, a weak-scale fundamental Planck mass is subject to collider constraints. These are fairly mild, and are consistent with $M_* = 10$ TeV. There are also several astrophysical and cosmological constraints due to the effects of the light Kaluza-Klein modes of the graviton. These bounds are more strict, and typically rule out $M_* = 10$ TeV for $n = 2$. However, we note that they are subject to large systematic errors, and depend on the details of the decay of the KK modes. See §106 of [101] for the latest constraints on M_*. In Section 5.5 we describe the qualitative effects of choosing a larger value for M_*.

5.4 Modified constraints from the extragalactic photon background

In this section we present the constraints on the density of higher-dimensional PBHs that arise from the contribution they would make to the extragalactic photon background. It transpires that the strongest constraints come from the X-ray and gamma ray background, as in the 4D case. In the $n = 1$ case the black holes radiate primarily in the UV and soft X-ray regions of the electromagnetic spectrum. There are only very poor measurements of the extragalactic UV background, but this is of no consequence since $n = 1$ is ruled out by gravitational experiments.

We assume for simplicity a monochromatic mass distribution — that is, that all of the primordial black holes are formed at the same time with the same mass. This is not particularly realistic, and it is known in the 4D case that constraints tend to become more stringent with extended mass distributions, if qualitatively similar [84]. A monochromatic distribution is nevertheless sufficient to indicate the large modifications to the constraints that occur in the extra-dimensional scenario. We also emphasise that the quantity $\rho_{\rm PBH}$ we plot in Figure 5.3 is the fraction of the

dark matter density the black holes constitute *at formation*, and likewise the mass M is their mass at formation. In order to constitute a fraction of the dark matter today, the PBHs must have an initial mass larger than that mass M_0 which would be evaporating now, tabulated in Table 5.2.

5.4.1 Methodology

To compute the spectrum of radiation emitted by a black hole, the public code `BlackHawk` [102] was used. In its original form, this code computes the emission rate of all Standard Model particles from a given black hole, accounting for greybody factors and using `PYTHIA` to compute the subsequent decay of all unstable particles. The code makes the simplifying assumption that a black hole begins radiating a given particle only when its temperature exceeds the particle's mass, and thereafter begins radiating it as though it were massless.

The code needs some modification to produce the emission rate in the large extra dimensions scenario. Naturally the mass-radius and mass-temperature relations are modified according to Eqs. (5.3) and (5.4). Furthermore, the greybody factors differ in different dimensions. These greybody factors were computed for all spins and for all dimensions n, using the numerical recipes outlined in [103, 104]. Accuracy of the numerical results could be compared to the results in [103, 105]. We found excellent agreement with the former, although not with the latter. We note that the numerical results in [105] do not agree with the expected low-energy analytic expressions (in particular, all spin-2 greybody factors should go to zero at low energy), so we put the discrepancy between our results down to an error in theirs. To produce the high-energy and low-energy asymptotics of the greybody factors, the analytic results from [106, 107] were used.

Given the spectrum of radiation from a black hole at each moment of its lifetime, the density of background photons today (in units of energy per unit volume per unit energy) is given by the formula

$$n = \int_{t_{\rm dec}}^{t_{\rm max}} (1+z) \frac{\mathrm{d}^2 N}{\mathrm{d}t\, \mathrm{d}E}((1+z)E)\, \mathrm{d}t\,, \tag{5.8}$$

where the derivative in the integrand is the energy being emitted by the black holes per unit time per unit volume per unit energy. The integral is taken between the time of photon decoupling $t_{\rm dec}$ and $t_{\rm max} = \min(t_0, \tau)$, where t_0 is the time today and τ the lifetime of the black hole. Those photons with energies between E and $E + {\rm d}E$, if produced at an earlier time t, must have been emitted with blueshifted energy $(1+z)E$ and belonged to a wider energy window $(1+z){\rm d}E$. This accounts for the two redshift factors in the integrand. Since the majority of the evaporation occurs during matter domination (at least for those black holes which haven't completely evaporated by photon decoupling), we take $1 + z(t) = (t_0/t)^{2/3}$.

An isotropic photon background gives rise to an observed flux of

$$I = \frac{c}{4\pi} n \,. \tag{5.9}$$

The data for the gamma ray region of the electromagnetic spectrum are collected by space-based telescopes, in particular EGRET and COMPTEL aboard the Compton Gamma Ray Observatory and LAT aboard the Fermi Gamma Ray Space Telescope [108–110]. More data exist for the intensity of the X-ray background, for which we use a fit from [111]. In Figure 5.2 we plot these data. In determining the PBH constraints we make the conservative assumption that the entirety of the photon background in the X-ray and gamma ray region of the electromagnetic spectrum is due to black hole evaporation products.

5.4.2 Results

Our results are plotted in Figure 5.3. We see that independent of n, the shape of the constraints is broadly similar. The explanation for this shape is as outlined in Section 5.2.2: those black holes which are evaporating today contribute most energy to the photon background, with the constraints disappearing for black holes small enough to have evaporated before photon decoupling. The primary qualitative difference is due to the fact that the mass M_0 of those black holes evaporating today is dimension-dependent. These masses are tabulated in Table 5.2. For $n \geq 4$ we note that the constraints cut off sharply above a certain mass. This is the mass M_c above which the

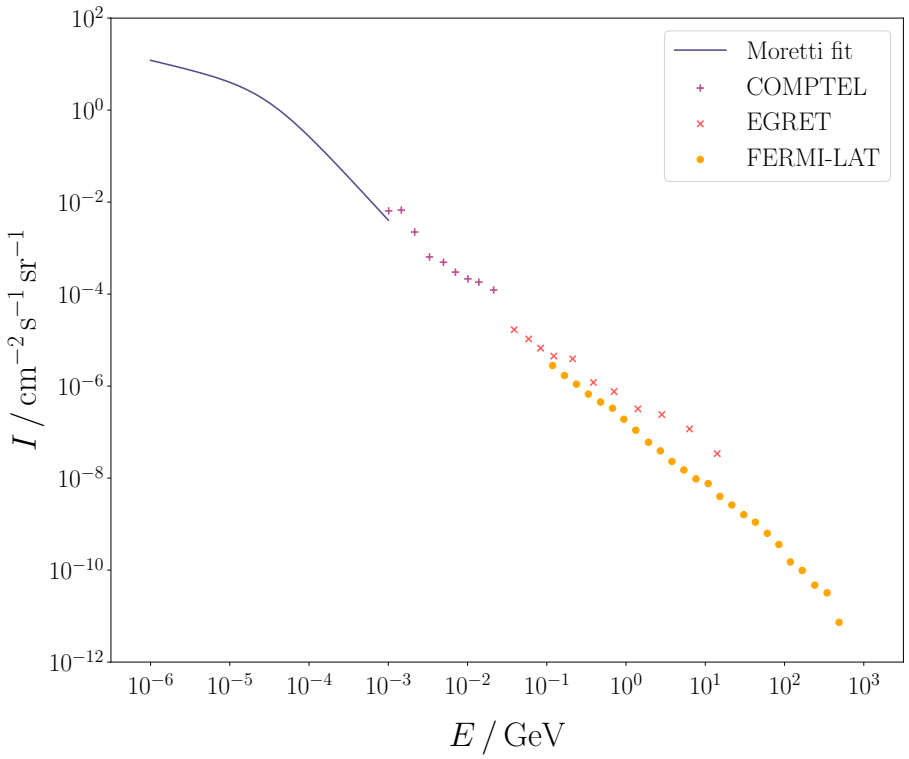

Figure 5.2: The observed background photon flux in units of energy per square centimetre per second per steradian per unit energy, as a function of energy. The energy range plotted corresponds to the X-ray and gamma ray region of the electromagnetic spectrum.

n	M_0 / g
2	2.44×10^7
3	5.33×10^{10}
4	1.83×10^{13}
5	2.53×10^{15}
6	1.45×10^{15}

Table 5.2: The mass M_0 in grams of a black hole evaporating today, assuming formation at the start of the universe.

4D description of the black holes is valid, tabulated in Table 5.1. The total radiation rate is substantially reduced above this mass (as explained in Section 5.3.2), which is why the constraints significantly soften. Indeed, comparison with Figure 5.1 shows that above this mass, the constraints coincide with those in the 4D case. Since we have not treated the crossover behaviour of the black hole solution precisely, the results are not reliable at this mass.

From Eqs. (5.7) and (5.4) one can show that for a black hole which survives until today, the typical temperature of the Hawking radiation is higher for larger n. This explains why the constraints are slightly stronger for larger n (and indeed why they are noisier), the dominant constraints coming from the higher-energy region of the electromagnetic spectrum (see Figure 5.2). The constraints also cover a wider mass range than the 4D constraints, on account that the lifetime of the black holes Eq. (5.7) depends less strongly on mass than in the 4D case.

One might wonder whether radiation into gravitons would dominate photon production for large n, and constraints might substantially weaken, on account that the number of degrees of freedom in the graviton is quadratic in n ($g = (n+1)(n+4)/2$). Our results do not bear this hypothesis out. To understand this, we note that the graviton greybody factor is suppressed at low energies relative to those for the photon and neutrinos, and more so for larger n. See Figure 5.4 in Appendix 5.A.

For $n = 7$, the mass M_c is approximately equal to the mass of a 4D black hole evaporating today ($M_0 \simeq 7.09 \times 10^{14}$ g). Black holes smaller than this, for which the

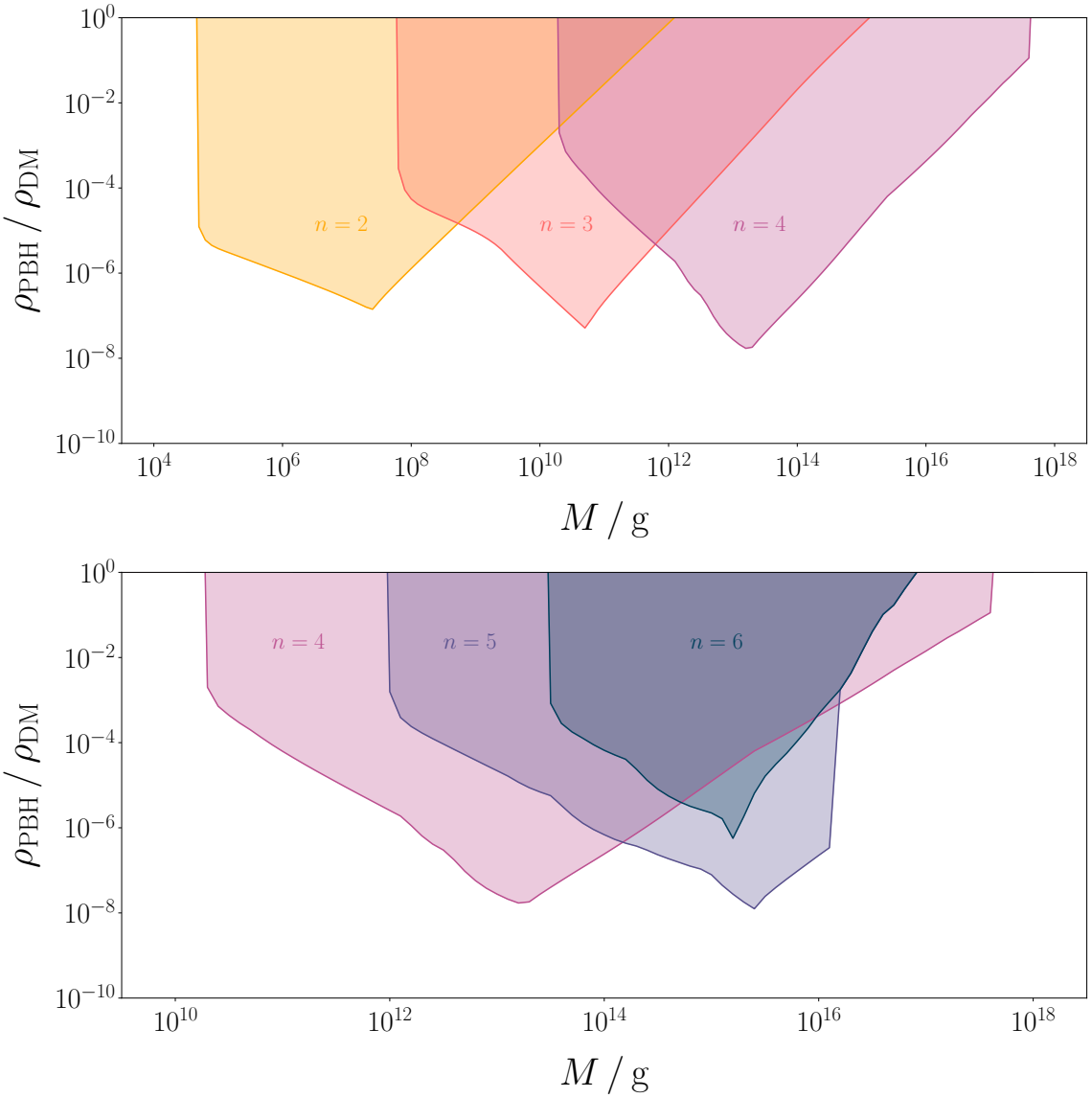

Figure 5.3: Constraints on the PBH density (at formation) as a fraction of the dark matter density for different choices of n, assuming a monochromatic mass distribution. Shaded regions are excluded. In the upper panel are plotted (left to right) the constraints for $n = 2, 3, 4$ and in the lower panel those for $n = 4, 5, 6$.

extra-dimensional picture is valid, have disappeared by today and therefore could not constitute the dark matter. On the other hand, for black holes larger than this the 4D description, and hence the 4D constraints, apply. Since M_c decreases for larger n, we find that for all $n > 6$ the constraints on the fraction of the dark matter the black holes could constitute are unchanged from those in the 4D case.

We note that only for $n = 2$ and $n = 3$ are there wide mass windows in which PBHs could constitute the entirety of the dark matter — $M \gtrsim 10^{12}$ g for $n = 2$ and $M \gtrsim 10^{15}$ g for $n = 3$. For larger n our results show that the photon background places similar constraints on the PBH mass as in the 4D case, requiring M to be larger than about 10^{17} g, beyond which other gravitational constraints need to be taken into consideration.

5.5 Discussion

The most important question to address next is the modification of the constraints from BBN in the extra-dimensional scenario. Just as for the photon background, we expect that the dominant constraints will arise from those black holes which evaporate completely during BBN. Since such black holes will be lighter than their 4D counterparts, we expect the constraints from BBN to be shifted to lower mass, and more so for lower n. We leave a detailed study of this to future work.

It is also necessary to understand how other evaporative and gravitational constraints change with the introduction of extra dimensions. As mentioned in Section 5.4.2, the typical temperature of the black holes increases as n is increased. For low n, numerical results indicate that the only evaporation products are neutrinos, gravitons, and photons, and we hence expect the constraints from positron annihilation or antiprotons to be non-existent. For large n, black holes larger than $10^{17}g$ behave as 4D objects, and so we expect existing gravitational constraints to apply. Lensing constraints in the low n case, and other evaporative constraints in the large n case, would need to be studied in greater detail.

In this chapter we have demonstrated the significant qualitative changes to the

constraints on the PBH density that occur when extra dimensions are present. In doing so we have made some simplifying assumptions — that the black hole mass distribution is monochromatic, and that the black holes are not rotating. In any number of dimensions, the Hawking temperature of a black hole depends quite sensitively on its angular momentum; the constraints on a population of spinning black holes could thus be appreciably different. To understand how these two factors affect the constraints in the 4D case, see [112].

A final natural question to ask is how the constraints would differ for a different choice of M_*. We have here chosen the lowest value of M_* consistent with experiment. From Eq. (5.7) we see that a black hole evaporating today would have larger mass for a larger choice of M_*. We thus expect the constraints to be shifted to larger mass as M_* is increased, though with the same qualitative shape. For $M_* = 10$ TeV we find that the constraints for $n > 6$ are just as in the 4D case, and we expect that the larger we take M_*, the fewer choices of n will give rise to novel constraints.

5.A Radiation in higher dimensions

In this appendix we state the formulae for computing the total emission rate

$$\frac{\mathrm{d}^2 N}{\mathrm{d}t\,\mathrm{d}\omega}\,, \tag{5.10}$$

as appears in Eq. (5.8), for both bulk and brane emission. The most straightforward expression, which applies in any number of dimensions, is Eq. (2.79):

$$\frac{\mathrm{d}^2 N}{\mathrm{d}t\,\mathrm{d}\omega} = \frac{1}{2\pi}\sum_{\text{states}} \frac{\mathcal{A}(\omega)}{\exp(\omega/T) \mp 1}\,, \tag{5.11}$$

where $\mathcal{A}$ is the absorption probability for a particle incident upon the black hole. Making closer connection with the usual Planck law, we can also write

$$\frac{\mathrm{d}^2 N}{\mathrm{d}t\,\mathrm{d}\omega} = \frac{g\Omega_{n+2}}{(2\pi)^{n+3}}\omega^{n+2}\frac{\sigma(\omega)}{\exp(\omega/T) \mp 1}\,, \tag{5.12}$$

where g is the number of degrees of freedom of the particle. Here the quantity $(4 + n)$ describes the number of dimensions the emitted particles feel — even for a

higher-dimensional black hole, we should take $n = 0$ for brane emission. These two expressions can be seen to be equivalent using the relation between the greybody factor $\sigma(\omega)$ and the absorption probability $\mathcal{A}(\omega)$ (cf. Eq. (2.80)):

$$\sigma(\omega) = \frac{2^n \pi^{(n+1)/2} (n+1) \Gamma((n+1)/2)}{\omega^{n+2}} \sum_\ell N_\ell \mathcal{A}_\ell(\omega) \,, \tag{5.13}$$

where N_ℓ is the number of degrees of freedom per angular momentum mode ℓ, implicit in the sum over states in Eq. (5.11). In four dimensions we have $N_\ell = 2\ell + 1$, though this is no longer true in higher dimensions, and indeed N_ℓ depends on whether the degree of freedom being emitted is a scalar, vector, or tensor perturbation. We remark that Eq. (2.8) in [103] is not correct in general since it assumes the scalar form of N_ℓ.

For a perfect black body, the greybody factor is independent of ω and equal to the cross-sectional 'area' of the body, πr^2 for a 4D black hole. In this case we can multiply Eq. (5.12) by energy and integrate to produce the total rate of radiation. It is particularly simple (cf. Eq. (2.81)):

$$P = \frac{g(n+3)}{\pi} T^{n+4} r_h^{n+2} \begin{cases} \zeta(n+4) & \text{bosons} \,, \\ \eta(n+4) & \text{fermions} \,, \end{cases} \tag{5.14}$$

where $\zeta(z)$ is the Riemann zeta function and $\eta(z)$ the Dirichlet eta function, both approximately unity for large n. To an order of magnitude, we thus have

$$P \sim T^{n+4} r_h^{n+2} \,. \tag{5.15}$$

Since the horizon radius and Hawking temperature are inversely proportional, as in Eq. (5.5), we arrive at the conclusion that the rate of loss of mass of the black hole is always proportional to T^2, independent of the number of dimensions, as claimed in Eq. (5.6). Studying Eq. (5.14) in more detail, we can conclude that for a given n the rates of bulk and brane emission are of the same order of magnitude. However, note that the numerical factors in the expression for the temperature Eq. (5.4) are not unimportant, and result in orders-of-magnitude faster evaporation for $n = 6$ as compared to $n = 1$. For this reason, constraints on the PBH density substantially weaken once the radius of the black hole exceeds the size of the extra dimensions.

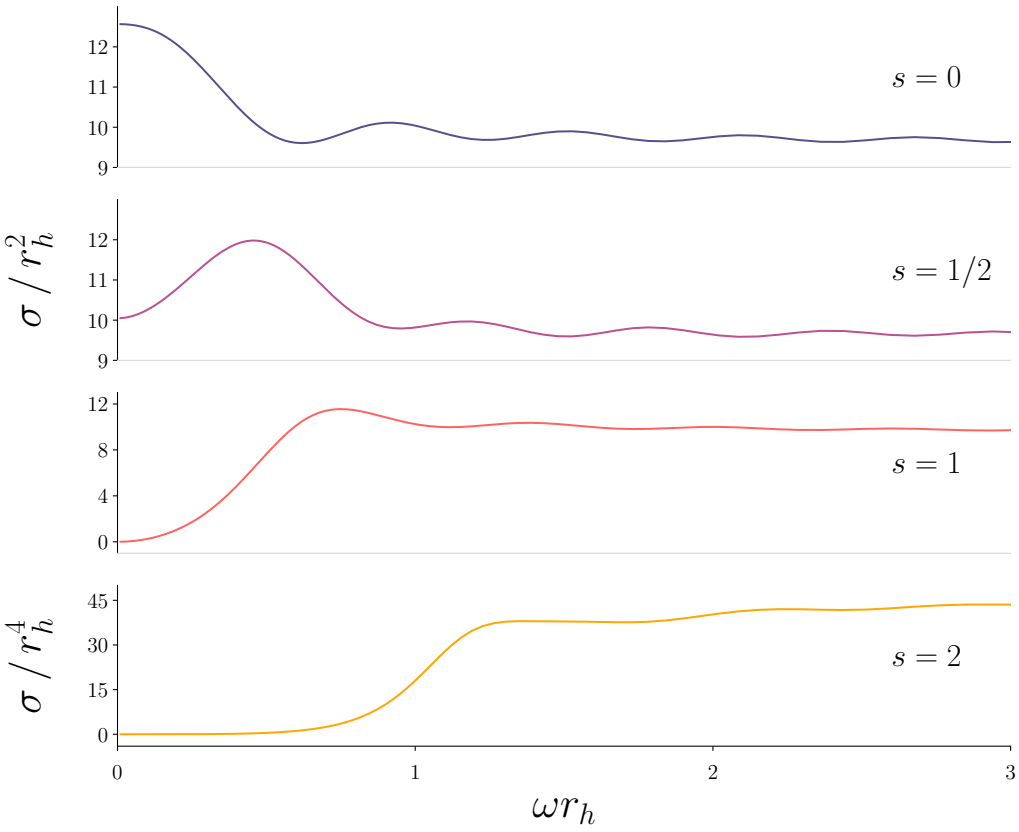

Figure 5.4: Sample greybody factors for $n = 2$, for all types of particle. Note the different scales on the y-axes, and the low-energy suppression of graviton radiation.

For black holes larger than the size of the extra dimensions, the spectrum contains the 4D graviton and a tower of Kaluza-Klein modes, which the black hole can also radiate in principle. However, the lightest of these has mass of order $1/R$, which by Eq. (5.5) only begins to be radiated when $r_h \sim R$. Such radiation can hence be neglected for large black holes, and evaporation treated just as in the 4D case. The exact spectrum of Kaluza-Klein modes depends on the geometry of the extra dimensions, but Weyl's law (or a generalisation thereof) guarantees that as the black hole becomes much smaller than the size of the extra dimensions, the spectrum tends towards that for infinite space.

6
Conclusions

That black holes should generically emit radiation has been known for almost 50 years. In this thesis we have considered how the nature of the spectrum, the mechanism of emission, and the observational consequences of the radiation, depend on the details of the black hole and of the radiated object. Particular focus was placed on the interaction of the radiation with the background gravitational (and electric) fields that exist outside black holes. We have also seen how modifications to the temperature of black holes, and thereby the rate at which they radiate, can substantially modify the constraints that exist on the number of black holes in the universe.

In Chapter 3 we analysed the emission from black holes of objects which are not pointlike but rather spatially extended. Such objects are subject to large tidal forces upon emission, and this significantly modifies the rate at which they are radiated. In particular, as the object becomes sufficiently large, emission becomes exponentially suppressed. This is not a theoretical curiosity — many objects in nature are finite in extent, including fundamental objects such as strings. Indeed, it may be that all objects in nature are spatially extended when considered on sufficiently small distance scales, and this could lead to profound effects on the final stages of black hole evaporation.

In Chapter 4 we studied the emission of charged particles from charged black holes. In this context there are two mechanisms for particle creation — the usual mechanism of Hawking, as well as Schwinger pair production by the external electric field. The interplay between the gravitational and electromagnetic effects gives rise

to a complex radiation spectrum. We elucidated the exact formulae that govern the loss of energy (and charge) from such black holes, and gave analytic expressions for these rates in certain limits. In particular, when the black hole is large relative to the wavelength of the radiated particle, emission can be considered in terms of point-particle tunnelling. We connected the tunnelling pictures of [48] and [76] to provide a single, unified description of tunnelling from charged black holes.

In Chapter 5 we turned our attention to the cosmological and astrophysical implications of black hole radiation. We considered the proposal that the dark matter consists (at least in part) of primordial black holes, formed very early in the universe's history. For certain choices of mass, evaporation of these black holes leaves a large imprint on the extragalactic photon background, which constrains their number density. However, since the temperature and evaporation rate of black holes depends sensitively on the number of dimensions they live in, we expected that the nature of these constraints would be substantially modified in the case of evaporation into dimensions other than four. The existence of large extra dimensions is not merely a theoretical possibility, but is motivated by attempts to explain the relative size difference between the Higgs mass and the Planck mass. We determined the nature of the constraints on the primordial black hole density in dimensions from five to ten, and found that in the case of two or three extra dimensions (assuming a weak-scale fundamental Planck mass), it is possible for primordial black holes to constitute the entirety of the dark matter.

There are still many unanswered questions pertaining to the work in each of the aforementioned chapters. We discussed several avenues for further research in Sections 3.5, 4.5, and 5.5. In particular, there are natural extensions of the work in Chapter 3 to particles which are not scalar, and to black holes which are not Schwarzschild. Likewise, the ideas in Chapter 4 can be applied to charged black holes in other backgrounds, or to those which are rotating, and to particles of spin higher than half. The diversity of constraints that exist on the cosmic black hole density is sensitive to diverse aspects of the nature of the black holes. We expect that many of these constraints will be substantially different in theories with large extra dimensions.

More broadly, the focus of black hole physics over the coming years will likely be directed towards the following fundamental problems.

The final stages of black hole evaporation are still a mystery, involving curvatures on the scale of the Planck mass. Hawking's semiclassical calculation does not apply here, and in principle only a correct quantum theory of gravity will suffice to explain the process. However, this problem can be turned on its head. On basic physical grounds there are certain characteristics we can expect of a black hole's final moments, and this informs our search for the theory of quantum gravity. For instance, it appears that black holes must completely evaporate *somehow*, for the alternative leads to a variety of disastrous consequences [42], and in conjunction with simple arguments involving energy and charge conservation this restricts the possible spectra of particles a theory of quantum gravity could contain. This proposal is known as the weak gravity conjecture [64], and has been used to rule out many otherwise-viable candidate effective field theories.

Constraints on the fraction of dark matter that black holes could constitute are becoming increasingly strict. It now seems unlikely that conventional black holes, as we currently understand them, could account for the entirety of the invisible matter in the universe. However, of the variety of proposed explanations for the nature of the dark matter none stands out as singularly compelling, with experimental searches for BSM dark matter thus far yielding only negative results. For this reason some form of black hole dark matter remains an attractive possibility.

There is still much work to be done in understanding the black hole information problem. Most of this thesis has been concerned with coarse-grained, macroscopic properties of black hole radiation, such as the expected number of particles produced with a given energy per unit time. Resolving the information problem requires more precise consideration of the quantum state of the radiation, including the entanglement of late-time evaporation products with early-time infalling matter. Hints towards a solution to this conundrum are afforded by the AdS/CFT correspondence. This gives us a rigorous definition of quantum theories of spacetime (albeit only on an anti-de Sitter background), and though practical computations are typically difficult

(by virtue of the strong-weak duality), they are nevertheless well-defined. Though many deep questions about quantum gravity are unaddressed within this framework — what actually happens at a black hole singularity; whether the big bang was in fact the beginning of time; how to understand the causal structure of spacetime if it fluctuates quantum mechanically — the correspondence sheds light on other questions. It compels us to view spacetime as emergent: an approximate, collective description of the underlying fundamental degrees of freedom. More pertinently, the manifest unitarity of the conformal field theory provides a direct answer to the question of whether indeed information is destroyed through the process of black hole formation and evaporation: it is not.

Taking this answer seriously, it remains to understand in detail how information is conveyed from the black hole interior, and where Hawking's calculation fails. Until very recently these questions remained a mystery, but presently a picture is beginning to crystallise. It is now thought that the apparent generation of entropy is a result of calculating the entropy by the wrong formula — the appropriate fine-grained expression for the entropy in a gravitational theory is the Ryu-Takayanagi entropy [113] (or its quantum mechanical generalisation [114]). When applied naively this does not resolve the problem, but clues from AdS/CFT suggest there should be additional contributions to this entropy from regions of spacetime disconnected from the exterior radiation, known as 'islands' [115]. Recent work has shed light on how to understand these contributions from first principles, without appealing to AdS/CFT. In particular, the entropy as calculated via the gravitational path integral receives contributions from previously ignored saddle points termed 'replica wormholes' [116]. Taken together, these ideas imply that the entropy of the radiation rises from zero at early times, reaches a maximum when the horizon area has roughly halved, and returns to zero at late times — that is, it follows the Page curve [117]. Further discussion of this story can be found in [118–120]. Whilst only a non-perturbatively small amount of information escapes the black hole at early times, the existence of this transmission is critical to enabling all information to later escape. Developing these ideas more fully will be the main focus of black hole physics in the years to come.

Bibliography

[1] C. R. Stephens, G. 't Hooft and B. F. Whiting, *Black Hole Evaporation without Information Loss*, *Class. Quant. Grav.* **11** (1994) 621–648, [gr-qc/9310006].

[2] L. Susskind, *The World as a Hologram*, *J. Math. Phys.* **36** (1995) 6377–6396, [hep-th/9409089].

[3] J. M. Maldacena, *The Large N Limit of Superconformal Field Theories and Supergravity*, *Int. J. Theor. Phys.* **38** (1999) 1113–1133, [hep-th/9711200].

[4] S. W. Hawking, *Black hole explosions?*, *Nature* **248** (1974) 30–31.

[5] S. W. Hawking, *Particle Creation by Black Holes*, *Commun. Math. Phys.* **43** (1975) 199–220.

[6] D. Finkelstein, *Past-Future Asymmetry of the Gravitational Field of a Point Particle*, *Phys. Rev.* **110** (May, 1958) 965–967.

[7] R. Penrose, *Gravitational Collapse and Space-Time Singularities*, *Phys. Rev. Lett.* **14** (Jan, 1965) 57–59.

[8] S. Gillessen, F. Eisenhauer, S. Trippe, T. Alexander, R. Genzel, F. Martins et al., *Monitoring stellar orbits around the Massive Black Hole in the Galactic Center*, *Astrophys. J.* **692** (2009) 1075–1109, [0810.4674].

[9] LIGO Scientific, Virgo collaboration, B. P. Abbott et al., *Observation of Gravitational Waves from a Binary Black Hole Merger*, *Phys. Rev. Lett.* **116** (2016) 061102, [1602.03837].

[10] Event Horizon Telescope collaboration, K. Akiyama et al., *First M87 Event Horizon Telescope Results. I. The Shadow of the Supermassive Black Hole*, *Astrophys. J.* **875** (2019) L1, [1906.11238].

[11] Y. B. Zeldovich, *Amplification of Cylindrical Electromagnetic Waves Reflected from a Rotating Body*, *Soviet Journal of Experimental and Theoretical Physics* **35** (Jan, 1972) 1085.

[12] W. G. Unruh, *Notes on black-hole evaporation*, *Phys. Rev.* **D14** (1976) 870.

[13] D. N. Page, *Particle emission rates from a black hole. II. Massless particles from a rotating hole*, *Phys. Rev.* **D14** (1976) 3260–3273.

[14] D. N. Page, *Particle emission rates from a black hole. III. Charged leptons from a nonrotating hole*, *Phys. Rev.* **D16** (1977) 2402–2411.

[15] W. G. Unruh, *Absorption cross section of small black holes*, *Phys. Rev.* **D14** (1976) 3251–3259.

[16] D. N. Page, *Particle emission rates from a black hole: Massless particles from an uncharged, nonrotating hole*, *Phys. Rev.* **D13** (1976) 198–206.

[17] A. Strominger and C. Vafa, *Microscopic origin of the Bekenstein-Hawking entropy*, *Phys. Lett.* **B379** (1996) 99–104, [hep-th/9601029].

[18] R. K. Kaul and P. Majumdar, *Logarithmic Correction to the Bekenstein-Hawking Entropy*, *Phys. Rev. Lett.* **84** (Jun, 2000) 5255–5257.

[19] A. Ghosh and P. Mitra, *On the log correction to the black hole area law*, *Phys. Rev.* **D71** (2005) 027502, [gr-qc/0401070].

[20] A. O. Barvinsky, V. P. Frolov and A. I. Zelnikov, *Wavefunction of a Black Hole and the Dynamical Origin of Entropy*, *Phys. Rev.* **D51** (1995) 1741–1763, [gr-qc/9404036].

[21] R. D. Sorkin, *The Statistical Mechanics of Black Hole Thermodynamics*, in *Symposium on Black Holes and Relativistic Stars, Chicago, Illinois, December 14–15, 1996*. gr-qc/9705006.

[22] G. 't Hooft, *On the Quantum Structure of a Black Hole*, *Nucl. Phys.* **B256** (1985) 727–745.

[23] L. Bombelli, R. K. Koul, J. Lee and R. D. Sorkin, *Quantum source of entropy for black holes*, *Phys. Rev. D* **34** (Jul, 1986) 373–383.

[24] S. W. Hawking, *Gravitationally collapsed objects of very low mass*, *Mon. Not. Roy. Astron. Soc.* **152** (1971) 75.

[25] B. J. Carr, K. Kohri, Y. Sendouda and J. Yokoyama, *New cosmological constraints on primordial black holes*, *Phys. Rev.* **D81** (2010) 104019, [0912.5297].

[26] M. Visser, *Thermality of the Hawking flux*, *JHEP* **07** (2015) 009, [1409.7754].

[27] C. Barcelo, S. Liberati, S. Sonego and M. Visser, *Minimal conditions for the existence of a Hawking-like flux*, *Phys. Rev.* **D83** (2011) 041501, [1011.5593].

[28] E. Corbelli and P. Salucci, *The Extended Rotation Curve and the Dark Matter Halo of M33*, *Mon. Not. Roy. Astron. Soc.* **311** (2000) 441–447, [astro-ph/9909252].

[29] X.-P. Wu, T. Chiueh, L.-Z. Fang and Y.-J. Xue, *A comparison of different cluster mass estimates: consistency or discrepancy?*, *Mon. Not. Roy. Astron. Soc.* **301** (1998) 861, [astro-ph/9808179].

[30] A. Refregier, *Weak Gravitational Lensing by Large-Scale Structure*, *Ann. Rev. Astron. Astrophys.* **41** (2003) 645–668, [astro-ph/0307212].

[31] D. Clowe, M. Bradac, A. H. Gonzalez, M. Markevitch, S. W. Randall, C. Jones et al., *A direct empirical proof of the existence of dark matter*, *Astrophys. J.* **648** (2006) L109–L113, [astro-ph/0608407].

[32] W. Israel, *Event Horizons in Static Vacuum Space-Times*, *Phys. Rev.* **164** (1967) 1776–1779.

[33] S. W. Hawking, *Black Holes in General Relativity*, *Commun. Math. Phys.* **25** (1972) 152–166.

[34] B. Carter, *Axisymmetric Black Hole Has Only Two Degrees of Freedom*, *Phys. Rev. Lett.* **26** (1971) 331–333.

[35] P. O. Mazur, *Proof of uniqueness of the Kerr-Newman black hole solution*, *J. Phys.* **A15** (1982) 3173–3180.

[36] G. L. Bunting and A. K. M. Masood-ul Alam, *Nonexistence of Multiple Black Holes in Asymptotically Euclidean Static Vacuum Space-Time*, *General Relativity and Gravitation* **19** (Feb, 1987) 147–154.

[37] S. W. Hawking and G. F. R. Ellis, *The Large Scale Structure of Space-Time*. Cambridge Monographs on Mathematical Physics. Cambridge University Press, 2011.

[38] J. M. Bardeen, B. Carter and S. W. Hawking, *The Four Laws of Black Hole Mechanics*, *Commun. Math. Phys.* **31** (1973) 161–170.

[39] J. D. Bekenstein, *Black Holes and Entropy*, *Phys. Rev. D* **7** (Apr, 1973) 2333–2346.

[40] J. R. Ellis, J. S. Hagelin, D. V. Nanopoulos and M. Srednicki, *Search for Violations of Quantum Mechanics*, *Nucl. Phys.* **B241** (1984) 381.

[41] T. Banks, L. Susskind and M. E. Peskin, *Difficulties for the Evolution of Pure States Into Mixed States*, *Nucl. Phys.* **B244** (1984) 125–134.

[42] L. Susskind, *Trouble For Remnants*, `hep-th/9501106`.

[43] L. Parker, *Particle Creation in Expanding Universes*, *Phys. Rev. Lett.* **21** (1968) 562–564.

[44] J. S. Schwinger, *On Gauge Invariance and Vacuum Polarization*, *Phys. Rev.* **82** (1951) 664–679.

[45] M. D. Schwartz, *Quantum Field Theory and the Standard Model*. Cambridge University Press, 2014.

[46] W. Heisenberg and H. Euler, *Consequences of Dirac's Theory of The Positron*, *Z. Phys.* **98** (1936) 714–732, [`physics/0605038`].

[47] G. W. Gibbons and S. W. Hawking, *Action Integrals and Partition Functions in Quantum Gravity*, *Phys. Rev.* **D15** (1977) 2752–2756.

[48] M. K. Parikh and F. Wilczek, *Hawking Radiation as Tunneling*, *Phys. Rev. Lett.* **85** (2000) 5042–5045, [`hep-th/9907001`].

[49] P. Kraus and F. Wilczek, *Self-Interaction Correction to Black Hole Radiance*, *Nucl. Phys.* **B433** (1995) 403–420, [`gr-qc/9408003`].

[50] M. K. Parikh, *A Secret Tunnel Through The Horizon*, *Int. J. Mod. Phys.* **D13** (2004) 2351–2354, [`hep-th/0405160`].

[51] L. Vanzo, G. Acquaviva and R. Di Criscienzo, *Tunnelling Methods and Hawking's radiation: achievements and prospects*, *Class. Quant. Grav.* **28** (2011) 183001, [1106.4153].

[52] S. R. Coleman, J. Preskill and F. Wilczek, *Quantum Hair on Black Holes*, *Nucl. Phys.* **B378** (1992) 175–246, [hep-th/9201059].

[53] N. Arkani-Hamed, S. Dimopoulos and G. R. Dvali, *The Hierarchy Problem and New Dimensions at a Millimeter*, *Phys. Lett.* **B429** (1998) 263–272, [hep-ph/9803315].

[54] V. A. Rubakov and M. E. Shaposhnikov, *Do We Live Inside a Domain Wall?*, *Phys. Lett.* **125B** (1983) 136–138.

[55] G. R. Dvali and M. A. Shifman, *Dynamical Compactification as a Mechanism of Spontaneous Supersymmetry Breaking*, *Nucl. Phys.* **B504** (1997) 127–146, [hep-th/9611213].

[56] D. Bailin and A. Love, *Kaluza-Klein theories*, *Rept. Prog. Phys.* **50** (1987) 1087–1170.

[57] W. D. Goldberger, *Les Houches lectures on effective field theories and gravitational radiation*, in *Les Houches Summer School — Session 86, Les Houches, France, July 31–August 25, 2006*. hep-ph/0701129.

[58] F. Bastianelli and A. Zirotti, *Worldline formalism in a gravitational background*, *Nucl. Phys.* **B642** (2002) 372–388, [hep-th/0205182].

[59] C. Misner, K. Thorne and J. Wheeler, *Gravitation*. W. H. Freeman, 1973.

[60] M. Abramowitz and I. Stegun, *Handbook of Mathematical Functions: with Formulas, Graphs, and Mathematical Tables*. Applied mathematics series. Dover Publications, 1965.

[61] E. Jung and D. K. Park, *Effect of scalar mass in the absorption and emission spectra of Schwarzschild black hole*, *Class. Quant. Grav.* **21** (2004) 3717–3732, [hep-th/0403251].

[62] S. P. Kim and D. N. Page, *Remarks on Schwinger Pair Production by Charged Black Holes*, *Nuovo Cim.* **B120** (2005) 1193–1208, [gr-qc/0401057].

[63] I. B. Khriplovich, *Particle creation by charged black holes*, *Phys. Rept.* **320** (1999) 37–49.

[64] N. Arkani-Hamed, L. Motl, A. Nicolis and C. Vafa, *The string landscape, black holes and gravity as the weakest force*, *JHEP* **06** (2007) 060, [hep-th/0601001].

[65] G. W. Gibbons, *Vacuum Polarization and the Spontaneous Loss of Charge by Black Holes*, *Commun. Math. Phys.* **44** (1975) 245–264.

[66] A. I. Nikishov, *Pair production by a constant external field*, *Zh. Eksp. Teor. Fiz.* **57** (1969) 1210–1216.

[67] O. J. C. Dias, R. Emparan and A. Maccarrone, *Microscopic theory of black hole superradiance*, *Phys. Rev.* **D77** (2008) 064018, [0712.0791].

[68] A. I. Nikishov, *Barrier scattering in field theory removal of Klein paradox*, *Nucl. Phys.* **B21** (1970) 346–358.

[69] A. Hansen and F. Ravndal, *Klein's Paradox and Its Resolution*, *Phys. Scripta* **23** (1981) 1036.

[70] K. Umetsu, *Recent Attempts in the Analysis of Black Hole Radiation*. PhD thesis, Nihon U., IQS, 2010. 1003.5534.

[71] D. N. Page, *Hawking radiation and black hole thermodynamics*, *New J. Phys.* **7** (2005) 203, [hep-th/0409024].

[72] S. A. Teukolsky, *Perturbations of a Rotating Black Hole. I. Fundamental Equations for Gravitational, Electromagnetic, and Neutrino-Field Perturbations*, *Astrophys. J.* **185** (1973) 635–647.

[73] E. Newman and R. Penrose, *An Approach to Gravitational Radiation by a Method of Spin Coefficients*, *J. Math. Phys.* **3** (1962) 566–578.

[74] C. L. Benone and L. C. B. Crispino, *Superradiance in static black hole spacetimes*, *Phys. Rev.* **D93** (2016) 024028, [1511.02634].

[75] S. P. Kim and D. N. Page, *Schwinger pair production in electric and magnetic fields*, *Phys. Rev.* **D73** (2006) 065020, [hep-th/0301132].

[76] S. P. Kim and D. N. Page, *Schwinger pair production via instantons in a strong electric field*, *Phys. Rev.* **D65** (2002) 105002, [hep-th/0005078].

[77] A. Dzieciol, N. Fröman, P. Fröman, A. Hökback, S. Linnaeus, B. Lundborg et al., *Phase-Integral Method: Allowing Nearlying Transition Points*. Springer Tracts in Natural Philosophy. Springer New York, 1998.

[78] Y. Habara, Y. Nagatani, H. B. Nielsen and M. Ninomiya, *Dirac Sea and Hole Theory for Bosons I: A new formulation of quantum field theories*, *Int. J. Mod. Phys.* **A23** (2008) 2733–2769, [hep-th/0603242].

[79] R. Penrose and R. M. Floyd, *Extraction of Rotational Energy from a Black Hole*, *Nature* **229** (1971) 177–179.

[80] H. A. Weldon, *Fermions without vierbeins in curved space-time*, *Phys. Rev.* **D63** (2001) 104010, [gr-qc/0009086].

[81] D. R. Brill and J. A. Wheeler, *Interaction of Neutrinos and Gravitational Fields*, *Rev. Mod. Phys.* **29** (1957) 465–479.

[82] C. Bender and S. Orszag, *Advanced Mathematical Methods for Scientists and Engineers I: Asymptotic Methods and Perturbation Theory*. Springer New York, 2013.

[83] B. Carr, F. Kuhnel and M. Sandstad, *Primordial Black Holes as Dark Matter*, *Phys. Rev.* **D94** (2016) 083504, [1607.06077].

[84] B. Carr, M. Raidal, T. Tenkanen, V. Vaskonen and H. Veermäe, *Primordial black hole constraints for extended mass functions*, *Phys. Rev.* **D96** (2017) 023514, [1705.05567].

[85] A. Barnacka, J. F. Glicenstein and R. Moderski, *New constraints on primordial black holes abundance from femtolensing of gamma-ray bursts*, *Phys. Rev.* **D86** (2012) 043001, [1204.2056].

[86] A. Katz, J. Kopp, S. Sibiryakov and W. Xue, *Femtolensing by Dark Matter Revisited*, *JCAP* **1812** (2018) 005, [1807.11495].

[87] H. Niikura et al., *Microlensing constraints on primordial black holes with Subaru/HSC Andromeda observations*, *Nat. Astron.* **3** (2019) 524–534, [1701.02151].

[88] EROS-2 collaboration, P. Tisserand et al., *Limits on the Macho Content of the Galactic Halo from the EROS-2 Survey of the Magellanic Clouds*, *Astron. Astrophys.* **469** (2007) 387–404, [astro-ph/0607207].

[89] F. Capela, M. Pshirkov and P. Tinyakov, *Constraints on primordial black holes as dark matter candidates from capture by neutron stars*, *Phys. Rev.* **D87** (2013) 123524, [1301.4984].

[90] P. W. Graham, S. Rajendran and J. Varela, *Dark Matter Triggers of Supernovae*, *Phys. Rev.* **D92** (2015) 063007, [1505.04444].

[91] Y. Ali-Haïmoud and M. Kamionkowski, *Cosmic microwave background limits on accreting primordial black holes*, *Phys. Rev.* **D95** (2017) 043534, [1612.05644].

[92] M. Boudaud and M. Cirelli, *Voyager 1 $e^{\pm}$ Further Constrain Primordial Black Holes as Dark Matter*, *Phys. Rev. Lett.* **122** (2019) 041104, [1807.03075].

[93] W. DeRocco and P. W. Graham, *Constraining Primordial Black Hole Abundance with the Galactic 511 keV Line*, *Phys. Rev. Lett.* **123** (2019) 251102, [1906.07740].

[94] R. Lehoucq, M. Casse, J. M. Casandjian and I. Grenier, *New constraints on the primordial black hole number density from Galactic gamma-ray astronomy*, *Astron. Astrophys.* **502** (2009) 37, [0906.1648].

[95] A. Barrau, D. Blais, G. Boudoul and D. Polarski, *Galactic cosmic rays from PBHs and primordial spectra with a scale*, *Phys. Lett.* **B551** (2003) 218–225, [astro-ph/0210149].

[96] H. Tashiro and N. Sugiyama, *Constraints on Primordial Black Holes by Distortions of Cosmic Microwave Background*, *Phys. Rev.* **D78** (2008) 023004, [0801.3172].

[97] E. G. Adelberger, J. H. Gundlach, B. R. Heckel, S. Hoedl and S. Schlamminger, *Torsion balance experiments: A low-energy frontier of particle physics*, *Prog. Part. Nucl. Phys.* **62** (2009) 102–134.

[98] P. Kanti, *Black Holes in Theories with Large Extra Dimensions: a Review*, *Int. J. Mod. Phys.* **A19** (2004) 4899–4951, [hep-ph/0402168].

[99] R. C. Myers and M. J. Perry, *Black Holes in Higher Dimensional Space-Times*, *Annals Phys.* **172** (1986) 304.

[100] P. C. Argyres, S. Dimopoulos and J. March-Russell, *Black holes and sub-millimeter dimensions*, *Phys. Lett.* **B441** (1998) 96–104, [hep-th/9808138].

[101] Particle Data Group collaboration, M. Tanabashi et al., *Review of particle physics*, *Phys. Rev. D* **98** (Aug, 2018) 030001.

[102] A. Arbey and J. Auffinger, *BlackHawk: a public code for calculating the Hawking evaporation spectra of any black hole distribution*, *Eur. Phys. J.* **C79** (2019) 693, [1905.04268].

[103] C. M. Harris and P. Kanti, *Hawking Radiation from a (4+n)-dimensional Black Hole: Exact Results for the Schwarzschild Phase*, *JHEP* **10** (2003) 014, [hep-ph/0309054].

[104] S. Creek, O. Efthimiou, P. Kanti and K. Tamvakis, *Graviton emission in the bulk from a higher-dimensional Schwarzschild black hole*, *Phys. Lett.* **B635** (2006) 39–49, [hep-th/0601126].

[105] A. S. Cornell, W. Naylor and M. Sasaki, *Graviton emission from a higher-dimensional black hole*, *JHEP* **02** (2006) 012, [hep-th/0510009].

[106] P. Kanti and J. March-Russell, *Calculable Corrections to Brane Black Hole Decay I: The Scalar Case*, *Phys. Rev.* **D66** (2002) 024023, [hep-ph/0203223].

[107] P. Kanti and J. March-Russell, *Calculable Corrections to Brane Black Hole Decay II: Greybody Factors for Spin 1/2 and 1*, *Phys. Rev.* **D67** (2003) 104019, [hep-ph/0212199].

[108] G. Weidenspointner, M. Varendorff, S. C. Kappadath, K. Bennett, H. Bloemen, R. Diehl et al., *The cosmic diffuse gamma-ray background measured with COMPTEL*, *AIP Conference Proceedings* **510** (2000) 467–470.

[109] A. W. Strong, I. V. Moskalenko and O. Reimer, *A New Determination of the Extragalactic Diffuse Gamma-Ray Background from EGRET Data*, *Astrophys. J.* **613** (2004) 956–961, [astro-ph/0405441].

[110] Fermi-LAT collaboration, M. Ackermann et al., *The spectrum of isotropic diffuse gamma-ray emission between 100 MeV and 820 GeV*, *Astrophys. J.* **799** (2015) 86, [1410.3696].

[111] A. Moretti et al., *A new measurement of the cosmic X-ray background*, *AIP Conf. Proc.* **1126** (2009) 223–226, [0811.1444].

[112] A. Arbey, J. Auffinger and J. Silk, *Constraining primordial black hole masses with the isotropic gamma ray background*, *Phys. Rev.* **D101** (2020) 023010, [1906.04750].

[113] S. Ryu and T. Takayanagi, *Holographic derivation of entanglement entropy from AdS/CFT*, *Phys. Rev. Lett.* **96** (2006) 181602, [hep-th/0603001].

[114] N. Engelhardt and A. C. Wall, *Quantum Extremal Surfaces: Holographic Entanglement Entropy beyond the Classical Regime*, *JHEP* **01** (2015) 073, [1408.3203].

[115] A. Almheiri, R. Mahajan, J. Maldacena and Y. Zhao, *The Page curve of Hawking radiation from semiclassical geometry*, *JHEP* **03** (2020) 149, [1908.10996].

[116] A. Almheiri, T. Hartman, J. Maldacena, E. Shaghoulian and A. Tajdini, *Replica Wormholes and the Entropy of Hawking Radiation*, *JHEP* **05** (2020) 013, [1911.12333].

[117] D. N. Page, *Information in black hole radiation*, *Phys. Rev. Lett.* **71** (1993) 3743–3746, [hep-th/9306083].

[118] T. Faulkner, A. Lewkowycz and J. Maldacena, *Quantum corrections to holographic entanglement entropy*, *JHEP* **11** (2013) 074, [1307.2892].

[119] A. Almheiri, N. Engelhardt, D. Marolf and H. Maxfield, *The entropy of bulk quantum fields and the entanglement wedge of an evaporating black hole*, *JHEP* **12** (2019) 063, [1905.08762].

[120] A. Almheiri, R. Mahajan and J. Maldacena, *Islands outside the horizon*, 1910.11077.